

Multi-Label Noise Transition Matrix Estimation with Label Correlations: Theory and Algorithm

Shikun Li, Xiaobo Xia, Hansong Zhang, Shiming Ge[†], *Senior Member, IEEE*,
Tongliang Liu, *Senior Member, IEEE*

Abstract—Noisy multi-label learning has garnered increasing attention due to the challenges posed by collecting large-scale accurate labels, making noisy labels a more practical and cost-effective alternative. Motivated by noisy multi-class learning, where the noise transition matrix is employed to represent the probabilities that clean labels flip into noisy labels, the introduction of transition matrices can help model multi-label noise and enable the development of statistically consistent algorithms for noisy multi-label learning. However, estimating multi-label noise transition matrices remains a challenging task, as most existing estimators in noisy multi-class learning rely on anchor points and accurate fitting of noisy class posteriors, which is hard to satisfy in noisy multi-label learning. In this paper, we address this problem by first investigating the identifiability of class-dependent transition matrices in noisy multi-label learning. Building upon the insights gained from the identifiability results, we propose a novel estimator that leverages label correlations without the need for anchor points or precise fitting of noisy class posteriors. Specifically, we first estimate the occurrence probability of two noisy labels to capture noisy label correlations. Subsequently, we employ sample selection techniques to extract information implying clean label correlations, which are then used to estimate the occurrence probability of one noisy label when a certain clean label appears. By exploiting the mismatches in label correlations implied by these occurrence probabilities, we demonstrate that the transition matrix becomes identifiable and can be acquired by solving a straightforward bilinear decomposition problem. Theoretically, we establish an estimation error bound for our multi-label transition matrix estimator and derive a generalization error bound for our statistically consistent algorithm with true transition matrices. Empirically, we validate the effectiveness of our estimator in estimating multi-label noise transition matrices, leading to excellent classification performance.

Index Terms—noisy multi-label learning, noise transition matrix, label correlation, robustness, generalization



1 INTRODUCTION

IN real-world scenarios, an instance is naturally associated with multiple labels, and these labels have *complex entangled correlations* [1]. Recently, the problem of label-noise learning in multi-label classification has received more and more attention [2], [3], [4], [5], [6], [7], [8], since it is time-consuming and expensive to collect large-scale accurate labels and the noisy labels are much cheaper and easier to acquire. In the setting of *noisy multi-label learning*, the multiple labels assigned to an instance may be corrupted simultaneously. That is to say, any label for each class can be flipped with its respective *transition matrix* that denotes the transition relationship from clean labels to noisy labels.

The noise transition matrix has been utilized to build a series of *statistically consistent* algorithms for *noisy multi-class learning* [9], [10], [11], [12]. The main advantage of these consistent algorithms is that they can guarantee to vanish the differences between the classifiers learned from noisy data and the optimal ones from clean data by increasing the size of noisy examples [10], [13], [14], [15].

Fortunately, these statistically consistent algorithms for noisy multi-class learning can also be applied in such noisy multi-label learning with a little modification [4]. However, the effectiveness of these algorithms heavily relies on estimating the transition matrix. Although the estimation of the transition matrix has been investigated in noisy multi-class learning, the estimation of the transition matrix in noisy multi-label learning has not been studied and remains challenging. Specifically, a series of methods [10], [13], [14], [16], [17] have been proposed to estimate the transition matrix for noisy multi-class learning. Most of them assume the existence of anchor points [13], [14], [16] that are defined as the training examples belonging to a particular clean class surely. Nevertheless, the assumption is strong and hard to check when we only have noisy data [10]. Also, the methods need to accurately fit the noisy or intermediate class posterior of anchor points, which is rather difficult in multi-label cases, due to severe positive-negative imbalance [18].

In this paper, to address the problem of estimating the noise transition matrix in noisy multi-label learning, we consider utilizing label correlations among noisy multiple labels [19]. Specifically, some label correlations that should *not exist* in practice are included in noisy multi-label learning. For example, as illustrated in Fig. 1, “fish” and “water” always co-occur, while “bird” and “sky” always co-occur. Nevertheless, due to label errors, there is a *slight correlation* between “fish” and “sky”, which is impractical. At a high level, we can utilize the *mismatch of label correlations* to identify the transition matrix without neither anchor points

[†] Corresponding author.

- S. Li, H. Zhang, and S. Ge are with the Institute of Information Engineering, Chinese Academy of Sciences, Beijing 100095, China, and also with the School of Cyber Security at University of Chinese Academy of Sciences, Beijing 100049, China (e-mail: {lishikun,hansongzhang,geshiming}@iie.ac.cn).
- X. Xia and T. Liu are with the Sydney AI Center, School of Computer Science, Faculty of Engineering, The University of Sydney, Darlington, NSW2008, Australia (e-mail: xxia5420@uni.sydney.edu.au; tongliang.liu@sydney.edu.au).

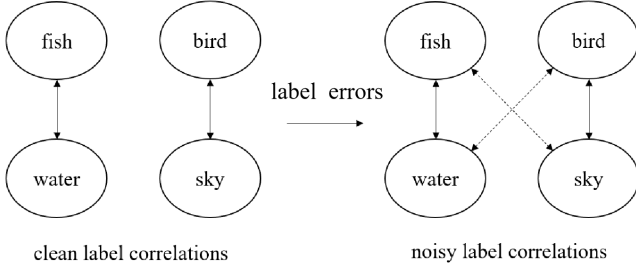


Fig. 1: The illustration of the mismatch of label correlations among multiple class labels.

nor accurate fitting of noisy class posterior.

In more detail, we first focus on the *identifiability problem* of the class-dependent transition matrix in noisy multi-label learning. Accordingly, a new method that estimates the transition matrix by exploiting label correlations is proposed. That is, motivated by the identifiability result that the label correlation of two noisy labels can not suffice to identify the transition matrix in noisy multi-label learning, we utilize *sample selection* to extract useful information from noisy data, which implies clean label correlations to achieve the identifiability. Afterward, we not only estimate the *occurrence probability* of two noisy labels in noisy data, but also of one noisy label when a certain clean label appears in selected data. By utilizing the mismatch of label correlations implied in these occurrence probabilities, we can prove the identifiability, and transform the problem of estimating the transition matrix using label correlations into a problem of *bilinear decomposition*. Finally, with easy frequency counting, we can get a great estimation of the noise transition matrix.

We conduct extensive experiments to justify our claims. Empirical results illustrate the effectiveness of the proposed estimator for estimating the transition matrix in noisy multi-label learning, and the consistent algorithms with our estimator can achieve better classification performance over various comparison methods.

A preliminary version of this work was presented at the Thirty-seventh Conference on Neural Information Processing Systems (NeurIPS 2022) and selected to be “Spotlight” [20]. Compared to the preliminary version, we include new theoretical analyses and more experimental results. Specifically, in Section 4, we derive theoretical analyses that present an estimation error bound for our multi-label transition matrix estimator and a generalization error bound for the statistically consistent algorithm [13], [21] with true transition matrices. The proofs of the established error bounds are also provided in Appendices. Additional discussions and empirical results with instance-dependent label noise are included in Section 5.2. More experiments about ablation studies are also presented in Section 6, which are consistent with our theoretical analyses. Our implementation is open-sourced at: <https://github.com/tmlab/Multi-Label-T>.

1.1 Contributions

Before delving into details, we highlight the main contributions of this paper as follows:

- We focus on an important but little explored problem of noisy multi-label learning, *i.e.*, the estimation of

multi-label noise transition matrices. In particular, we first prove some identifiability results of class-dependent transition matrices in such a setting.

- Inspired by the identifiability results, we propose a new estimator to learn the transition matrix by utilizing the wealth of label correlations without anchor points and accurate fitting of noisy class posterior.
- We provide an estimation error bound for our multi-label transition matrix estimator and a generalization error bound for the statistically consistent algorithm with true transition matrices, which theoretically justify the effectiveness of the proposed method.
- Empirical results across various noisy multi-label benchmarks with simulated class-dependent, instance-dependent, and real-world label noise, demonstrate the superiority of our transition matrix estimator. Comprehensive ablation studies and discussions are also provided.

1.2 Organization

The rest of the paper is organized as follows. In Section 2, we introduce the problem setting of label-noise learning in multi-label classification. In Section 3, we discuss the identifiability of the noise transition matrix under such a noisy multi-label setting, and introduce our estimation method. In Section 4, we provide theoretical analyses to justify the effectiveness of our proposed method. Experimental results are provided in Section 5. Ablation studies about transition matrix estimation, multi-label classifier learning and the choice of hyperparameter are presented in Section 6. Finally, we conclude the paper in Section 7. To improve readability, more discussions, proofs, and experimental results are provided in supplemental materials.

2 PROBLEM SETTING

In this section, we introduce the problem setting of noisy multi-label learning. In what follows, scalars/vectors are in lowercase letters, and matrices/variables are in uppercase letters. For simplicity, let $[q] = \{1, \dots, q\}$.

Preliminaries. Let D be the distribution of a pair of random variables (X, Y) , where $X \in \mathcal{X} \subseteq \mathbb{R}^d$ denotes the variable of instances, and $Y = \{Y^1, Y^2, \dots, Y^q\} \in \{0, 1\}^q$ denotes the variable of targets with q possible class labels. As for Y , $Y^j = 1$ indicates that the instance x is associated with the class j ; $Y^j = 0$, otherwise. In multi-label learning, the goal is to learn a function about D which maps each unseen instance $x \in \mathcal{X}$ to proper labels y . However, as discussed, Y is hard to be annotated precisely. Before being observed, their true labels are independently flipped and what we can obtain are noisy training examples $\mathcal{D}_t = \{(x_i, \bar{y}_i)\}_{i=1}^n$, where $\bar{y}_i = \{\bar{y}_i^1, \bar{y}_i^2, \dots, \bar{y}_i^q\}$ denotes noisy labels. Let \bar{D} be the distribution of the noisy random variables $(X, \bar{Y}) \in \mathcal{X} \times \{0, 1\}^q$. In noisy multi-label learning, our goal is to infer proper labels for each unseen instance by *only* using noisy training examples.

Noise transition matrix. The random variables \bar{Y}^j and Y^j for the class j are related through a noise transition matrix $T^j \in [0, 1]^{2 \times 2}$, $j \in [q]$. Generally, the transition matrix depends on instances, *i.e.*, its element $T_{ik}^j(X = x)$

represents the probability $\mathbb{P}(\bar{Y}^j = k \mid Y^j = i, X = x)$. Nevertheless, given only noisy examples, the instance-dependent transition matrix is *non-identifiable* without any additional assumption [10], [22]. For example, both $\mathbb{P}(\bar{Y}^j = k \mid X = x) = \sum_{i=0}^1 T_{ik}^j(X = x)\mathbb{P}(Y^j = i \mid X = x)$ and $\mathbb{P}(\bar{Y}^j = k \mid X = x) = \sum_{i=0}^1 T_{ik}^j(X = x)\mathbb{P}'(Y^j = i \mid X = x)$ are valid, for any $\mathbb{P}'(Y^j = 0 \mid X = x) \in [0, 1]$, $\mathbb{P}'(Y^j = 1 \mid X = x) = 1 - \mathbb{P}'(Y^j = 0 \mid X = x)$, and $T_{ik}^j(X = x) = T_{ik}^j(X = x)\mathbb{P}(Y^j = i \mid X = x)/\mathbb{P}'(Y^j = i \mid X = x)$. Therefore, in this paper, we assume that the transition matrix is class-dependent and instance-independent [14], i.e., $\mathbb{P}(\bar{Y}^j = k \mid Y^j = i, X = x) = \mathbb{P}(\bar{Y}^j = k \mid Y^j = i)$. The definition of the class-dependent label noise can be found in Appendix A, where we further discuss its differences with the class-dependent label noise in the multi-class cases.

Statistically consistent algorithms. The transition matrix bridges the class posterior probabilities for noisy and clean data, i.e., $\mathbb{P}(\bar{Y} = k \mid X = x) = \sum_{i=0}^1 T_{ik}\mathbb{P}(Y = i \mid X = x)$. Therefore, it has been exploited to achieve many statistically consistent algorithms in noisy multi-class learning. Specifically, it has been utilized to build risk-consistent estimators via correcting loss functions [10], [13], [14], and to design classifier-consistent estimators via limiting hypotheses, e.g., [14], [23], [24]. Since the multi-label task can be decomposed into multiple conditionally independent binary classification problems, we also can apply these consistent methods in noisy multi-label learning [4]. In this paper, without loss of generality, by employing the importance reweighting (abbreviated as ‘‘Reweight’’) algorithm [10], [13], we build the risk-consistent estimator $\bar{R}_{n,w}(\{T^j\}_{j=1}^q, f)$ to learn statistically consistent classifiers with noise transition matrices:

$$\begin{aligned} & \bar{R}_{n,w}(\{T^j\}_{j=1}^q, f) \\ &= \frac{1}{n} \sum_{i=1}^n \sum_{j=1}^q \frac{\hat{\mathbb{P}}(Y^j = \bar{y}_i^j \mid X = x_i)}{\hat{\mathbb{P}}(\bar{Y}^j = \bar{y}_i^j \mid X = x_i)} \ell(f_j(x_i), \bar{y}_i^j), \end{aligned} \quad (1)$$

where ℓ is the binary cross entropy function, and $f = (f_1, f_2, \dots, f_q)$ is the learnable q classification functions; the subscript w denotes that the loss function is weighted. More details of the Reweight algorithm for noisy multi-label learning can be found in Appendix B.

Transition matrix estimation. As inaccurate transition matrices will degenerate the performances of these consistent algorithms, a series of estimation methods [13], [16], [17], [25], [26] have been proposed for noisy multi-class learning to efficiently identify the transition matrix. However, most of them require the assumption of anchor points [14], [16], [17], which is strong and hard to check in multi-label cases when only noisy data are provided [10]. Besides, severe positive-negative imbalance in multi-label learning [18] will make it difficult to accurately approximate the noisy or intermediate class posterior of anchor points, which is crucial for these methods. This motivates us to seek for a better estimator that can do without anchor points and avoid estimating noisy posterior in noisy multi-label learning.

3 ESTIMATING TRANSITION MATRICES WITH LABEL CORRELATIONS

In this section, we first study the identifiability problem [27] of class-dependent transition matrices in the cases of multi-

label learning (Section 3.1). Furthermore, inspired by these results, we propose a new estimator to estimate the noise transition matrix by utilizing label correlations (Section 3.2).

3.1 Identifiability of Transition Matrix

Recently, Liu et al. [27] built identifiability of the noise transition matrix on Kruskal’s identifiability results. Inspired by them, with the complex correlations among class labels, we can get some identifiability results of the class-dependent transition matrix in noisy multi-label learning.

Following [27], to define identifiability, we denote an observation space by Ω . For a general parametric space Θ , we denote the distribution (probability density function) induced by the parameter $\theta \in \Theta$ on the observation space Ω as \mathbb{P}_θ [28]. The identifiability for a general parametric space is defined as follows.

Definition 1 (Identifiability [27]). *The parameter θ is identifiable if $\mathbb{P}_\theta \neq \mathbb{P}_{\theta'}, \forall \theta \neq \theta'$.*

For the class-dependent transition matrix T^j for class j , the identifiability can be defined as the following, when T^j is a part of θ .

Definition 2 (Identifiability of T^j). *T^j is identifiable if $\mathbb{P}_\theta \neq \mathbb{P}_{\theta'}$ for $\theta \neq \theta'$, up to the label permutation of class j .*

Remark 1. The label permutation of class j means swapping 1 and 0 class values in class j , and the rows of T^j will also swap. Note that Ω does not necessarily include all observable variables. We use an example to better understand it. For example, let $\Omega := \{\bar{Y}^j, X\}$, $\theta := \{T^j, \mathbb{P}(Y^j \mid X)\}$, and $\mathbb{P}_\theta := \mathbb{P}(\bar{Y}^j \mid X)$, the identifiability of T^j can be achieved with the anchor point assumption [14], [16], [17].

To use notations without confusion, for the identifiability of T^j using label correlations, we let $\Omega := \{\bar{Y}^j, \bar{Y}^{-j}\}$, where $-j$ means other classes having correlations with class j , $\theta := \{T^j, \mathbb{P}(Y^j), \mathbb{P}(\bar{Y}^{-j} \mid Y^j)\}$, and $\mathbb{P}_\theta := \mathbb{P}(\bar{Y}^j, \bar{Y}^{-j})$. Also, Ω does not necessarily include all noisy class labels. As we need Ω to provide useful information to achieve identifiability, the exploration of an effective Ω and necessary conditions is one of the focuses of the paper.

3.1.1 Assumptions

In the following, we discuss some assumptions that are used to simplify theoretical analysis.

Assumption 1. $\mathbb{P}(\bar{Y}^j = 0 \mid Y^j = 1) + \mathbb{P}(\bar{Y}^j = 1 \mid Y^j = 0) < 1, j \in [q]$.

Remark 2. Assumption 1 means that the noisy label agrees with the clean label on average, which is a standard condition for analysis under the class-dependent transition matrix [9], [29].

Assumption 2. $\mathbb{P}(Y^i = 0 \mid Y^j = 0) \neq \mathbb{P}(Y^i = 0 \mid Y^j = 1)$, $i, j \in [q]$ and $i \neq j$.

Remark 3. Assumption 2 means that the multiple labels have correlations between each other, which is satisfied by most of (i, j) pairs in the real-world dataset (more details are provided in Appendix C).

3.1.2 Theoretical results

When considering multi-label learning, the simplest case is having two class labels. In this case, the following theoretical results can be obtained.

Theorem 1. *Two noisy labels $\{\bar{Y}^j, \bar{Y}^i\}$ will not suffice to identify T^j .*

This result tells us that the label correlations of two noisy labels can not offer enough information to achieve the identifiability of T^j . We provide Theorem 2 based on the Kruskal’s identifiability result [30], [31].

Theorem 2. *If \bar{Y}^i and \bar{Y}^k are independent given Y^j , three noisy labels $\{\bar{Y}^j, \bar{Y}^i, \bar{Y}^k\}$ are sufficient to identify T^j .*

The assumption that \bar{Y}^i and \bar{Y}^k are independent given Y^j can be satisfied in certain cases, e.g., the occurrences of “blue” and “dolphin” may be independent given “sea” appearing or not. Nevertheless, due to the complex correlations among labels, sometimes, this condition is hard to hold in most cases. When the condition can not hold, these label correlations are no longer sufficient to determine T^j , as shown in Theorem 3 below.

Theorem 3. *If \bar{Y}^i and \bar{Y}^k are not independent given Y^j , three noisy labels $\{\bar{Y}^j, \bar{Y}^i, \bar{Y}^k\}$ will not suffice to identify T^j .*

The inspiration from Theorem 3 is that, the increase of the number of noisy labels may make the identifiability decrease due to the entangled correlations (see Appendix H and J). To handle this problem, we prove Theorem 4 by assuming the transition relationship between the noisy label for class i and the clean label for class j is known.

Theorem 4. *If $\mathbb{P}(\bar{Y}^i | Y^j)$ is known, two noisy labels $\{\bar{Y}^j, \bar{Y}^i\}$ are sufficient to identify T^j .*

Theorem 4 theoretically guarantees that the identifiability of the class-dependent transition matrix can be achieved by utilizing the occurrence probabilities $\mathbb{P}(\bar{Y}^i, \bar{Y}^j)$ and $\mathbb{P}(\bar{Y}^i | Y^j)$. Note that $\mathbb{P}(\bar{Y}^i, \bar{Y}^j)$ can represent noisy label correlations, and $\mathbb{P}(\bar{Y}^i | Y^j) = \sum_{Y^i} \mathbb{P}(\bar{Y}^i | Y^i) \mathbb{P}(Y^i | Y^j)$, which can imply clean label correlations. At a high level, the mismatch of label correlations implied in the occurrence probabilities can achieve the identifiability.

The detailed proofs of Theorems 1-4 are provided in Appendix F-I respectively.

3.2 The Proposed Estimator

Our estimator is based on Theorem 4, which needs extra information to estimate $\mathbb{P}(\bar{Y}^i | Y^j)$. Recently, the *memorization effect* [32] of deep networks has received much attention in learning with noisy labels, which shows that deep networks will first memorize the training data with clean labels and then those with noisy labels. Prior works utilize this characteristic to develop *sample selection* methods [33], [34], [35], [36], [37], [38], [39], [40], where we select some examples with more likely clean labels for each class j respectively in the early learning phase. The selected examples can serve as useful extra information that implies clean label correlations, through which we can achieve estimation via counting. However, when implementing sample-selection-based methods, a major concern is whether the sampling bias will lead to large estimation errors.

Generally speaking, according to the memorization effect, the sampling bias is about selecting easy examples for class j , which usually means these examples have easy-to-discriminate features. We can reasonably assume that given Y^j , the distribution of the features about class j is biased, while the distribution of the features about another class i is unbiased, i.e.,

$$\begin{aligned} \mathbb{P}_{D_s^j}(\bar{Y}^i | Y^j) &= \int \mathbb{P}_{D_s^j}(\bar{Y}^i | X^i) \mathbb{P}_{D_s^j}(X^i | Y^j) dx \\ &= \int \mathbb{P}_{\bar{D}_s^j}(\bar{Y}^i | X^i) \mathbb{P}_{\bar{D}_s^j}(X^i | Y^j) dx \\ &= \mathbb{P}_{\bar{D}_s^j}(\bar{Y}^i | Y^j), \end{aligned} \quad (2)$$

where D_s^j is the distribution of (X, Y_s) , $Y_s = \{\bar{Y}^1, \bar{Y}^2, \dots, Y^j, \dots, \bar{Y}^q\}$, \bar{D}_s^j is the biased distribution of (X, Y_s) , and X^i is the part of X , which represents all information about class i appearing or not. When the assumption is satisfied, the sample selection will not lead to large estimation errors on $\mathbb{P}(\bar{Y}^i | Y^j)$, and it can converge to zero exponentially fast by counting [41].

In real-world scenarios, due to the complex label correlations, this assumption will not strictly hold. While, it may be roughly met when class labels i and j do not share the major discriminative features. Intuitively speaking, the classifying of simplest examples for one label is not easily affected by the presence or absence of other significantly different labels. Also, since most label pairs from typical real-world multi-label datasets are significantly different (see Appendix D), the assumption can be roughly held for those label pairs in typical cases. In Section 5.1.1, our empirical results justify this by showing a little gap between the estimation error of our estimator with a biased sample selection and an unbiased one.

Based on the above discussions, we can approximate $\mathbb{P}(\bar{Y}^i, \bar{Y}^j)$ and $\mathbb{P}(\bar{Y}^i | Y^j)$ with *frequency counting*, and utilize the *mismatch* of label correlations implied in these occurrence probabilities to estimate the transition matrix. In this work, we propose to estimate transition matrices $\{T^j\}_{j=1}^q$ below.

First, we utilize sample selection to obtain useful information that implies clean label correlations. Specifically, we train a classifier with the standard multi-label classification loss on noisy training examples \mathcal{D}_t for a few epochs, and then perform sample selection to get a selected clean set D_s^j for each class label j . Specially, we use a commonly used sample selection way [35], [42] in learning with noisy labels, which extracts the subset of examples with small losses by modeling the distribution of losses for class j with a Gaussian mixture model (GMM).

Second, we perform co-occurrence estimation by frequency counting, and then estimate the transition matrix by solving a simple bilinear decomposition problem. For class label j , we first choose another class label i and estimate $\mathbb{P}(\bar{Y}^i, \bar{Y}^j)$ and $\mathbb{P}(\bar{Y}^i | Y^j)$ via frequency counting, i.e.,

$$\hat{\mathbb{P}}(\bar{Y}^i = v, \bar{Y}^j = k) = \frac{1}{n} \sum_{(x, \bar{y}) \in \mathcal{D}_t} \mathbb{I}[\bar{y}^i = v, \bar{y}^j = k], \quad (3)$$

$$\hat{\mathbb{P}}(\bar{Y}^i = v | Y^j = k) = \frac{\sum_{(x, \bar{y}) \in D_s^j} \mathbb{I}[\bar{y}^i = v, \bar{y}^j = k]}{\sum_{(x, \bar{y}) \in D_s^j} \mathbb{I}[\bar{y}^j = k]}, \quad (4)$$

where $\mathbb{I}[\cdot]$ is the indicator function which takes 1 if the identity index is true and 0 otherwise.

Then, these co-occurrence probabilities, which imply the mismatch of label correlations, can lead to four equations involving T^j :

$$\begin{aligned} \mathbb{P}(\bar{Y}^j = 0, \bar{Y}^i = 0) &= \mathbb{P}(Y^j = 0)T_{00}^j \mathbb{P}(\bar{Y}^i = 0|Y^j = 0) \\ &\quad + \mathbb{P}(Y^j = 1)T_{10}^j \mathbb{P}(\bar{Y}^i = 0|Y^j = 1), \\ \mathbb{P}(\bar{Y}^j = 0, \bar{Y}^i = 1) &= \mathbb{P}(Y^j = 0)T_{00}^j \mathbb{P}(\bar{Y}^i = 1|Y^j = 0) \\ &\quad + \mathbb{P}(Y^j = 1)T_{10}^j \mathbb{P}(\bar{Y}^i = 1|Y^j = 1), \\ \mathbb{P}(\bar{Y}^j = 1, \bar{Y}^i = 0) &= \mathbb{P}(Y^j = 0)T_{01}^j \mathbb{P}(\bar{Y}^i = 0|Y^j = 0) \\ &\quad + \mathbb{P}(Y^j = 1)T_{11}^j \mathbb{P}(\bar{Y}^i = 0|Y^j = 1), \\ \mathbb{P}(\bar{Y}^j = 1, \bar{Y}^i = 1) &= \mathbb{P}(Y^j = 0)T_{01}^j \mathbb{P}(\bar{Y}^i = 1|Y^j = 0) \\ &\quad + \mathbb{P}(Y^j = 1)T_{11}^j \mathbb{P}(\bar{Y}^i = 1|Y^j = 1). \end{aligned} \quad (5)$$

For simplicity, we denote

$$\begin{aligned} E &= \begin{pmatrix} \mathbb{P}(\bar{Y}^j = 0, \bar{Y}^i = 0) & \mathbb{P}(\bar{Y}^j = 0, \bar{Y}^i = 1) \\ \mathbb{P}(\bar{Y}^j = 1, \bar{Y}^i = 0) & \mathbb{P}(\bar{Y}^j = 1, \bar{Y}^i = 1) \end{pmatrix} = \begin{pmatrix} e_{00} & e_{01} \\ e_{10} & e_{11} \end{pmatrix}, \\ P &= \begin{pmatrix} \mathbb{P}(Y^j = 0) & 0 \\ 0 & \mathbb{P}(Y^j = 1) \end{pmatrix} = \begin{pmatrix} 1-p & 0 \\ 0 & p \end{pmatrix}, \\ T^j &= \begin{pmatrix} \mathbb{P}(\bar{Y}^j = 0 | Y^j = 0) & \mathbb{P}(\bar{Y}^j = 1 | Y^j = 0) \\ \mathbb{P}(\bar{Y}^j = 0 | Y^j = 1) & \mathbb{P}(\bar{Y}^j = 1 | Y^j = 1) \end{pmatrix} \\ &= \begin{pmatrix} 1-\rho_- & \rho_- \\ \rho_+ & 1-\rho_+ \end{pmatrix}, \quad \text{and} \\ M &= \begin{pmatrix} \mathbb{P}(\bar{Y}^i = 0 | Y^j = 0) & \mathbb{P}(\bar{Y}^i = 1 | Y^j = 0) \\ \mathbb{P}(\bar{Y}^i = 0 | Y^j = 1) & \mathbb{P}(\bar{Y}^i = 1 | Y^j = 1) \end{pmatrix} \\ &= \begin{pmatrix} 1-\rho'_- & \rho'_- \\ \rho'_+ & 1-\rho'_+ \end{pmatrix}. \end{aligned}$$

Then the system of equations can be expressed as

$$E = (T^j)^\top PM, \text{ i.e.,}$$

$$\begin{pmatrix} e_{00} & e_{01} \\ e_{10} & e_{11} \end{pmatrix} = \begin{pmatrix} 1-\rho_- & \rho_- \\ \rho_+ & 1-\rho_+ \end{pmatrix}^\top \begin{pmatrix} 1-p & 0 \\ 0 & p \end{pmatrix} \begin{pmatrix} 1-\rho'_- & \rho'_- \\ \rho'_+ & 1-\rho'_+ \end{pmatrix}. \quad (6)$$

Denote the estimation of E, P, T^j , and M as

$$\hat{E} = \begin{pmatrix} \hat{e}_{00} & \hat{e}_{01} \\ \hat{e}_{10} & \hat{e}_{11} \end{pmatrix}, \hat{P} = \begin{pmatrix} 1-\hat{p} & 0 \\ 0 & \hat{p} \end{pmatrix}, \hat{T}^j = \begin{pmatrix} 1-\hat{\rho}_- & \hat{\rho}_- \\ \hat{\rho}_+ & 1-\hat{\rho}_+ \end{pmatrix},$$

$$\text{and } \hat{M} = \begin{pmatrix} 1-\hat{\rho}'_- & \hat{\rho}'_- \\ \hat{\rho}'_+ & 1-\hat{\rho}'_+ \end{pmatrix}.$$

As \hat{E} and \hat{M} can be derived from Eq. (3) and Eq. (4), the problem is hence equivalent to a bilinear decomposition problem:

$$\hat{E}(\hat{M})^{-1} = (\hat{T}^j)^\top \hat{P}. \quad (7)$$

By solving the above matrix equation, we can get

$$\hat{p} = \frac{(1-\hat{\rho}'_-) - (\hat{e}_{00} + \hat{e}_{10})}{1-\hat{\rho}'_- - \hat{\rho}'_+}, \quad (8)$$

and the estimation of the transition matrix

$$\hat{T}^j = [\hat{E}(\hat{M})^{-1}(\hat{P})^{-1}]^\top. \quad (9)$$

Implementation of our estimator. The pseudo-code of our estimator is described in Algorithm 1. A little difference from the above is that in order to make better use of correlations among labels, we perform R times co-occurrence estimation and bilinear decomposition for different classes i in the second stage to get R estimations, $\hat{T}_r^j, r = 1, 2, \dots, R$. Finally, we estimate the transition matrix T^j by the below

Algorithm 1 Estimating Multi-Label Noise Transition Matrices with Label Correlations.

Require: Noisy training examples \mathcal{D}_t , the number of classes q , the early warmup training epoch E_{warm} , the threshold of sample selection τ , and repeated estimation times R .

Stage1: Standard Training and Sample Selection

- 1: Standard training with the standard multi-label loss for E_{warm} epochs.
 - 2: **for** $j = 1, 2, \dots, q$ **do**
 - 3: Model losses with a trained classifier on \mathcal{D}_t by a GMM.
 - 4: Get the selected set D_s^j for class label j with the threshold τ .
 - 5: **end for**
 - Stage2: Co-occurrence Estimation and Bilinear Decomposition**
 - 6: **for** $j = 1, 2, \dots, q$ **do**
 - 7: **for** $r = 1, 2, \dots, R$ **do**
 - 8: Choose another class label i .
 - 9: Estimate $\mathbb{P}(\bar{Y}^i, \bar{Y}^j)$ by $\hat{\mathbb{P}}(\bar{Y}^i, \bar{Y}^j)$ with Eq. (3) on \mathcal{D}_t , and $\mathbb{P}(\bar{Y}^i | Y^j)$ by $\hat{\mathbb{P}}(\bar{Y}^i | Y^j)$ with Eq. (4) on D_s^j .
 - 10: Solve a bilinear decomposition problem (Eq. (7)) to get an estimation \hat{T}_r^j by Eq. (9).
 - 11: **end for**
 - 12: Estimate T^j by \hat{T}^j which has the minimum error with Eq. (10) from R estimations.
 - 13: **end for**
- Ensure:** The estimated transition matrices $\{\hat{T}_r^j\}_{j=1}^q$.

aggregation rule from :

$$\hat{T}^j = \arg \min_{\hat{T}_r^j} \sum_{i=1}^R \|\hat{T}_r^j - \hat{T}_i^j\|_1, \quad (10)$$

where $\|\cdot\|_1$ denotes ℓ_1 norm.

4 THEORETICAL ANALYSES

In this section, we provide an estimation error bound for our multi-label transition matrix estimator (Section 4.1) and a generalization error bound for the statistically consistent algorithm with true transition matrices (Section 4.2), which theoretically justify the effectiveness of the proposed method.

4.1 Estimation Error Bound

In this subsection, we theoretically justify what factors will influence the effectiveness of our multi-label transition matrix estimator and how accurate it will be with a finite sample. As shown in Section 3.2, our estimator of T^j need to perform R times of estimations with different class i . Then, for the r -th estimation, let

$$\begin{aligned} \mathbb{P}(\bar{Y}^i = v, \bar{Y}^j = k) &= e_{kv}^r, \\ \mathbb{P}(\bar{Y}^j = 1 | Y^j = 0) &= \rho_-^r, \mathbb{P}(\bar{Y}^j = 0 | Y^j = 1) = \rho_+^r, \\ \mathbb{P}_{D_s^j}(\bar{Y}^i = 1 | Y^j = 0) &= \rho_-'^r, \mathbb{P}_{D_s^j}(\bar{Y}^i = 0 | Y^j = 1) = \rho_+'^r, \\ \mathbb{P}_{D_s^j}(\bar{Y}^i = 1 | Y^j = 0) - \mathbb{P}_{D_s^j}(\bar{Y}^i = 1 | Y^j = 0) &= \Delta_0^r, \\ \mathbb{P}_{D_s^j}(\bar{Y}^i = 0 | Y^j = 1) - \mathbb{P}_{D_s^j}(\bar{Y}^i = 0 | Y^j = 1) &= \Delta_1^r. \end{aligned} \quad (11)$$

Besides, let λ_k be the ratio of selected examples with $\bar{y}^j = k$ in training examples. We assume $\lambda_1 < \lambda_0$.

To derive an estimation error bound of \hat{T}^j , we first introduce the following two assumptions.

Assumption 3. $|\Delta_0^r| \leq \Delta, |\Delta_1^r| \leq \Delta, r \in \{1, \dots, R\}$.

Assumption 3 means that for convenience, we assume the influence of sampling bias is smaller than a certain constant Δ .

Assumption 4. $\|T^j - \hat{T}^j\|_1 \leq \|T^j - \bar{T}^j\|_1$, for $j \in \{1, \dots, q\}$, where $\hat{T}^j = \arg \min_{\hat{T}^j} \sum_{r=1}^R \|\hat{T}_i^j - \hat{T}_r^j\|_1$ and $\bar{T}^j = \arg \min_{\bar{T}^j} \sum_{r=1}^R \|\hat{T}^j - \bar{T}_r^j\|_1 = \sum_{r=1}^R \frac{1}{R} \hat{T}_r^j$.

Assumption 4 means that the error of the final estimation \hat{T}^j by Eq. (10) is smaller than that of the average of R estimations. Note that this assumption has been verified by the experiments in Section 6.1. With the above assumptions, we are ready to present our theoretical results.

Theorem 5. Let C be the maximum absolute value of the first derivative of $\hat{\rho}_+^x$ and $\hat{\rho}_-^x$ w.r.t. the estimated co-occurrence probabilities. Under Assumptions 3 and 4, with a size n of training examples, for any $\delta > 0$, with probability at least $1 - \delta$,

$$\|T^j - \hat{T}^j\|_1 \leq 8C\Delta + \min \left(4C\sqrt{\left(\frac{3}{4n} + \frac{1}{2\lambda_1 n}\right) \frac{2}{R\delta}}, \right. \\ \left. 4C\sqrt{\left(\frac{3}{4n} + \frac{1}{2\lambda_1 n}\right) \frac{2\log(4/\delta)}{R} + \frac{8\log(4/\delta)}{3R}} \right).$$

Further, if sample selection is unbiased ($\Delta \rightarrow 0$), then $\hat{T}^j \xrightarrow{p} T^j$ as $n \rightarrow \infty$.

A detailed proof is provided in Appendix K.

Remark 4. First, this bound theoretically shows that the effectiveness of our estimator is neither dependent on the existence of anchor points nor accurate fitting of noisy class posterior, which are major problems of existing estimators. Second, the derived estimation error bound shows that a sufficiently large number of training samples n can ensure that the estimation error is mainly due to the error from sampling bias Δ . When sample selection is unbiased ($\Delta \rightarrow 0$), the proposed estimator \hat{T}^j will converge to the true transition matrix T^j in probability as n increases, which we empirically verify in the ablation experiments (See Section 6.1). It guarantees the effectiveness of the proposed estimator in typical scenarios with large samples. Third, it reveals that obtaining a final transition matrix via multiple estimations can promote its accuracy as the times of estimations R increases. In addition, this bound tells us a limitation that when the number of one label appearing is too few, leading to very small λ_1 , the estimation of the transition matrix for this class label will be difficult to be accurate.

4.2 Generalization Error Bound

Here, we theoretically justify how the Reweight method [13] generalizes for learning classifiers in noisy multi-label cases given true transition matrices $\{T^j\}_{j=1}^q$.

Assume the neural network has d layers, parameter matrices W_1, \dots, W_d , and activation functions $\sigma_1, \dots, \sigma_{d-1}$

for each layer. Let denote the mapping of the neural network by $h : x \mapsto W_d \sigma_{d-1}(W_{d-1} \sigma_{d-2}(\dots \sigma_1(W_1 x))) \in \mathbb{R}^q$. The output of the sigmoid function is defined by $g_j(x) = 1/(1 + \exp(-h_j(x)))$, $j = 1, \dots, q$. Let $f_j(x) = \mathbb{I}[g_j(x) > 0.5]$, $j = 1, \dots, q$, be the classifier learned from the hypothesis space F determined by the real-valued parameters of the neural network, i.e., $\hat{f} = \arg \min_{f \in F} \bar{R}_{n,w}(f)$.

To derive a generalization bound, following [10], we assume that instances are upper bounded by B , i.e., $\|x\| \leq B$ for all $x \in \mathcal{X}$, and that the loss function $\mathcal{L}(f(x), \bar{y})$ is L -Lipschitz continuous w.r.t. $f(x)$ and upper bounded by M , i.e., for any $f, f' \in F$ and any (x, \bar{y}) , $|\mathcal{L}(f(x), \bar{y}) - \mathcal{L}(f'(x), \bar{y})| \leq L|f(x) - f'(x)|$, and for any (x, \bar{y}) , $\mathcal{L}(f(x), \bar{y}) \leq M$.

Theorem 6. Assume the Frobenius norm of the weight matrices W_1, \dots, W_d are at most M_1, \dots, M_d . Let the activation functions be 1-Lipschitz, positive-homogeneous, and applied element-wise (such as the ReLU). Let the loss function be the binary cross-entropy loss, i.e., $\mathcal{L}(f(x), \bar{y}) = \sum_{j=1}^q -\bar{y}^j \log(g_j(x)) - (1 - \bar{y}^j) \log(1 - g_j(x))$. Let \hat{f} be the learned classifier. Assume the true transition matrices $\{T^j\}_{j=1}^q$ is given. Let $U = \frac{1}{\min_j (1 - \max(\mathbb{P}(Y^j=0|Y^j=1), \mathbb{P}(Y^j=1|Y^j=0)))}$. Then, for any $\delta > 0$, with probability at least $1 - \delta$,

$$\mathbb{E}[\bar{R}_{n,w}(\{T^j\}_{j=1}^q, \hat{f})] - \bar{R}_{n,w}(\{T^j\}_{j=1}^q, \hat{f}) \\ \leq \frac{2BqL(\sqrt{2d\log 2} + 1)\prod_{i=1}^d M_i}{\sqrt{n}} + UM\sqrt{\frac{\log(1/\delta)}{2n}}.$$

A detailed proof is provided in Appendix L.

Remark 5. The factor $(\sqrt{2d\log 2} + 1)\prod_{i=1}^d M_i$ is induced by the hypothesis complexity of the deep neural network [43] (see Theorem 1 therein). This derived generalization error bound shows that the Reweight algorithm in multi-label cases can achieve a small difference between training error ($\bar{R}_{n,w}(\{T^j\}_{j=1}^q, \hat{f})$) and test error ($\mathbb{E}[\bar{R}_{n,w}(\{T^j\}_{j=1}^q, \hat{f})]$) with the rate of convergence $\mathcal{O}(\sqrt{1/n})$. Also, note that deep learning is powerful in yielding a small training error. Therefore, if the training sample size n is large, then the upper bound in Theorem 6 is small, which implies a small $\mathbb{E}[\bar{R}_{n,w}(\{T^j\}_{j=1}^q, \hat{f})]$ and justifies why such a method with true transition matrices will have small test errors in the experiment section. Meanwhile, in Section 5.1.2, we show that given true transition matrices $\{T^j\}_{j=1}^q$, the Reweight method in multi-label cases can overall outperform the state-of-the-art methods in classification performance, implying that the small generalization error is not obtained at the cost of enlarging the approximation error.

Overall, according to Theorem 5 and Theorem 6, it can be guaranteed that when sampling bias is small and given sufficiently large examples, the estimated multi-label transition matrices will be accurate, and then, with such accurate transition matrices, the classifier learned by the Reweight algorithm will achieve a good generalization performance.

5 EXPERIMENTS

5.1 Experiments on Class-Dependent Noisy Multi-Label Datasets

Dataset. We verify the effectiveness of the proposed method on three synthetic noisy multi-label datasets, i.e., Pascal-

TABLE 1: Comparison for estimating transition matrices on Pascal-VOC2007 dataset.

Noise rates (ρ_-, ρ_+)	(0,0.2)	(0,0.6)	(0.2,0)	(0.6,0)	(0.1,0.1)	(0.2,0.2)	(0.017,0.2)	(0.034,0.4)
T-estimator max	3.89±0.03	10.52±0.58	3.01±0.12	4.47±0.22	3.18±0.22	5.28±0.20	3.99±0.10	6.28±0.44
T-estimator 97%	4.95±0.17	4.42±0.18	1.77±0.03	2.13±0.12	6.99±0.10	6.94±0.17	5.38±0.14	5.17±0.09
Dual T-estimator max	1.94±0.13	7.29±0.16	1.03±0.04	2.68±0.13	2.13±0.23	4.02±0.18	1.71±0.08	2.67 ±0.27
Dual T-estimator 97%	12.59±0.06	7.43±0.06	1.09±0.03	2.41±0.33	14.39±0.10	11.78±0.06	13.71±0.16	11.15±0.09
Our estimator	1.63±0.16	1.54±0.30	0.36±0.08	1.17±0.37	2.94±0.24	3.10±0.28	2.09±0.06	1.85±0.13
Our estimator gold	0.44±0.05	0.51±0.09	0.38±0.08	0.37±0.11	0.83±0.05	2.15±0.30	0.65±0.10	1.40±0.20

TABLE 2: Comparison for estimating transition matrices on Pascal-VOC2012 dataset.

Noise rates (ρ_-, ρ_+)	(0,0.2)	(0,0.6)	(0.2,0)	(0.6,0)	(0.1,0.1)	(0.2,0.2)	(0.017,0.2)	(0.034,0.4)
T-estimator max	3.90±0.01	10.28±0.33	2.87±0.09	4.55±0.08	3.29±0.07	5.25±0.15	4.05±0.04	6.82±0.20
T-estimator 97%	5.42±0.09	3.98±0.09	1.53±0.06	1.91±0.07	6.43±0.16	6.20±0.17	5.76±0.27	5.16±0.14
Dual T-estimator max	1.02±0.20	5.13±0.26	1.07±0.07	2.06±0.12	1.94±0.05	2.59±0.16	1.17±0.13	1.93±0.08
Dual T-estimator 97%	12.94±0.06	7.49±0.03	1.14±0.04	2.94±0.18	14.23±0.08	11.56±0.05	13.97±0.09	11.10±0.08
Our estimator	0.83±0.10	1.94±0.15	0.26±0.03	0.91±0.12	1.74±0.22	1.79±0.17	0.94±0.07	1.07±0.14
Our estimator gold	0.33±0.05	0.34±0.05	0.25±0.05	0.45±0.05	0.51±0.05	1.67±0.29	0.42±0.06	0.91±0.16

TABLE 3: Comparison for estimating transition matrices on MS-COCO dataset.

Noise rates (ρ_-, ρ_+)	(0,0.2)	(0,0.6)	(0.2,0)	(0.6,0)	(0.1,0.1)	(0.2,0.2)	(0.008,0.2)	(0.015,0.4)
T-estimator max	16.14±0.33	39.09±0.47	10.39±0.21	11.49±0.60	13.95±0.41	20.50±0.04	16.70±0.06	28.16±0.45
T-estimator 97%	50.49±0.01	25.70±0.08	4.04±0.08	3.70±0.02	51.17±0.16	39.45±0.11	49.96±0.18	37.54±0.10
Dual T-estimator max	5.04±0.04	11.22±0.70	4.65±0.07	9.55±0.84	13.02±0.45	15.79±0.38	7.04±0.31	6.34±0.11
Dual T-estimator 97%	61.49±0.02	30.97±0.03	1.53±0.00	7.86±0.12	64.20±0.02	48.67±0.01	63.12±0.02	46.91±0.01
Our estimator	7.42±0.38	11.23±0.11	0.50±0.03	0.83±0.06	8.88±0.10	10.27±0.19	7.51±0.43	8.77±0.20
Our estimator gold	0.82±0.03	0.80±0.04	0.40±0.04	0.66±0.04	1.94±0.04	8.14±0.06	0.95±0.05	2.02±0.08

VOC2007 [44], Pascal-VOC2012 [45], and MS-COCO [46]. Pascal-VOC2007 [44] and Pascal-VOC2012 [45] datasets are two popular datasets for object recognition. They both contain images from the same 20 object classes, with an average of $n_a = 1.5$ labels per image. Pascal-VOC2007 contains a training set of 5,011 images and a test set of 4,952 images. Pascal-VOC2012 consists of 11,540 images as the training set and 10,991 images as the test set [47]. As the labels of the test set in Pascal-VOC2012 are not publicly available, we use the test set in Pascal-VOC2007 for Pascal-VOC2012 evaluation. MS-COCO [46] is a widely used multi-label dataset. It contains 82,081 images as the training set and 40,137 images as the test set and covers 80 object classes with an average of $n_a = 2.9$ labels per image. For these datasets, we corrupted the training sets manually according to true transition matrices $\{T^j\}_{j=1}^q$. For convenience, we use the same true transition matrices for all classes, *i.e.*, $T^j = T = \begin{pmatrix} 1 - \rho_- & \rho_- \\ \rho_+ & 1 - \rho_+ \end{pmatrix}$, but do not divulge this information for algorithms. We generate four different types of synthetic datasets by using different transition matrices: (1) $\rho_- = 0, \rho_+ = \rho$, which annotates some positive examples as negative examples, also known as multi-label learning with missing labels [48], [49] (termed MLML); (2) $\rho_- = \rho, \rho_+ = 0$, which annotates some negative examples as positive examples, also known as partial multi-label learning [50], [51] (termed PML); (3) $\rho_- = \rho, \rho_+ = \rho$, where positive examples and negative examples are mislabeled with the same probability ρ (termed uniform label flipping, ULF); (4) $\rho_- = \frac{n_a}{q-n_a}\rho, \rho_+ = \rho$, where positive examples and negative examples are mislabeled with the same number (termed asymmetric label flipping, ALF). In the experiments, we test the algorithms on various ρ (two cases for each noise type). For all datasets, we leave out 10% of the noisy training examples as a noisy validation set. We use mAP on noisy validation set as the criterion for model selection.

Implementation details. For a fair comparison, we implement all methods with default parameters by PyTorch on NVIDIA RTX 3090. We use a ResNet-50 network [52] pre-trained on ImageNet [53] for all datasets, and the optimizer is Adam optimizer [54] with $\beta = (0.9, 0.999)$. The batch size is 128, the learning rate is 5e-5. The number of training epochs is 20 for Pascal-VOC2007/VOC2012, and 30 for MS-COCO. For the transition matrix estimation method, E_{warm} is the same as the normal training epoch. For our estimator, we perform sample selection based on the average losses of 5 epochs before a certain warmup epoch (10th epoch for Pascal-VOC2007/VOC2012, 15th epoch for MS-COCO), $R = q - 1$ and $\tau = 0.5$ in all experiments. All experiments are run at least three times with different random seeds, and the average and standard deviation values of results are reported. The best results are in **bold**, and the second-best results are in **blue**.

5.1.1 Comparison for estimating transition matrices

Baselines. For evaluating the effectiveness of estimating the transition matrix under multi-label cases, we compare the proposed method with the following methods: (1) T-estimator max [13], [14], which estimates the transition matrix via the noisy class posterior probabilities for anchor points that have the largest estimated noisy class posteriors. (2) T-estimator 97% [13], [14], which selects the points with 97% largest estimated noisy class posteriors to be anchor points. (3) Dual T-estimator max [16], which introduces an intermediate class to avoid directly estimating the noisy class posterior, and selects the points with the largest estimated intermediate class posteriors to be the anchor points. (4) Dual T-estimator 97% [16], which selects the points with the 97% largest estimated intermediate class posteriors to be the anchor points.

Metrics. We use the sum of estimation error for the transition matrices as the estimation evaluation metric, *i.e.*, $\sum_{j=1}^q \|T^j - \hat{T}^j\|_1$.

TABLE 4: Comparison for classification performance on Pascal-VOC2007 dataset with class-dependent label noise.

	Noise type	MLML	PML	ULF	ALF	Avg.
mAP	Standard	80.71	75.68	80.97	82.45	79.95
	GCE	78.59	75.25	81.54	82.54	79.48
	CDR	81.03	75.81	81.12	82.76	80.18
	AGCN	79.37	73.78	77.44	79.38	77.49
	CSRA	82.29	75.15	80.90	83.23	80.39
	WSIC	80.16	74.56	80.67	82.46	79.46
	Reweight-T max	80.59	77.20	81.29	82.54	80.41
	Reweight-T 97%	81.49	78.52	80.76	82.90	80.92
	Reweight-DualT max	81.06	78.75	81.71	83.19	81.18
	Reweight-DualT 97%	80.04	80.16	77.48	79.62	79.33
	Reweight-Ours	81.58	79.27	82.24	82.53	81.41
	Reweight-TrueT	81.04	79.94	82.26	82.96	81.55
	OF1	Standard	53.63	46.97	77.55	67.83
GCE		56.15	47.07	78.00	68.53	62.44
CDR		55.08	47.02	77.67	67.94	61.93
AGCN		52.95	46.15	75.67	65.86	60.16
CSRA		55.30	46.83	78.64	70.05	62.71
WSIC		45.75	46.95	75.72	62.78	57.80
Reweight-T max		59.26	63.67	76.79	71.86	67.90
Reweight-T 97%		73.00	75.42	70.16	76.28	73.72
Reweight-DualT max		73.60	72.72	72.62	62.80	70.44
Reweight-DualT 97%		64.99	76.64	44.87	62.48	62.25
Reweight-Ours		72.15	74.14	77.58	76.80	75.17
Reweight-TrueT		72.44	77.22	77.76	77.35	76.19
CF1		Standard	51.59	45.90	73.27	62.59
	GCE	53.09	46.01	73.99	65.13	59.56
	CDR	53.07	45.92	73.44	63.75	59.05
	AGCN	53.43	44.66	72.65	63.95	58.67
	CSRA	53.77	45.50	75.48	66.79	60.39
	WSIC	41.89	45.05	69.56	54.42	52.73
	Reweight-T max	56.71	63.82	75.26	68.54	66.08
	Reweight-T 97%	74.03	72.44	71.53	76.09	73.52
	Reweight-DualT max	60.29	70.28	73.38	71.99	68.99
	Reweight-DualT 97%	67.89	73.20	56.67	65.79	65.89
	Reweight-Ours	69.08	72.34	76.06	74.73	73.05
	Reweight-TrueT	69.57	73.22	73.25	73.97	72.50

Results. In Tab. 1, 2 and 3, we can see that for all cases on three datasets, the proposed estimation method leads to the smallest or second-smallest estimator errors across various noise rates. Note that since the fitting of the noisy or intermediate class posterior is hard to be accurate in noisy multi-label learning, the T-estimator and Dual T-estimator need to carefully tune a hyperparameter for better estimation under different noise rates, and it’s very sensitive in some cases, *e.g.*, MS-COCO datasets with noise rates (0.1, 0.1). In contrast, our method uses the same hyperparameters on one dataset to get good results for all cases, which reflects its robustness to various noise rates. Besides, to study the ablation of sampling bias, we also run our method with an unbiased sample selection, named “our estimator gold”. We can see that sample bias is the main factor that contributes to the error for our estimator, but the little error gap between our estimator and our estimator gold shows it will not lead to large estimation errors.

5.1.2 Comparison for classification performance

Baselines. We exploit 10 baselines: (1) Standard, which trains with a standard multi-label classification loss. (2) GCE [55], which proposes a Generalized Cross-Entropy loss for robustness. (3) CDR [56], which performs different update rules for two types of parameters to achieve robust learning. (4) AGCN [57], which adopts a dynamic GCN to model the relation of content-aware class representations. (5) CSRA [58], which generates class-specific features for every category by proposing a spatial attention score. (6) WSIC [59] proposes to use a small set with clean labels

TABLE 5: Comparison for classification performance on Pascal-VOC2012 dataset with class-dependent label noise.

	Noise type	MLML	PML	ULF	ALF	Avg.
mAP	Standard	83.00	80.92	84.23	84.47	82.72
	GCE	82.37	80.49	84.74	84.40	82.53
	CDR	83.31	81.07	84.40	84.70	82.93
	AGCN	82.42	81.23	82.42	83.30	82.02
	CSRA	84.32	80.24	83.56	85.19	82.71
	WSIC	83.57	81.27	83.84	84.63	82.89
	Reweight-T max	82.23	82.20	84.43	83.95	82.95
	Reweight-T 97%	83.51	82.97	84.24	84.64	83.57
	Reweight-DualT max	82.31	83.24	85.22	84.79	83.59
	Reweight-DualT 97%	81.95	84.11	80.50	82.14	82.19
	Reweight-Ours	83.17	83.33	84.83	84.74	83.78
	Reweight-TrueT	84.26	83.95	85.04	85.12	84.42
	OF1	Standard	52.88	47.70	79.89	69.75
GCE		51.46	47.81	80.13	70.79	59.80
CDR		53.74	47.78	79.96	69.88	60.49
AGCN		53.59	47.96	78.15	68.71	59.90
CSRA		55.49	47.80	79.97	70.41	61.09
WSIC		53.23	47.83	79.17	68.04	60.08
Reweight-T max		60.86	65.06	80.08	73.35	68.67
Reweight-T 97%		75.55	78.33	74.55	76.55	76.14
Reweight-DualT max		72.06	78.09	79.88	78.02	76.68
Reweight-DualT 97%		59.62	79.08	43.35	61.43	60.68
Reweight-Ours		74.81	78.58	79.45	79.03	77.61
Reweight-TrueT		77.72	79.88	80.15	79.51	79.25
CF1		Standard	52.46	46.97	77.33	68.20
	GCE	50.75	47.19	77.49	69.02	58.48
	CDR	53.41	47.03	77.35	68.07	59.26
	AGCN	53.75	47.12	75.69	66.24	58.85
	CSRA	54.37	47.17	77.70	67.97	59.75
	WSIC	53.33	47.24	76.30	65.58	58.96
	Reweight-T max	57.60	64.70	78.03	71.18	66.78
	Reweight-T 97%	76.30	76.56	74.97	77.16	75.94
	Reweight-DualT max	68.67	76.34	77.83	72.19	74.28
	Reweight-DualT 97%	64.93	75.99	58.69	66.18	66.54
	Reweight-Ours	72.79	76.33	77.90	77.27	75.67
	Reweight-TrueT	75.39	76.91	77.76	77.56	76.69

to learn a residual net for regularization in noisy multi-label learning, and we only provide noisy datasets to it for a fair comparison. (7) Reweight-T max, which learns with a reweighting algorithm using transition matrices estimated by T-estimator max [14]. (8) Reweight-T 97%, which learns with a reweighting algorithm using transition matrices estimated by T-estimator 97% [14]. (9) Reweight-DualT max, which learns with a reweighting algorithm using transition matrices estimated by Dual T-estimator max [16]. (10) Reweight-DualT 97%, which learns with a reweighting algorithm using transition matrices estimated by Dual T-estimator 97% [16]. Note that Standard, AGCN, and CSRA are designed for clean multi-label data, and GCE and CDR are designed for noisy multi-class learning.

Metrics. Following conventional setting [1], [18], [44], [60], we compute the mean average precision (mAP), overall F1-measure (OF1) and per-class F1-measure (CF1) as classification evaluation metrics. For each image, we assign a positive label if its prediction probability is greater than 0.5.

Results. As shown in Tab. 4, 5 and 6, we report the results of four noise types (MLML, PML, ULF, and ALF) and the overall average results on three multi-label datasets, where some observations are concluded. ¹ First, we can find those statistically consistent methods achieve the best or second-best results on all three metrics in the vast majority of cases, while other methods can only achieve good results in some cases. For example, on the Pascal-VOC2012 dataset

¹ Note that to present the results more concise here, we only report the average number of two cases for each noise type. The complete numerical results can be found in Appendix O

TABLE 6: Comparison for classification performance on MS-COCO dataset with class-dependent label noise.

	Noise type	MLML	PML	ULF	ALF	Avg.
mAP	Standard	66.87	61.11	65.14	68.29	64.37
	GCE	66.24	60.67	65.92	68.36	64.28
	CDR	66.96	61.26	65.33	68.36	64.52
	AGCN	68.62	62.58	66.69	69.38	65.96
	CSRA	68.23	59.71	65.32	69.39	64.42
	WSIC	66.01	59.92	64.87	67.62	63.60
	Reweight-T max	66.97	62.84	65.57	68.00	65.13
	Reweight-T 97%	65.25	63.72	62.86	66.27	63.94
	Reweight-DualT max	63.98	63.50	65.09	67.26	64.19
	Reweight-DualT 97%	61.91	59.43	52.89	60.74	58.08
	Reweight-Ours	66.93	65.63	66.58	68.55	66.38
	Reweight-TrueT	68.14	65.93	67.38	69.25	67.15
OF1	Standard	42.83	38.32	66.74	58.89	49.30
	GCE	43.14	38.43	67.21	59.31	49.59
	CDR	43.03	38.39	66.72	59.26	49.38
	AGCN	41.58	38.84	67.87	59.50	49.43
	CSRA	46.03	38.60	67.30	59.59	50.64
	WSIC	44.85	38.02	65.05	59.23	49.31
	Reweight-T max	53.30	64.55	60.86	60.04	59.57
	Reweight-T 97%	55.86	67.26	38.73	53.61	53.95
	Reweight-DualT max	60.12	63.53	54.71	63.69	59.45
	Reweight-DualT 97%	29.35	59.56	17.17	37.54	35.36
	Reweight-Ours	65.92	68.15	61.53	67.67	65.20
	Reweight-TrueT	68.29	68.46	68.77	69.38	68.51
CF1	Standard	41.50	35.87	59.58	52.70	45.65
	GCE	40.91	36.16	60.16	52.47	45.74
	CDR	41.34	36.17	59.52	52.63	45.68
	AGCN	40.55	36.67	61.53	52.12	46.25
	CSRA	43.32	36.43	59.94	52.78	46.56
	WSIC	44.14	35.37	56.8	53.02	45.44
	Reweight-T max	47.19	60.75	61.64	54.66	56.53
	Reweight-T 97%	54.23	60.34	44.34	53.76	52.97
	Reweight-DualT max	58.48	59.07	63.81	63.03	60.45
	Reweight-DualT 97%	31.24	49.50	21.38	39.19	34.04
	Reweight-Ours	62.32	62.03	63.89	64.68	62.75
	Reweight-TrueT	62.71	62.11	62.68	64.06	62.50

TABLE 7: Comparison for classification performance on multi-label datasets with instance-dependent label noise.

	Dataset	Pascal-VOC2007	Pascal-VOC2012	MS-COCO
mAP	Standard	81.86	83.49	65.72
	GCE	81.80	83.75	66.02
	CDR	81.81	83.63	65.79
	AGCN	79.54	82.04	66.89
	CSRA	82.59	83.81	66.45
	WSIC	81.47	83.81	65.13
	Reweight-T max	81.32	83.08	65.77
	Reweight-T 97%	81.00	83.32	63.30
	Reweight-DualT max	81.58	83.67	63.63
	Reweight-DualT 97%	79.04	79.87	58.38
	Reweight-Ours	81.45	83.73	66.25
	OF1	Standard	74.11	75.64
GCE		73.96	75.47	62.15
CDR		74.26	75.49	62.21
AGCN		72.56	74.46	61.68
CSRA		75.32	75.78	62.21
WSIC		71.88	74.25	62.92
Reweight-T max		75.21	76.90	63.94
Reweight-T 97%		75.94	76.25	53.39
Reweight-DualT max		76.56	78.48	62.40
Reweight-DualT 97%		64.17	61.35	33.75
Reweight-Ours		77.11	78.22	66.61
CF1		Standard	69.62	72.63
	GCE	69.81	72.41	55.67
	CDR	69.90	72.67	55.67
	AGCN	69.26	71.64	56.05
	CSRA	72.35	73.45	56.20
	WSIC	65.45	71.35	57.22
	Reweight-T max	71.92	74.19	57.17
	Reweight-T 97%	74.27	75.70	51.82
	Reweight-DualT max	73.33	74.14	61.32
	Reweight-DualT 97%	67.49	66.41	37.33
	Reweight-Ours	75.00	76.97	63.49

with MLML label noise, CSRA achieves the best result in the mAP metric with the help of its well-designed network, but its performance is far lower than those consistent methods on the OF1 and CF1 metrics, which shows the learned model can not approximate well the true class posterior $\mathbb{P}(Y|X)$. Note that since network structure and

loss correction are compatible, the risk-consistent methods can also help AGCN and CSRA perform better (shown in Section 6.2). Second, to show the performance of the consistent algorithm with true transition matrices, we also evaluate the performance of the Reweight method with true transition matrix (named "Reweight-TrueT"). Its excellent performance not only verifies the small generalization error with a sufficiently large number of training samples as analyzed in Section 4.2, but also implies that it is not obtained at the cost of enlarging the approximation error. Third, among those consistent methods with the estimated transition matrices, Reweight algorithm with our estimator (named "Reweight-Ours") obtains the best or second-best results on the three metrics, which is due to the smaller error of our estimation. Especially on the challenging and large-scale MS-COCO dataset, Reweight-Ours outperforms all state-of-the-art methods on the CF1 metric.

5.2 Experiments on Instance-Dependent Noisy Multi-Label Datasets

Datasets. To illustrate the applicability in realistic scenarios, we perform the experiments with two types of instance-dependent label noise on Pascal-VOC2007, Pascal-VOC2012 and MS-COCO datasets: (1) Pair-wise label noise [34], where one class label is mistaken as another class label with a certain probability; (2) PMD label noise [61], where data points near the decision boundary are harder to distinguish and more likely to be mislabeled. Both of them are dependent on class labels and instances, which are much more realistic than class-dependent label noise. In the experiments, we test the algorithms on cases for each noise type. Same to Section 5.1, for all datasets, we also leave out 10% of the noisy training examples as a noisy validation set, and use mAP on noisy validation set as the criterion for model selection. Note that as class labels in those multi-label datasets are unbalanced, we only mislabel one class into another class when the class change does not occur.

Implementation details. We use the same baselines and implementation way as the experiments in Section 5.1.

Results. The comparison for classification performance with instance-dependent label noise can be seen in Tab. 7, where we report the overall average classification performance in three noisy multi-label datasets. The results show the proposed method with our estimator (Reweight-Ours) can achieve the best or second-best performance among the state-of-the-art methods in the OF1 and CF1 metrics. Especially, on the MS-COCO dataset, it outperforms all baselines by a large margin (at least +2.67%) in the OF1 metric. Besides, in terms of the mAP metric, Reweight-Ours consistently outperforms the Reweight algorithm with other estimators across three datasets, showing the superiority of our multi-label transition matrix estimator.

6 ABLATION STUDY

6.1 Ablation Study about Our Multi-Label Transition Matrix Estimation

Influence of repeated multiple estimations. To exploit the correlations among multiple labels, our estimator performs

TABLE 8: Ablation study of the influence of repeated multiple estimations on Pascal-VOC2007 dataset with class-dependent label noise. The best results are in **bold**.

Noise rates (ρ_-, ρ_+)	(0,0.2)	(0,0.6)	(0.2,0)	(0.6,0)	(0.1,0.1)	(0.2,0.2)	(0.017,0.2)	(0.034,0.4)
Our estimator ($R = 1$)	2.05±0.33	2.04±0.44	0.76±0.10	3.06±0.74	4.20±0.40	4.65±0.56	2.91±0.26	3.49±0.33
Our estimator (Avg.)	1.81±0.16	1.31±0.26	0.52±0.02	3.16±0.42	3.51±0.24	2.84±0.27	2.21±0.13	1.39±0.18
Our estimator	1.63±0.16	1.54±0.30	0.36±0.08	1.17±0.37	2.94±0.24	3.10±0.28	2.09±0.06	1.85±0.13

TABLE 9: Comparison for estimation error with different numbers of training samples on Pascal-VOC dataset with class-dependent label noise.

Noise rates (ρ_-, ρ_+)	(0,0.2)	(0,0.6)	(0.2,0)	(0.6,0)	(0.1,0.1)	(0.2,0.2)	(0.017,0.2)	(0.034,0.4)
$n = 1000$	0.22±0.22	0.31±0.37	0.65±0.09	0.58±0.10	1.45±0.23	3.07±0.36	1.12±0.20	2.96±0.33
$n = 5000$	0.13±0.12	0.21±0.07	0.38±0.14	0.49±0.16	0.76±0.10	2.32±0.12	0.48±0.14	1.35±0.21
$n = 10000$	0.16±0.09	0.18±0.10	0.25±0.02	0.47±0.10	0.64±0.04	1.96±0.21	0.40±0.09	0.94±0.09
$n = 20000$	0.07±0.02	0.10±0.06	0.19±0.01	0.38±0.09	0.36±0.07	1.30±0.09	0.23±0.02	0.58±0.03

TABLE 10: Comparison for estimation error of T^{49} using different levels of label correlations on the MS-COCO dataset. The best results are in **bold**.

Noise rates (ρ_-, ρ_+)	(0,0.2)	(0,0.6)	(0.2,0)	(0.6,0)	(0.1,0.1)	(0.2,0.2)	(0.017,0.2)	(0.034,0.4)
Using the correlations with label A	0.02±0.02	0.02±0.02	0.09±0.04	0.07±0.06	0.10±0.05	0.10±0.08	0.09±0.04	0.08±0.03
Using the correlations with label B	0.05±0.06	0.05±0.07	0.13±0.11	0.15±0.14	0.19±0.12	0.18±0.11	0.17±0.10	0.17±0.11

TABLE 11: Comparison for classification performance with different loss correction ways on Pascal-VOC2007 dataset with class-dependent label noise.

	Noise type	MLML	PML	ULF	ALF	Avg.
mAP	Reweight-Ours	81.58	79.27	82.24	82.53	81.41
	Backward-Ours	75.32	72.48	74.72	75.25	74.44
	Forward-Ours	82.60	77.43	79.98	82.39	80.60
	Revision-Ours	82.13	79.41	82.55	83.56	81.91
OFI	Reweight-Ours	72.15	74.14	77.58	76.80	75.17
	Backward-Ours	45.67	46.56	68.98	54.03	53.81
	Forward-Ours	75.24	69.90	76.85	77.55	74.89
	Revision-Ours	71.52	74.97	77.95	77.53	75.49
CFI	Reweight-Ours	69.08	72.34	76.06	74.73	73.05
	Backward-Ours	42.83	45.02	56.23	44.67	47.19
	Forward-Ours	71.25	69.70	74.09	74.75	72.45
	Revision-Ours	67.69	72.58	76.25	74.99	72.88

TABLE 12: Comparison for classification performance with different base multi-label learning algorithms on Pascal-VOC2007 dataset with class-dependent label noise.

	Noise type	MLML	PML	ULF	ALF	Avg.
mAP	Standard	80.71	75.68	80.97	82.45	79.95
	+R-Ours	81.58(+0.87)	79.27(+3.59)	82.24(+1.27)	82.53(+0.08)	81.41(+1.46)
	AGCN	79.37	73.78	77.44	79.38	77.49
	+R-Ours	82.71(+3.34)	74.74(+0.96)	80.99(+3.55)	82.57(+3.19)	80.25(+2.76)
	CSRA	82.29	75.15	80.9	83.23	80.39
OFI	+R-Ours	81.74(+0.55)	80.04(+4.89)	82.85(+1.95)	84.19(+0.96)	82.21(+1.82)
	Standard	53.63	46.97	77.55	67.83	61.5
	+R-Ours	72.15(+18.52)	74.14(+27.17)	77.58(+0.03)	76.80(+8.97)	75.17(+13.67)
	AGCN	52.95	46.15	75.67	65.86	60.16
	+R-Ours	75.82(+22.87)	62.98(+16.83)	76.10(+0.43)	77.64(+11.78)	73.14(+12.98)
CFI	CSRA	55.30	46.83	78.64	70.05	62.71
	+R-Ours	71.05(+15.75)	69.35(+22.52)	78.24(+0.40)	79.22(+9.17)	74.47(+11.76)
	Standard	51.59	45.9	73.27	62.59	58.34
	+R-Ours	69.08(+17.49)	72.34(+26.44)	76.06(+2.79)	74.73(+12.14)	73.05(+14.71)
	AGCN	53.43	44.66	72.65	63.95	58.67
CFI	+R-Ours	73.66(+20.23)	64.54(+19.88)	74.93(+2.28)	76.21(+12.26)	72.34(+13.67)
	CSRA	53.77	45.5	75.48	66.79	60.39
	+R-Ours	68.97(+15.2)	70.46(+24.96)	77.13(+1.65)	76.95(+10.16)	73.38(+12.99)

R estimations and obtains the final estimation by Eq. (10). To study the ablation of repeated estimations, we test its estimation error when performing one estimation, *i.e.*, our estimator ($R = 1$) and our estimator (Avg.). As shown in Tab. 8, our estimator can consistently get a significantly better estimation than our estimator ($R = 1$) across various cases, revealing the improvement brought by repeated estimations. Further, we evaluate the estimation error with the

average aggregation rule. The results in most cases verified the assumption that the error of the obtained estimation by Eq. (10) is smaller than that of the average estimation from multiple estimations.

Influence of the number of training examples. To study the ablation of the number of training samples for our estimator, we consider testing its estimation errors with different training samples. Note that to eliminate the influence of sampling bias here, we actually test the estimation errors of "our estimator gold" where the sample selection is unbiased. As shown in Tab. 9, the estimated multi-label transition matrices will become more accurate as the number of training examples n increases, which verifies our theoretical analyses in Section 4.1.

Influence of label correlations According to the results in Appendix C, we divide all labels on the MS-COCO dataset into two categories: one is very likely to have a correlation with class label 50 (the label belonging to this category is termed "label A") and the other is less likely to has a correlation with class label 50 (the label belonging to this category is termed as "label B"). Tab. 10 shows the estimation error of the transition matrix for class label 50 using the correlations with label A (or B) in various cases. The results represent using the correlations with label A, the estimation error of T^{49} will be smaller, showing stronger label correlations can lead to better estimation in our approach.

6.2 Ablation Study about Our Multi-Label Classifier Learning

Influence of loss correction ways. Many statistically consistent algorithms [10], [13], [14] consist of a two-step training procedure. The first step estimates the transition matrix, and the second step builds statistically consistent algorithms via modifying loss functions. Our proposed estimator can be seamlessly embedded into their frameworks. Here, we compare classification performance of applying our estimation method to four different loss correction ways: Reweight [13] (named Reweight-Ours), Backward [9] (named Backward-Ours), Forward [14] (named Forward-

Ours) and T-Revision [10] (named Revision-Ours) on Pascal-VOC2007 dataset. As shown in Tab. 11, T-Revision with our estimator achieves the best performance in most cases, which may be because it can further tune the transition matrices via classification learning.

Influence of base multi-label learning algorithms. Recently, many advanced multi-label learning algorithms [47], [57], [58], which designed exquisite networks for multi-label learning, have been proposed, and they perform well on the clean dataset. As they also use binary cross entropy loss function, we can also apply the Reweight method with our estimator to their frameworks. Here, we compare the classification performance of applying the Reweight method with our estimator to three different base learning algorithms: Standard, AGCN [57] and CSRA [58] on Pascal-VOC2007 dataset. Besides, to show the importance of consistent algorithms, we also present the performance of base learning algorithms here. As shown in Tab. 12, the consistent algorithms with our estimator can work well with more advanced networks.

6.3 Ablation Study about the Hyperparameter τ

The sample selection we adopted [35], [62] is to estimate this clean probability of examples by modeling loss values with a GMM model using the Expectation-Maximization algorithm. If the clean sample can be distinguished according to loss values and its estimated probability is accurate, the best threshold will be about 0.5. Hence, $\tau = 0.5$ is a typical value in related works [35], [62], and we follow this practice in our experiments. Here, we conduct the ablation study about the sample selection threshold on Pascal-VOC2007 dataset with class-dependent label noise. As shown in Fig. 2, $\tau = 0.5$ is a good choice both according to mAP scores on the noisy validation set and according to mAP scores on the clean test dataset.

7 CONCLUSION

In this paper, we study the estimation problem of the transition matrices in the noisy multi-label setting. We prove some identifiability results of class-dependent transition matrices in such a setting, inspired by which we propose a new estimator to estimate the transition matrix. The proposed estimator utilizes the information of label correlations, and demands neither anchor points nor accurate fitting of noisy class posterior. The estimation error bound and generalization error bound theoretically justify the effectiveness of the proposed method. Experiments on popular multi-label datasets illustrate the superiority of the proposed estimator to accurately estimate transition matrices, and the consistent algorithms with this estimator achieve better classification performance.

REFERENCES

[1] Z. Chen, X. Wei, P. Wang, and Y. Guo, "Multi-label image recognition with graph convolutional networks," in *IEEE/CVF Computer Vision and Pattern Recognition Conference*, 2019, pp. 5177–5186.
 [2] W. Liu, X. Shen, H. Wang, and I. W. Tsang, "The emerging trends of multi-label learning," *IEEE Transactions on Pattern Analysis and Machine Intelligence*, 2021.

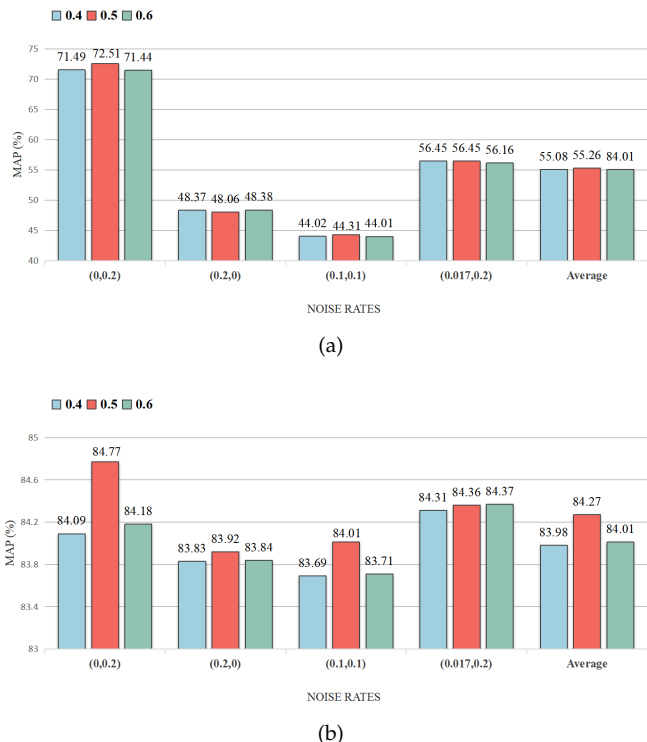


Fig. 2: (a) mAP scores on the noisy validation set of the Reweight method with our estimator with $\tau = 0.4, 0.5, 0.6$; (b) mAP scores on the clean test dataset of the Reweight method with our estimator with $\tau = 0.4, 0.5, 0.6$.

[3] C. O. Pene, A. Ghiassi, T. Younesian, R. Birke, and L. Y. Chen, "Multi-label gold asymmetric loss correction with single-label regulators," *arXiv*, vol. abs/2108.02032, 2021.
 [4] M. Xie and S. Huang, "CCMN: A general framework for learning with class-conditional multi-label noise," *IEEE Transactions on Pattern Analysis and Machine Intelligence*, 2022.
 [5] X. Xia, T. Liu, B. Han, M. Gong, J. Yu, G. Niu, and M. Sugiyama, "Sample selection with uncertainty of losses for learning with noisy labels," in *International Conference on Learning Representations*, 2022.
 [6] S. Wu, X. Xia, T. Liu, B. Han, M. Gong, N. Wang, H. Liu, and G. Niu, "Class2simi: A noise reduction perspective on learning with noisy labels," in *International Conference on Machine Learning*, 2021, pp. 11 285–11 295.
 [7] Z. Wu, X. Xia, R. Wang, J. Li, J. Yu, Y. Mao, and T. Liu, "Lr-svm+: Learning using privileged information with noisy labels," *IEEE Transactions on Multimedia*, 2021.
 [8] H. Song, M. Kim, D. Park, and J.-G. Lee, "Learning from noisy labels with deep neural networks: A survey," *IEEE Transactions on Neural Networks and Learning Systems*, 2022.
 [9] N. Natarajan, I. S. Dhillon, P. K. Ravikumar, and A. Tewari, "Learning with noisy labels," in *Conference on Neural Information Processing Systems*, vol. 26, 2013.
 [10] X. Xia, T. Liu, N. Wang, B. Han, C. Gong, G. Niu, and M. Sugiyama, "Are anchor points really indispensable in label-noise learning?" in *Conference on Neural Information Processing Systems*, 2019, pp. 6835–6846.
 [11] X. Xia, B. Han, N. Wang, J. Deng, J. Li, Y. Mao, and T. Liu, "Extended T: Learning with mixed closed-set and open-set noisy labels," *IEEE Transactions on Pattern Analysis and Machine Intelligence*, 2022.
 [12] D. Cheng, Y. Ning, N. Wang, X. Gao, H. Yang, Y. Du, B. Han, and T. Liu, "Class-dependent label-noise learning with cycle-consistency regularization," in *Conference on Neural Information Processing Systems*, 2022.
 [13] T. Liu and D. Tao, "Classification with noisy labels by importance reweighting," *IEEE Transactions on Pattern Analysis and Machine Intelligence*, vol. 38, no. 3, pp. 447–461, 3 2016.

- [14] G. Patrini, A. Rozza, A. K. Menon, R. Nock, and L. Qu, "Making deep neural networks robust to label noise: A loss correction approach," in *IEEE/CVF Computer Vision and Pattern Recognition Conference*, 2017, pp. 2233–2241.
- [15] J. Shu, Q. Zhao, Z. Xu, and D. Meng, "Meta transition adaptation for robust deep learning with noisy labels," *arXiv preprint arXiv:2006.05697*, 2020.
- [16] Y. Yao, T. Liu, B. Han, M. Gong, J. Deng, G. Niu, and M. Sugiyama, "Dual T: reducing estimation error for transition matrix in label-noise learning," in *Conference on Neural Information Processing Systems*, 2020.
- [17] X. Li, T. Liu, B. Han, G. Niu, and M. Sugiyama, "Provably end-to-end label-noise learning without anchor points," in *International Conference on Machine Learning*, 2021, pp. 6403–6413.
- [18] T. Ridnik, E. B. Baruch, N. Zamir, A. Noy, I. Friedman, M. Protter, and L. Zelnik-Manor, "Asymmetric loss for multi-label classification," in *International Conference on Computer Vision*, 2021, pp. 82–91.
- [19] X. Xia, J. Deng, W. Bao, Y. Du, B. Han, S. Shan, and T. Liu, "Holistic label correction for noisy multi-label classification," in *ICCV*, 2023.
- [20] S. Li, X. Xia, H. Zhang, Y. Zhan, S. Ge, and T. Liu, "Estimating noise transition matrix with label correlations for noisy multi-label learning," in *Conference on Neural Information Processing Systems*, 2022, pp. 24184–24198.
- [21] X. Xia, T. Liu, B. Han, N. Wang, M. Gong, H. Liu, G. Niu, D. Tao, and M. Sugiyama, "Part-dependent label noise: Towards instance-dependent label noise," in *Conference on Neural Information Processing Systems*, 2020.
- [22] Y. Yao, T. Liu, M. Gong, B. Han, G. Niu, and K. Zhang, "Instance-dependent label-noise learning under a structural causal model," in *Conference on Neural Information Processing Systems*, 2021.
- [23] H. Cheng, Z. Zhu, X. Li, Y. Gong, X. Sun, and Y. Liu, "Learning with instance-dependent label noise: A sample sieve approach," in *International Conference on Learning Representations*, 2021.
- [24] Z. Zhu, T. Liu, and Y. Liu, "A second-order approach to learning with instance-dependent label noise," in *IEEE/CVF Computer Vision and Pattern Recognition Conference*, 2021, pp. 10113–10123.
- [25] X. Xia, T. Liu, B. Han, N. Wang, M. Gong, H. Liu, G. Niu, D. Tao, and M. Sugiyama, "Part-dependent label noise: Towards instance-dependent label noise," in *Conference on Neural Information Processing Systems*, 2020.
- [26] Z. Zhu, Y. Song, and Y. Liu, "Clusterability as an alternative to anchor points when learning with noisy labels," in *International Conference on Machine Learning*, M. Meila and T. Zhang, Eds., 2021, pp. 12912–12923.
- [27] Y. Liu, H. Cheng, and K. Zhang, "Identifiability of label noise transition matrix," *CoRR*, vol. abs/2202.02016, 2022.
- [28] E. S. Allman, C. Matias, and J. A. Rhodes, "Identifiability of parameters in latent structure models with many observed variables," *Annals of Statistics*, vol. 37, pp. 3099–3132, 2009.
- [29] A. K. Menon, B. van Rooyen, C. S. Ong, and B. Williamson, "Learning from corrupted binary labels via class-probability estimation," in *International Conference on Machine Learning*, vol. 37, 2015, pp. 125–134.
- [30] J. B. Kruskal, "Three-way arrays: rank and uniqueness of trilinear decompositions, with application to arithmetic complexity and statistics," *Linear algebra and its applications*, vol. 18, no. 2, pp. 95–138, 1977.
- [31] N. D. Sidiropoulos and R. Bro, "On the uniqueness of multilinear decomposition of n-way arrays," *Journal of Chemometrics: A Journal of the Chemometrics Society*, vol. 14, no. 3, pp. 229–239, 2000.
- [32] D. Arpit, S. Jastrzebski, N. Ballas, D. Krueger, E. Bengio, M. S. Kanwal, T. Maharaj, A. Fischer, A. Courville, Y. Bengio et al., "A closer look at memorization in deep networks," in *International Conference on Machine Learning*, 2017, pp. 233–242.
- [33] L. Jiang, Z. Zhou, T. Leung, L.-J. Li, and L. Fei-Fei, "Mentornet: Learning data-driven curriculum for very deep neural networks on corrupted labels," in *International Conference on Machine Learning*, 2018, pp. 2309–2318.
- [34] B. Han, Q. Yao, X. Yu, G. Niu, M. Xu, W. Hu, I. Tsang, and M. Sugiyama, "Co-teaching: Robust training of deep neural networks with extremely noisy labels," in *Conference on Neural Information Processing Systems*, 2018, pp. 8536–8546.
- [35] J. Li, R. Socher, and S. C. H. Hoi, "DivideMix: learning with noisy labels as semi-supervised learning," in *International Conference on Learning Representations*, 2020.
- [36] T. Kim, J. Ko, S. Cho, J. Choi, and S. Yun, "FINE samples for learning with noisy labels," in *Conference on Neural Information Processing Systems*, 2021, pp. 24137–24149.
- [37] H. Song, M. Kim, and J.-G. Lee, "Selfie: Refurbishing unclean samples for robust deep learning," in *International Conference on Machine Learning*, 2019, pp. 5907–5915.
- [38] H. Song, M. Kim, D. Park, Y. Shin, and J.-G. Lee, "Robust learning by self-transition for handling noisy labels," in *ACM SIGKDD Conference on Knowledge Discovery and Data Mining*, 2021, pp. 1490–1500.
- [39] S. Li, X. Xia, S. Ge, and T. Liu, "Selective-supervised contrastive learning with noisy labels," in *IEEE/CVF Computer Vision and Pattern Recognition Conference*, 2022, pp. 316–325.
- [40] X. Xia, B. Han, Y. Zhan, J. Yu, M. Gong, C. Gong, and T. Liu, "Combating noisy labels with sample selection by mining high-discrepancy examples," in *International Conference on Computer Vision*, 2023.
- [41] S. Boucheron, G. Lugosi, and P. Massart, "Concentration inequalities - a nonasymptotic theory of independence," in *Concentration Inequalities*, 2013.
- [42] E. Arazo, D. Ortego, P. Albert, N. E. O'Connor, and K. McGuinness, "Unsupervised label noise modeling and loss correction," in *International Conference on Machine Learning*, K. Chaudhuri and R. Salakhutdinov, Eds., 2019, pp. 312–321.
- [43] N. Golowich, A. Rakhlin, and O. Shamir, "Size-independent sample complexity of neural networks," in *Conference on Learning Theory*, 2018, pp. 297–299.
- [44] M. Everingham, L. Van Gool, C. K. I. Williams, J. Winn, and A. Zisserman, "The PASCAL Visual Object Classes Challenge 2007 (VOC2007) Results," <http://www.pascal-network.org/challenges/VOC/voc2007/workshop/index.html>, 2007.
- [45] —, "The PASCAL Visual Object Classes Challenge 2012 (VOC2012) Results," <http://www.pascal-network.org/challenges/VOC/voc2012/workshop/index.html>, 2012.
- [46] T.-Y. Lin, M. Maire, S. Belongie, J. Hays, P. Perona, D. Ramanan, P. Dollár, and C. L. Zitnick, "Microsoft coco: Common objects in context," in *European Conference on Computer Vision*, 2014, pp. 740–755.
- [47] H.-Y. Z. Bin-Bin Gao, "Learning to Discover Multi-Class Attentional Regions for Multi-Label Image Recognition," *IEEE Transactions on Image Processing*, vol. 30, pp. 5920–5932, 2021.
- [48] B. Wu, Z. Liu, S. Wang, B.-G. Hu, and Q. Ji, "Multi-label learning with missing labels," in *International Conference on Pattern Recognition*, 2014, pp. 1964–1968.
- [49] B. Wu, F. Jia, W. Liu, B. Ghanem, and S. Lyu, "Multi-label learning with missing labels using mixed dependency graphs," *International Journal of Computer Vision*, vol. 126, pp. 875–896, 2018.
- [50] M.-K. Xie and S.-J. Huang, "Partial multi-label learning," in *AAAI Conference on Artificial Intelligence*, 2018.
- [51] —, "Partial multi-label learning with noisy label identification," *IEEE Transactions on Pattern Analysis and Machine Intelligence*, vol. 44, pp. 3676–3687, 2022.
- [52] K. He, X. Zhang, S. Ren, and J. Sun, "Deep residual learning for image recognition," in *IEEE/CVF Computer Vision and Pattern Recognition Conference*, 2016, pp. 770–778.
- [53] O. Russakovsky, J. Deng, H. Su, J. Krause, S. Satheesh, S. Ma, Z. Huang, A. Karpathy, A. Khosla, M. Bernstein et al., "Imagenet large scale visual recognition challenge," *International Journal of Computer Vision*, vol. 115, no. 3, pp. 211–252, 2015.
- [54] D. P. Kingma and J. Ba, "Adam: A method for stochastic optimization," in *International Conference on Learning Representations*, Y. Bengio and Y. LeCun, Eds., 2015.
- [55] Z. Zhang and M. Sabuncu, "Generalized cross entropy loss for training deep neural networks with noisy labels," in *Conference on Neural Information Processing Systems*, 2018, pp. 8778–8788.
- [56] X. Xia, T. Liu, B. Han, C. Gong, N. Wang, Z. Ge, and Y. Chang, "Robust early-learning: Hindering the memorization of noisy labels," in *International Conference on Learning Representations*, 2021.
- [57] J. Ye, J. He, X. Peng, W. Wu, and Y. Qiao, "Attention-driven dynamic graph convolutional network for multi-label image recognition," in *European Conference on Computer Vision*, 2020.
- [58] K. Zhu and J. Wu, "Residual attention: A simple but effective method for multi-label recognition," in *IEEE/CVF Computer Vision and Pattern Recognition Conference*, 2021, pp. 184–193.

- [59] M. Hu, H. Han, S. Shan, and X. Chen, "Weakly supervised image classification through noise regularization," in *IEEE/CVF Computer Vision and Pattern Recognition Conference*, 2019, pp. 11 517–11 525.
- [60] T. Ridnik, G. Sharir, A. Ben-Cohen, E. Ben-Baruch, and A. Noy, "ML-decoder: Scalable and versatile classification head," *arXiv*, 2021.
- [61] Y. Zhang, S. Zheng, P. Wu, M. Goswami, and C. Chen, "Learning with feature-dependent label noise: A progressive approach," in *International Conference on Learning Representations*, 2021.
- [62] E. A. Sanchez, D. Ortego, P. Albert, N. E. O'Connor, and K. McGuinness, "Unsupervised label noise modeling and loss correction," in *International Conference on Machine Learning*, 2019.
- [63] S. Li, S. Ge, Y. Hua, C. Zhang, H. Wen, T. Liu, and W. Wang, "Coupled-view deep classifier learning from multiple noisy annotators," in *AAAI Conference on Artificial Intelligence*, 2020, pp. 4667–4674.
- [64] S. Li, T. Liu, J. Tan, D. Zeng, and S. Ge, "Trustable co-label learning from multiple noisy annotators," *IEEE Transactions on Multimedia*, 2022.
- [65] I. Krasin, T. Duerig, N. Alldrin, V. Ferrari, S. Abu-El-Hajja, A. Kuznetsova, H. Rom, J. Uijlings, S. Popov, S. Kamali, M. Mallocci, J. Pont-Tuset, A. Veit, S. Belongie, V. Gomes, A. Gupta, C. Sun, G. Chechik, D. Cai, Z. Feng, D. Narayanan, and K. Murphy, "Openimages: A public dataset for large-scale multi-label and multi-class image classification," Dataset available from <https://storage.googleapis.com/openimages/web/index.html>, 2017.
- [66] A. Kuznetsova, H. Rom, N. Alldrin, J. Uijlings, I. Krasin, J. Pont-Tuset, S. Kamali, S. Popov, M. Mallocci, A. Kolesnikov *et al.*, "Hierarchy for the 600 boxable classes," https://storage.googleapis.com/openimages/2018_04/bbox_labels_600_hierarchy_visualizer/circle.html.
- [67] J. Wei, Z. Zhu, H. Cheng, T. Liu, G. Niu, and Y. Liu, "Learning with noisy labels revisited: A study using real-world human annotations," in *International Conference on Learning Representations*, 2022.
- [68] H. Song, M. Kim, and J. Lee, "SELFIE: refurbishing unclean samples for robust deep learning," in *International Conference on Machine Learning*, 2019, pp. 5907–5915.
- [69] J. M. Ten Berge and N. D. Sidiropoulos, "On uniqueness in candecomp/parafac," *Psychometrika*, vol. 67, no. 3, pp. 399–409, 2002.
- [70] S. Boucheron, G. Lugosi, and P. Massart, *Concentration inequalities: A nonasymptotic theory of independence*. Oxford university press, 2013.
- [71] P.-L. Chebyshev, "Des valeurs moyennes," *Journal de Mathématiques Pures et Appliquées*, vol. 12, pp. 177–184, 1867.
- [72] S. Bernstein, "The theory of probabilities," 1946.
- [73] M. Spivak, *Calculus*. Reverté, 2019.
- [74] P. L. Bartlett and S. Mendelson, "Rademacher and gaussian complexities: Risk bounds and structural results," *Journal of Machine Learning Research*, vol. 3, no. Nov, pp. 463–482, 2002.
- [75] M. Ledoux and M. Talagrand, *Probability in Banach Spaces: isoperimetry and processes*. Springer Science & Business Media, 2013.
- [76] J. Demšar, "Statistical comparisons of classifiers over multiple data sets," *Journal of Machine learning research*, vol. 7, pp. 1–30, 2006.



Shikun Li received the B.S. degree from the School of Information and Communication Engineering, Beijing University of Posts and Telecommunications (BUPT), Beijing, China. He is currently pursuing the Ph.D. degree with the Institute of Information Engineering, Chinese Academy of Sciences, Beijing, and the School of Cyber Security, University of Chinese Academy of Sciences, Beijing. His research interests include machine learning, data analysis and computer vision.



Xiaobo Xia received the B.E. degree in telecommunications engineering from Xidian University, in 2020. He is currently pursuing a Ph.D. degree in computer science from the University of Sydney. He has published more than 20 papers at top-tiered conferences or journals such as IEEE T-PAMI, ICML, ICLR, NeurIPS, CVPR, ICCV, and KDD. He also serves as the reviewer for top-tier conferences such as ICML, NeurIPS, ICLR, CVPR, ICCV, and ECCV. His research interest lies in machine learning, with a particular emphasis on weakly-supervised learning. He was a recipient of the Google Ph.D. Fellowship (machine learning) in 2022.



Hansong Zhang received the B.S. degree from the School of Mathematics and physics in North China Electric Power University, Beijing, China. He is currently a Ph.D. candidate in the Institute of Information Engineering, Chinese Academy of Sciences, Beijing, and the School of Cyber Security, University of Chinese Academy of Sciences, Beijing. His research interests include machine learning, data-centric AI, and computer vision.



Shiming Ge (M'13-SM'15) is a Professor with the Institute of Information Engineering, Chinese Academy of Sciences. He is also the member of Youth Innovation Promotion Association, Chinese Academy of Sciences. Prior to that, he was a senior researcher and project manager in Shanda Innovations, a researcher in Samsung Electronics and Nokia Research Center. He received the B.S. and Ph.D. degrees both in Electronic Engineering from the University of Science and Technology of China (USTC) in 2003 and 2008, respectively. His research mainly focuses on computer vision, data analysis, machine learning and AI security, especially efficient learning solutions towards scalable applications. He is a senior member of IEEE, CSIG and CCF.



Tongliang Liu (Senior Member, IEEE) is the Director of Sydney AI Centre at the University of Sydney. He is broadly interested in the fields of trustworthy machine learning and its interdisciplinary applications, with a particular emphasis on learning with noisy labels, adversarial learning, transfer learning, unsupervised learning, and statistical deep learning theory. He has authored and co-authored more than 200 research articles including ICML, NeurIPS, ICLR, CVPR, AAAI, IJCAI, JMLR, and TPAMI. His monograph on machine learning with noisy labels will be published by MIT Press. He is/was a (senior-) meta reviewer for many conferences, such as ICML, NeurIPS, ICLR, UAI, AAAI, IJCAI, and KDD, and was a notable AC for ICLR. Dr. Liu is an Associate Editor of TMLR and is on the Editorial Boards of JMLR and MLJ. He is a recipient of the AI's 10 to Watch Award from IEEE in 2023, the Future Fellowship Award from Australian Research Council (ARC) in 2022, and the Discovery Early Career Researcher Award (DECRA) from ARC in 2018.

APPENDIX A

DEFINITION OF CLASS-DEPENDENT LABEL NOISE

In this paper, the class-dependent multi-label noise for class label Y^j means that the flip probabilities of \bar{Y}^j are only dependent on the value of class label Y^j , *i.e.*, $Y^j = 0$ or $Y^j = 1$. The corresponding class-dependent transition matrix represents $\mathbb{P}(\bar{Y}^j|Y^j)$. The differences between this definition and the class-dependent label noise in the single-label cases are as follows.

First, the class-dependent label noise in the single-label cases represents the flip probability from class i to class j (i and j are two different classes), while in this paper, the class-dependent label noise for class label Y^j is only dependent on $Y^j = 0$ or $Y^j = 1$, which is independent on another class label Y^i , *i.e.*, $P(\bar{Y}^j|Y^j, Y^i) = P(\bar{Y}^j|Y^j)$.

Second, the class-dependent label noise in the single-label cases can be modeled by a $C \times C$ transition matrix, bridging the transition from clean single label to noisy single label, while in this paper, the class-dependent label noise for class label Y^j can be modeled by a 2×2 transition matrix, bridging the transition from clean label Y^j to noisy label \bar{Y}^j .

Third, the definition of class-dependent multi-label noise in this paper can be extended to instance-dependent multi-label noise, where the flip probabilities of \bar{Y}^j are dependent on class label Y^j and instance feature X . Such instance-dependent label model can sufficiently model various multi-label noise cases such as missing multi-labels [48], [49], partial multi-labels [50], [51], pair-wise label noise [34], [63], [64], and PMD label noise [61]. While the instance-dependent label noise in the single-label cases can not simultaneously model such complex multi-label noise.

APPENDIX B

REWEIGHT ALGORITHM FOR NOISY MULTI-LABEL LEARNING

In this appendix, we present applying a risk-consistent algorithm, *i.e.*, Reweight [10], [13], in noisy multi-label learning. First of all, we decompose the task into q independent binary classification problems given X , which is a widely used assumption for deep multi-label learning [1], [4], [18] and the surrogate loss is as:

$$\mathcal{L}(f(X), Y) = \sum_{j=1}^q \ell(f_j(X), Y^j) \quad (12)$$

where $f = (f_1, f_2, \dots, f_q)$ is the learnable q classification functions, and ℓ is the base loss function. In the deep learning community, f is usually modeled by a deep neural network with the outputs of q sigmoid functions, and ℓ is usually the binary cross entropy function.

Similar to the single-label case [10], [13], Reweight method employs the importance reweighting technique to rewrite the expected risk w.r.t. clean data:

$$\begin{aligned} R(f) &= \mathbb{E}_{(X,Y) \sim D}[\mathcal{L}(f(X), Y)] = \sum_{j=1}^q \mathbb{E}_{(X,Y)}[\ell(f_j(X), Y^j)] \\ &= \sum_{j=1}^q \int_x \sum_i \mathbb{P}_D(X = x, Y^j = i) \ell(f_j(x), i) dx \\ &= \sum_{j=1}^q \int_x \sum_i \mathbb{P}_{\bar{D}}(X = x, \bar{Y}^j = i) \frac{\mathbb{P}_D(X = x, Y^j = i)}{\mathbb{P}_{\bar{D}}(X = x, \bar{Y}^j = i)} \ell(f_j(x), i) dx \\ &= \sum_{j=1}^q \int_x \sum_i \mathbb{P}_{\bar{D}}(X = x, \bar{Y}^j = i) \frac{\mathbb{P}_D(Y^j = i | X = x)}{\mathbb{P}_{\bar{D}}(\bar{Y}^j = i | X = x)} \ell(f_j(x), i) dx \\ &= \sum_{j=1}^q \mathbb{E}_{(X,\bar{Y})}[\bar{\ell}_j(f_j(X), \bar{Y}^j)] = \mathbb{E}_{(X,\bar{Y}) \sim \bar{D}}[\bar{\mathcal{L}}(f(X), \bar{Y})], \end{aligned} \quad (13)$$

where D denotes the distribution for clean data, \bar{D} for noisy data, $\bar{\ell}_j(f_j(x), i) = \frac{\mathbb{P}_D(Y^j=i|X=x)}{\mathbb{P}_{\bar{D}}(\bar{Y}^j=i|X=x)} \ell(f_j(x), i)$, $\bar{\mathcal{L}}(f(x), \bar{y}) = \sum_{j=1}^q \bar{\ell}_j(f_j(x), \bar{y}^j)$, and the third last equation holds because label noise is assumed to be independent of instances. In the paper, we have omitted the subscript for P when no confusion is caused.

We use the output of the sigmoid function $g_j(x)$ to approximate $\mathbb{P}(Y^j = 1|X = x)$, *i.e.*, $\mathbb{P}(Y^j = 1|X = x) \approx \hat{\mathbb{P}}(Y^j = 1|X = x) = g_j(x)$ and $\mathbb{P}(Y^j = 0|X = x) \approx \hat{\mathbb{P}}(Y^j = 0|X = x) = 1 - g_j(x)$. Then, $\hat{\mathbb{P}}(\bar{Y}^j = k | X = x) = \sum_{i=0}^1 T_{ik}^j \hat{\mathbb{P}}(Y^j = i | X = x)$ is an approximation for $\mathbb{P}(\bar{Y}^j = k | X = x)$. By employing the Reweight algorithm, we build the risk-consistent estimator as:

$$\bar{R}_{n,w}(\{T^j\}_{j=1}^q, f) = \frac{1}{n} \sum_{i=1}^n \sum_{j=1}^q \frac{\hat{\mathbb{P}}(Y^j = \bar{y}_i^j | X = x_i)}{\hat{\mathbb{P}}(\bar{Y}^j = \bar{y}_i^j | X = x_i)} \ell(f_j(x_i), \bar{y}_i^j), \quad (14)$$

where $f_j(x) = \mathbb{I}[g_j(x) > 0.5]$, and $\mathbb{I}[\cdot]$ is the indicator function which takes 1 if the identity index is true and 0 otherwise; the subscript w denotes that the loss function is weighted.

APPENDIX C

VALIDATION OF ASSUMPTION 2

TABLE 13: The frequencies of $Y^i = 0$ given $Y^{50} = 0/1$ on MS-COCO training dataset. The frequencies whose difference between given $Y^{50} = 0$ and $Y^{50} = 1$ is greater than 0.015 are in **bold**.

$i = 1$	$i = 2$	$i = 3$	$i = 4$	$i = 5$	$i = 6$	$i = 7$	$i = 8$	$i = 9$	$i = 10$
0.960/0.983	0.979/0.992	0.991/0.920	0.974/0.985	0.999/0.961	0.999/0.959	0.984/0.999	0.955/0.980	0.974/0.936	0.989/0.958
$i = 11$	$i = 12$	$i = 13$	$i = 14$	$i = 15$	$i = 16$	$i = 17$	$i = 18$	$i = 19$	$i = 20$
0.955/0.987	0.980/0.970	0.943/0.964	0.925/0.929	0.920/0.954	0.969/0.996	0.983/0.952	0.975/0.975	0.931/0.866	0.975/0.995
$i = 21$	$i = 22$	$i = 23$	$i = 24$	$i = 25$	$i = 26$	$i = 27$	$i = 28$	$i = 29$	$i = 30$
0.937/0.989	0.982/0.941	0.912/0.874	0.950/0.971	0.958/0.964	0.974/0.990	0.918/0.923	0.886/0.908	0.957/0.968	0.987/0.987
$i = 31$	$i = 32$	$i = 33$	$i = 34$	$i = 35$	$i = 36$	$i = 37$	$i = 38$	$i = 39$	$i = 40$
0.976/0.986	0.981/0.989	0.966/0.972	0.994/0.972	0.959/0.993	0.998/0.999	0.989/0.902	0.982/0.969	0.990/0.990	0.972/0.991
$i = 41$	$i = 42$	$i = 43$	$i = 44$	$i = 45$	$i = 46$	$i = 47$	$i = 48$	$i = 49$	$i = 50$
0.997/0.967	0.962/0.962	0.966/0.973	0.980/0.992	0.987/0.957	0.974/0.993	0.977/0.992	0.965/0.984	0.993/0.995	1.000/0.000
$i = 51$	$i = 52$	$i = 53$	$i = 54$	$i = 55$	$i = 56$	$i = 57$	$i = 58$	$i = 59$	$i = 60$
0.970/0.975	0.954/0.969	0.972/0.986	0.981/0.967	0.974/0.985	0.989/0.994	0.977/0.994	0.930/0.984	0.999/0.945	0.999/0.952
$i = 61$	$i = 62$	$i = 63$	$i = 64$	$i = 65$	$i = 66$	$i = 67$	$i = 68$	$i = 69$	$i = 70$
0.999/0.975	0.965/0.973	0.997/0.936	0.980/0.990	0.984/0.977	0.998/0.950	0.976/0.987	0.999/0.948	0.997/0.944	0.997/0.999
$i = 71$	$i = 72$	$i = 73$	$i = 74$	$i = 75$	$i = 76$	$i = 77$	$i = 78$	$i = 79$	$i = 80$
0.945/0.994	0.991/0.992	0.969/0.961	0.964/0.975	0.959/0.938	0.950/0.970	0.991/0.947	0.948/0.987	0.984/0.974	0.966/0.998

In order to verify the assumption 2, we count the frequencies of $Y^i = 0$ given $Y^{50} = 0/1$ on MS-COCO training dataset, *i.e.*, $\hat{\mathbb{P}}(Y^i = 0|Y^{50} = 0)/\hat{\mathbb{P}}(Y^i = 0|Y^{50} = 1)$. According to Hoeffding’s inequality [41], when the frequencies whose difference between given $Y^{50} = 0$ and $Y^{50} = 1$ is greater than 0.015, we have at least 95% confidence to make sure $\mathbb{P}(Y^i = 0|Y^{50} = 0) \neq \mathbb{P}(Y^i = 0|Y^{50} = 1)$. As shown in Tab. 13, class 50 has a correlation with another 46 classes with a high probability, which means they are very likely to hold Assumption 2, accounting for the majority of all 79 classes.

In the implementation of our estimator, we always assume class j and class i have a strong correlation at first, and use them to estimate. While, when a reasonable solution cannot be obtained, we will abandon class i and choose another class.

APPENDIX D

DISCUSSION ABOUT SIGNIFICANTLY DIFFERENT LABEL PAIRS IN REAL-WORLD DATASETS

Although the real-world scenarios have complex label correlations, we claim significantly different class label pairs usually account for the majority of all label pairs in the typical multi-label datasets, *e.g.*, MS-COCO [46] and OpenImages [65] datasets. It is because, among a large number of classes, most label pairs belong to significantly different superclasses. For example, in MS-COCO datasets, there are 80 classes, which belong to 10 significantly different superclasses (outdoor, food, indoor, appliance, sports, person, animal, vehicle, furniture, accessory, electronic, kitchen). In the OpenImages dataset, there are 19,957 class labels, and also have significantly different superclasses, such as Toy, Building, Medical equipment, Clothing, Insect, and so on. A part of these superclasses can be seen in [66], which clearly shows most of the label pairs are significantly different and do not share the major discriminant features.

APPENDIX E

DISCUSSION ABOUT RELAXATION OF INSTANCE-INDEPENDENT ASSUMPTION

In this work, we assume that label noise is class-dependent but instance-independent. While, in real-world scenarios, label noise is instance-dependent. Actually, this instance-independent assumption can be roughly related to the assumption that the label noise of one class label is dependent on the label correlations with a few classes, and independent on the label correlations with most classes, which means most label pairs (i, j) s meet $P(\bar{Y}^j | Y^j, Y^i) = P(\bar{Y}^j | Y^j)$, $P(\bar{Y}^i | Y^j, Y^i) = P(\bar{Y}^i | Y^i)$. With such labels, the system of equations involving T^j in Section 3.2 holds, and our approach also works well. This relaxed assumption can be nearly satisfied in many real-world scenes because generally speaking, the multi-label label noises for class j are usually dependent on confusing features for itself, and the majority of classes will not share the same confusing features with class j . This claim agrees with the discussion about significantly different label pairs in Appendix D, and some research works about real-world label noise [67], [68] also show that noisy labels usually flip to some similar class labels in the real-world scene. For example, In CIFAR-100N, which is a re-annotated version of the CIFAR-100 with real-world human annotations, most classes are more likely to be mislabeled into less than four fine classes [67]. In ANIMAL-10N, the label noise mainly happens between five pairs of confusing animals [68]. Besides, the experiments in Section 5.2 also verify the effectiveness of our approach in two typical instance-dependent multi-label noise cases.

APPENDIX F

PROOF OF THEOREM 1

Lemma 1. \bar{Y}^i and \bar{Y}^j are independent given Y^j .

Proof. Since we assume that the transition matrix is class-dependent and instance-independent, \bar{Y}^j and any variable are independent given Y^j . Therefore, this lemma holds. \square

Lemma 2. *The product of two row-stochastic matrices is still a row-stochastic one.*

Proof. Let P and Q be row-stochastic matrices of the following form: $P = \begin{pmatrix} 1-p_- & p_- \\ p_+ & 1-p_+ \end{pmatrix}$ and $Q = \begin{pmatrix} 1-q_- & q_- \\ q_+ & 1-q_+ \end{pmatrix}$. Then the product of P and Q is $PQ = \begin{pmatrix} 1-q_-+p_-(-1+q_-+q_+) & q_- - p_-(-1+q_-+q_+) \\ q_+ - p_+(-1+q_-+q_+) & 1-q_+ + p_+(-1+q_-+q_+) \end{pmatrix}$. It can be readily verified that the sum of each row of PQ is equal to 1, meaning that PQ is a row-stochastic matrix. \square

Theorem 1. *Two noisy labels $\{\bar{Y}^j, \bar{Y}^i\}$ will not suffice to identify T^j .*

Proof. First, the information from \bar{Y}^j, \bar{Y}^i can be fully captured by the following four quantities: $\mathbb{P}(\bar{Y}^j = 0, \bar{Y}^i = 0)$, $\mathbb{P}(\bar{Y}^j = 1, \bar{Y}^i = 0)$, $\mathbb{P}(\bar{Y}^j = 0, \bar{Y}^i = 1)$, and $\mathbb{P}(\bar{Y}^j = 1, \bar{Y}^i = 1)$. According to Lemma 1, these four quantities can lead to four equations that depend on T^j :

$$\begin{aligned} \mathbb{P}(\bar{Y}^j = 0, \bar{Y}^i = 0) &= \mathbb{P}(Y^j = 0)T_{00}^j\mathbb{P}(\bar{Y}^i = 0|Y^j = 0) + \mathbb{P}(Y^j = 1)T_{10}^j\mathbb{P}(\bar{Y}^i = 0|Y^j = 1) \\ \mathbb{P}(\bar{Y}^j = 0, \bar{Y}^i = 1) &= \mathbb{P}(Y^j = 0)T_{00}^j\mathbb{P}(\bar{Y}^i = 1|Y^j = 0) + \mathbb{P}(Y^j = 1)T_{10}^j\mathbb{P}(\bar{Y}^i = 1|Y^j = 1) \\ \mathbb{P}(\bar{Y}^j = 1, \bar{Y}^i = 0) &= \mathbb{P}(Y^j = 0)T_{01}^j\mathbb{P}(\bar{Y}^i = 0|Y^j = 0) + \mathbb{P}(Y^j = 1)T_{11}^j\mathbb{P}(\bar{Y}^i = 0|Y^j = 1) \\ \mathbb{P}(\bar{Y}^j = 1, \bar{Y}^i = 1) &= \mathbb{P}(Y^j = 0)T_{01}^j\mathbb{P}(\bar{Y}^i = 1|Y^j = 0) + \mathbb{P}(Y^j = 1)T_{11}^j\mathbb{P}(\bar{Y}^i = 1|Y^j = 1). \end{aligned}$$

For simplicity, we denote

$$\begin{aligned} E &= \begin{pmatrix} \mathbb{P}(\bar{Y}^j = 0, \bar{Y}^i = 0) & \mathbb{P}(\bar{Y}^j = 0, \bar{Y}^i = 1) \\ \mathbb{P}(\bar{Y}^j = 1, \bar{Y}^i = 0) & \mathbb{P}(\bar{Y}^j = 1, \bar{Y}^i = 1) \end{pmatrix} = \begin{pmatrix} e_{00} & e_{01} \\ e_{10} & e_{11} \end{pmatrix}, \\ P &= \begin{pmatrix} \mathbb{P}(Y^j = 0) & 0 \\ 0 & \mathbb{P}(Y^j = 1) \end{pmatrix} = \begin{pmatrix} 1-p & 0 \\ 0 & p \end{pmatrix}, \\ T^j &= \begin{pmatrix} \mathbb{P}(\bar{Y}^j = 0 | Y^j = 0) & \mathbb{P}(\bar{Y}^j = 1 | Y^j = 0) \\ \mathbb{P}(\bar{Y}^j = 0 | Y^j = 1) & \mathbb{P}(\bar{Y}^j = 1 | Y^j = 1) \end{pmatrix} = \begin{pmatrix} 1-\rho_- & \rho_- \\ \rho_+ & 1-\rho_+ \end{pmatrix}, \text{ and} \\ M &= \begin{pmatrix} \mathbb{P}(\bar{Y}^i = 0 | Y^j = 0) & \mathbb{P}(\bar{Y}^i = 1 | Y^j = 0) \\ \mathbb{P}(\bar{Y}^i = 0 | Y^j = 1) & \mathbb{P}(\bar{Y}^i = 1 | Y^j = 1) \end{pmatrix} = \begin{pmatrix} 1-\rho'_- & \rho'_- \\ \rho'_+ & 1-\rho'_+ \end{pmatrix}. \end{aligned}$$

Then, the system of equations can be expressed as $E = (T^j)^\top PM$, i.e.,

$$\begin{pmatrix} e_{00} & e_{01} \\ e_{10} & e_{11} \end{pmatrix} = \begin{pmatrix} 1-\rho_- & \rho_- \\ \rho_+ & 1-\rho_+ \end{pmatrix}^\top \begin{pmatrix} 1-p & 0 \\ 0 & p \end{pmatrix} \begin{pmatrix} 1-\rho'_- & \rho'_- \\ \rho'_+ & 1-\rho'_+ \end{pmatrix}. \quad (15)$$

Assuming $\{T^0, P^0, M^0\}$ satisfies

$$E = (T^0)^\top P^0 M^0, \quad (16)$$

Next, we will prove that by selecting proper parameters, a different solution of Eq. (15) can be derived, which ruins the identifiability of T^j . Let $A = \begin{pmatrix} 1-a_- & a_- \\ a_+ & 1-a_+ \end{pmatrix}$ and $B = \begin{pmatrix} 1-b_- & b_- \\ b_+ & 1-b_+ \end{pmatrix}$ be invertible, row-stochastic matrices. Based on the invertibility of A and B , Eq. (16) can be rewritten as $E = (AT^0)^\top (A^\top)^{-1} P^0 B^{-1} B M^0$. According to Lemma 2, $T^1 = AT^0$ and $M^1 = B M^0$ are row-stochastic matrices, which is consistent with the form of T^j and M .

Last, denoting $P^0 = \begin{pmatrix} 1-p_0 & 0 \\ 0 & p_0 \end{pmatrix}$ and $P^1 = \begin{pmatrix} p_{00} & p_{01} \\ p_{10} & p_{11} \end{pmatrix}$, by letting $P^1 = (A^\top)^{-1} P^0 B^{-1} = \left[\begin{pmatrix} 1-a_- & a_- \\ a_+ & 1-a_+ \end{pmatrix}^\top \right]^{-1} \begin{pmatrix} 1-p_0 & 0 \\ 0 & p_0 \end{pmatrix} \begin{pmatrix} 1-b_- & b_- \\ b_+ & 1-b_+ \end{pmatrix} = \begin{pmatrix} p_{00} & p_{01} \\ p_{10} & p_{11} \end{pmatrix}$ be in the form of P , i.e., solving the following equations:

$$\begin{cases} p_{00} + p_{11} = 1, \\ p_{01} = 0, \\ p_{10} = 0, \end{cases}$$

we can get $a_+ = \frac{b_-(1-p_0)}{b_- - p_0}$ and $b_+ = \frac{a_-(1-p_0)}{a_- - p_0}$. It means that when we have a solution $\{T^0, P^0, M^0\}$ of Eq. (15), we can get another different solution $\{T^1, P^1, M^1\}$ by setting appropriate values of b_- and a_- . Hence, T^j is unidentifiable in this situation. \square

APPENDIX G

PROOF OF THEOREM 2

To make the proof clear, following [27], we reproduce the Kruskal's identifiability result here. The setup of Kruskal's identifiability result is as follows: suppose that there is an unobserved variable Z that takes values in $\{0, 1, \dots, K-1\}$. Z has a non-degenerate prior $\mathbb{P}(Z=i) > 0$. Instead of observing Z , we observe a set of conditionally independent variables $\{O^{(t)}\}_{t=1}^N$. Each $O^{(t)}$ has a finite state space with cardinality κ_t . Let $M^{(t)}$ be a matrix of size $K \times \kappa_t$, which j -th row is simply $\left[\mathbb{P}\left(O^{(t)} = 1 \mid Z = j\right), \dots, \mathbb{P}\left(O^{(t)} = \kappa_t \mid Z = j\right)\right]$. The previous works [30], [31] have proved the following Theorem 7.

Definition 3 (Kruskal rank [27]). *For a matrix M , the Kruskal rank of M is the largest number I such that every set of I rows of M are independent. The symbol is $\text{Kr}(M) = I$.*

Theorem 7 (Kruskal's identifiability result [30], [31]). *The model parameters are uniquely identifiable, up to label permutation, if*

$$\sum_{t=1}^N \text{Kr}\left(M^{(t)}\right) \geq 2K + N - 1.$$

We can prove Theorem 2 with the following lemmas:

Lemma 3. *\bar{Y}^i and Y^j are independent given Y^i .*

Proof. Since we assume that the transition matrix is class-dependent and instance-independent, \bar{Y}^i and any variable are independent given Y^i . Therefore, this lemma holds. \square

Lemma 4. *If $Y^j \in \{0, 1\}$ corresponds to Z , $\{\bar{Y}^j, \bar{Y}^i, \bar{Y}^k\}$ correspond to the observations $\{O^{(t)}\}_{t=1}^3$, then $\text{Kr}\left(M^{(t)}\right) = 2, t \in [3]$.*

Proof. As $M^{(1)} = T^j$ is a row-stochastic matrix, according to Assumption 1, every set of 2 rows of it are independent, thus its Kruskal rank is 2. Therefore, according to Definition 3, $\text{Kr}\left(T^j\right) = 2$.

The (p, q) entry of $M^{(2)}$ is

$$\begin{aligned} M_{pq}^{(2)} &= \mathbb{P}(\bar{Y}^i = q \mid Y^j = p) = \sum_{c=0}^1 \mathbb{P}(\bar{Y}^i = q, Y^i = c \mid Y^j = p) \\ &= \sum_{c=0}^1 \mathbb{P}(\bar{Y}^i = q \mid Y^i = c, Y^j = p) \mathbb{P}(Y^i = c \mid Y^j = p) \\ &= \sum_{c=0}^1 \mathbb{P}(\bar{Y}^i = q \mid Y^i = c) \mathbb{P}(Y^i = c \mid Y^j = p), \end{aligned} \quad (17)$$

where the last equation holds because of Lemma. 3.

Denote $M^{(2)} = \begin{pmatrix} \mathbb{P}(Y^i = 0 \mid Y^j = 0) & \mathbb{P}(Y^i = 1 \mid Y^j = 0) \\ \mathbb{P}(Y^i = 0 \mid Y^j = 1) & \mathbb{P}(Y^i = 1 \mid Y^j = 1) \end{pmatrix}$. Then Eq. (17) can be rewritten as the following matrix form:

$$M^{(2)} = M'^{(2)} T^i, \quad (18)$$

where T^i denotes the transition matrix of class i . According to Assumption 1, $\text{Kr}\left(T^i\right) = 2$. As $M'^{(2)}$ is a row-stochastic matrix, according to Assumption 2, every set of 2 rows of it are independent. Hence, according to Definition 3, $\text{Kr}\left(M'^{(2)}\right) = 2$.

Since T^i and $M'^{(2)}$ are full-rank matrices, based on Eq. (17), we can get the Kruskal rank of $M^{(2)}$ as $\text{Kr}\left(M^{(2)}\right) = 2$. Similarly, $\text{Kr}\left(M^{(3)}\right) = 2$. \square

Theorem 2. *If \bar{Y}^i and \bar{Y}^k are independent given Y^j , three noisy labels $\{\bar{Y}^j, \bar{Y}^i, \bar{Y}^k\}$ are sufficient to identify T^j .*

Proof. According to Lemma 1 and that \bar{Y}^i and \bar{Y}^k are independent given Y^j , we can relate our multi-label noise setting to the setup of Kruskal's identifiability scenario: $Y^j \in \{0, 1\}$ corresponds to the unobserved hidden variable Z ; $\mathbb{P}(Y^j = i)$ corresponds to the prior of this hidden variable; Noisy labels $\{\bar{Y}^j, \bar{Y}^i, \bar{Y}^k\}$ correspond to the observations $\{O^{(t)}\}_{t=1}^3$. κ_t is then simply the cardinality of the noisy label space, i.e., $\kappa_t = K = 2$; Each $O^{(t)}$ has a corresponding observation matrix $M^{(t)}$, and $M_{vk}^{(t)} = \mathbb{P}\left(O^{(t)} = k \mid Y^j = v\right)$. Now we can get the following result about identifiability of T .

According to Lemma 4, the Kruskal ranks satisfy

$$\sum_{t=1}^3 \text{Kr}(M^{(t)}) = 3K = 2K + 2 \geq 2K + N - 1, \text{ when } N = 3.$$

Calling Theorem 7 proves the uniqueness of $M^{(t)}$. As $M^{(1)} = T^j$, then T^j is identifiable. \square

APPENDIX H PROOF OF THEOREM 3

Lemma 5. \bar{Y}^i, \bar{Y}^j and \bar{Y}^k are independent given Y^j and Y^i .

Proof. Since we assume that the transition matrix is class-dependent and instance-independent, \bar{Y}^j and any variable are independent given Y^j , and \bar{Y}^i and any variable are independent given Y^i . Therefore, this lemma holds. \square

Lemma 6. If $M_{4 \times 2} = \mathbb{P}(\bar{Y}^i | Y^j, Y^i)$, the first two rows and last two rows of M are identical respectively, i.e., $M_{0p} = M_{1p}$ and $M_{2p} = M_{3p}, p = 0, 1$.

Proof.

$$\begin{aligned} M &= \begin{pmatrix} \mathbb{P}(\bar{Y}^i = 0 | Y^j = 0, Y^i = 0) & \mathbb{P}(\bar{Y}^i = 1 | Y^j = 0, Y^i = 0) \\ \mathbb{P}(\bar{Y}^i = 0 | Y^j = 1, Y^i = 0) & \mathbb{P}(\bar{Y}^i = 1 | Y^j = 1, Y^i = 0) \\ \mathbb{P}(\bar{Y}^i = 0 | Y^j = 0, Y^i = 1) & \mathbb{P}(\bar{Y}^i = 1 | Y^j = 0, Y^i = 1) \\ \mathbb{P}(\bar{Y}^i = 0 | Y^j = 1, Y^i = 1) & \mathbb{P}(\bar{Y}^i = 1 | Y^j = 1, Y^i = 1) \end{pmatrix} \\ &= \begin{pmatrix} \mathbb{P}(\bar{Y}^i = 0 | Y^i = 0) & \mathbb{P}(\bar{Y}^i = 1 | Y^i = 0) \\ \mathbb{P}(\bar{Y}^i = 0 | Y^i = 0) & \mathbb{P}(\bar{Y}^i = 1 | Y^i = 0) \\ \mathbb{P}(\bar{Y}^i = 0 | Y^i = 1) & \mathbb{P}(\bar{Y}^i = 1 | Y^i = 1) \\ \mathbb{P}(\bar{Y}^i = 0 | Y^i = 1) & \mathbb{P}(\bar{Y}^i = 1 | Y^i = 1) \end{pmatrix}, \end{aligned}$$

where the second equation holds because \bar{Y}^i is only dependent on Y^i . Accordingly, $M_{0p} = M_{1p}$ and $M_{2p} = M_{3p}, p = 0, 1$. \square

Theorem 3. If \bar{Y}^i and \bar{Y}^k are not independent given Y^j , three noisy labels $\{\bar{Y}^j, \bar{Y}^i, \bar{Y}^k\}$ will not suffice to identify T^j .

Proof. The likelihood of noisy labels can be formulated as a third-order tensor L , where the (p, q, m) entry is

$$L_{pqr} = \mathbb{P}(\bar{Y}^i = p, \bar{Y}^j = q, \bar{Y}^k = r). \quad (19)$$

According to Lemma 5, Eq. (19) can be expanded by the total probability rule:

$$\begin{aligned} L_{pqr} &= \sum_{c_0, c_1=0}^{c_0, c_1=1} \mathbb{P}(\bar{Y}^i = p, \bar{Y}^j = q, \bar{Y}^k = r | Y^j = c_0, Y^i = c_1) \mathbb{P}(Y^j = c_0, Y^i = c_1) \\ &= \sum_{c_0, c_1=0}^{c_0, c_1=1} \mathbb{P}(\bar{Y}^i = p | Y^j, Y^i) \mathbb{P}(\bar{Y}^j = q | Y^j, Y^i) \mathbb{P}(\bar{Y}^k = r | Y^j, Y^i) \mathbb{P}(Y^j, Y^i). \end{aligned} \quad (20)$$

where we omit the value of Y^i, Y^j in the last equation for simplicity. Let $M_{4 \times 2}^{(1)} = \mathbb{P}(\bar{Y}^j | Y^i, Y^j)$, $M_{4 \times 2}^{(2)} = \mathbb{P}(\bar{Y}^i | Y^i, Y^j)$, $M_{4 \times 2}^{(3)} = \mathbb{P}(\bar{Y}^k | Y^i, Y^j)$ and $\Lambda_{4 \times 1} = \mathbb{P}(Y^i, Y^j)$, and the Eq. (20) can be expressed as $L_{pqr} = \sum_{v=0}^3 M_{vp}^{(2)} M_{vq}^{(1)} M_{vm}^{(3)} \Lambda_v$.

Let $\{A^0, B^0, C^0, \Lambda^0\}$ be a solution of $\{M^{(1)}, M^{(2)}, M^{(3)}, \Lambda\}$, which means it fulfils the likelihood equations (Eq. (20)), i.e.,

$$L_{pqr} = \sum_{v=0}^3 B_{vp}^0 A_{vq}^0 C_{vm}^0 \Lambda_v^0. \quad (21)$$

Note that as stated in Lemma. 6, the first two rows and last two rows of B^0 are identical respectively. Next, we will show that a different solution can be constructed by simply switching the corresponding rows in A^0, C^0 and Λ^0 , which is consistent with the result in [69] when $\text{Kr}(M^{(2)}) = 1$. By letting

$$A^1 = \begin{pmatrix} A_{10}^0 & A_{11}^0 \\ A_{00}^0 & A_{01}^0 \\ A_{30}^0 & A_{31}^0 \\ A_{20}^0 & A_{21}^0 \end{pmatrix}, \quad C^1 = \begin{pmatrix} C_{10}^0 & C_{11}^0 \\ C_{00}^0 & C_{01}^0 \\ C_{30}^0 & C_{31}^0 \\ C_{20}^0 & C_{21}^0 \end{pmatrix}, \quad \text{and} \quad \Lambda^1 = \begin{pmatrix} \Lambda_1^0 \\ \Lambda_0^0 \\ \Lambda_3^0 \\ \Lambda_2^0 \end{pmatrix},$$

then the Eq. (21) is equivalent to

$$\begin{aligned}
L_{pqm} &= B_{0p}^0 A_{0q}^0 C_{0m}^0 \Lambda_0^0 + B_{1p}^0 A_{1q}^0 C_{1m}^0 \Lambda_1^0 + B_{2p}^0 A_{2q}^0 C_{2m}^0 \Lambda_2^0 + B_{3p}^0 A_{3q}^0 C_{3m}^0 \Lambda_3^0 \\
&= B_{1p}^0 A_{0q}^0 C_{0m}^0 \Lambda_0^0 + B_{0p}^0 A_{1q}^0 C_{1m}^0 \Lambda_1^0 + B_{3p}^0 A_{2q}^0 C_{2m}^0 \Lambda_2^0 + B_{2p}^0 A_{3q}^0 C_{3m}^0 \Lambda_3^0 \\
&= B_{1p}^0 A_{1q}^1 C_{1m}^1 \Lambda_1^1 + B_{0p}^0 A_{0q}^1 C_{0m}^1 \Lambda_0^1 + B_{3p}^0 A_{3q}^1 C_{3m}^1 \Lambda_3^1 + B_{2p}^0 A_{2q}^1 C_{2m}^1 \Lambda_2^1 \\
&= \sum_{v=0}^3 B_{vp}^0 A_{vq}^1 C_{vm}^1 \Lambda_v^1
\end{aligned} \tag{22}$$

where the second equation holds because the first two rows and last two rows of B^0 are identical respectively, i.e., $B_{0p}^0 = B_{1p}^0$ and $B_{2p}^0 = B_{3p}^0$. Note that A^1, C^1 and Λ^1 are consistent with the form of $M^{(1)}, M^{(3)}$ and Λ respectively. Then, according to Eq. (22), it can be readily observed that the $\{A^1, B^0, C^1, \Lambda^1\}$ is a new solution of $\{M^{(1)}, M^{(2)}, M^{(3)}, \Lambda\}$, hence the uniqueness is not guaranteed under this circumstance. As $M^{(1)} = \begin{pmatrix} T^j \\ T^j \end{pmatrix}$ is not unique, then T^j is unidentifiable. \square

Note that according to Definition 2, in the situation of Theorem 3, the model parameter $\theta := \{T^j, \mathbb{P}(Y^j), \mathbb{P}(\bar{Y}^i, \bar{Y}^k | Y^j)\}$. For convenience, in the proof of Theorem 3, we use $\theta^1 := \{T^j, \mathbb{P}(Y^j, Y^i), \mathbb{P}(\bar{Y}^i | Y^j, Y^i), \mathbb{P}(\bar{Y}^k | Y^j, Y^i)\}$ as the model parameter. It is easy to prove that the above different solutions of θ^1 can lead to two different solutions of θ .

APPENDIX I PROOF OF THEOREM 4

Theorem 4. *If $\mathbb{P}(\bar{Y}^i | Y^j)$ is known, two noisy labels $\{\bar{Y}^j, \bar{Y}^i\}$ are sufficient to identify T^j .*

Proof. The proof of Theorem 4 is much similar to that of Theorem 1, we can get a system of equations expressed as $E = (T^j)^\top P M$. The difference lies in that in Theorem 4, the matrix M which is parameterized by $\mathbb{P}(\bar{Y}^i | Y^j)$ is given. Since M is invertible (Similar to Lemma. 4), the problem can be converted to a simple bilinear decomposition problem:

$$E(M)^{-1} = (T^j)^\top P,$$

i.e.,

$$\begin{pmatrix} e_{00} & e_{01} \\ e_{10} & e_{11} \end{pmatrix} \begin{pmatrix} 1 - \rho'_- & \rho'_- \\ \rho'_+ & 1 - \rho'_+ \end{pmatrix}^{-1} = \begin{pmatrix} 1 - \rho_- & \rho_- \\ \rho_+ & 1 - \rho_+ \end{pmatrix}^\top \begin{pmatrix} 1 - p & 0 \\ 0 & p \end{pmatrix}. \tag{23}$$

Solving the above bilinear decomposition problem, the unique solution can be obtained as:

$$p = \frac{(1 - \rho'_-) - (e_{00} + e_{10})}{1 - \rho'_- - \rho'_+}. \tag{24}$$

Substituting Eq. (24) into Eq. (23), then right multiplying P^{-1} on both side of the equation, the matrix T^j can be derived as:

$$T^j = [E(M)^{-1}(P)^{-1}]^\top,$$

which indicates that T^j is identifiable given label correlation $\mathbb{P}(\bar{Y}^i | Y^j)$. \square

APPENDIX J SUMMARY OF THE INSPIRATIONS FROM THE PROOF OF THEOREM 1-4

From the proof of Theorem 1, we can know that the label correlations of two noisy labels $\{\bar{Y}^j, \bar{Y}^i\}$ can not offer enough information to achieve the identifiability of T^j .

From the proof of Theorem 2, three noisy labels $\{\bar{Y}^j, \bar{Y}^i, \bar{Y}^k\}$ can provide more information than two noisy labels $\{\bar{Y}^j, \bar{Y}^i, \bar{Y}^k\}$ to achieve the identifiability when \bar{Y}^i and \bar{Y}^k are independent given Y^j . Note that when satisfying the condition, the parameter $\mathbb{P}(\bar{Y}^i, \bar{Y}^k | Y^j)$ is reduced to $\mathbb{P}(\bar{Y}^i | Y^j)$ and $\mathbb{P}(\bar{Y}^k | Y^j)$.

From the proof of Theorem 3, due to the entangled correlations, when \bar{Y}^i and \bar{Y}^k are not independent given Y^j , modelling three noisy labels $\{\bar{Y}^j, \bar{Y}^i, \bar{Y}^k\}$ will increase too many model parameters, making the identifiability decrease from the situation in Theorem 2.

From the proof of Theorem 4, by reducing the unknown model parameters via some extra information, the label correlations of two noisy labels $\{\bar{Y}^j, \bar{Y}^i\}$ can achieve the identifiability.

The summary of $\Omega, \theta, \mathbb{P}_\theta$, conditions, and the identifiability in Theorem 1-4 is shown in Tab. 14.

TABLE 14: Summary of Ω , θ , \mathbb{P}_θ , condition, and the identifiability in Theorem 1-4 .

	Ω	θ	\mathbb{P}_θ	Condition	Identifiability of T^j
Theorem 1	Y^j, Y^i	$T^j, \mathbb{P}(Y^j), \mathbb{P}(Y^i Y^j)$	$\mathbb{P}(Y^j, Y^i)$	-	
Theorem 2	$\bar{Y}^j, \bar{Y}^i, \bar{Y}^k$	$T^j, \mathbb{P}(Y^j), \mathbb{P}(\bar{Y}^i Y^j), \mathbb{P}(\bar{Y}^k Y^j)$	$\mathbb{P}(\bar{Y}^j, \bar{Y}^i, \bar{Y}^k)$	\bar{Y}^i and \bar{Y}^k are independent given Y^j	✓
Theorem 3	$\bar{Y}^j, \bar{Y}^i, \bar{Y}^k$	$T^j, \mathbb{P}(Y^j), \mathbb{P}(\bar{Y}^i, \bar{Y}^k Y^j)$	$\mathbb{P}(\bar{Y}^j, \bar{Y}^i, \bar{Y}^k)$	-	
Theorem 4	\bar{Y}^j, \bar{Y}^i	$T^j, \mathbb{P}(Y^j)$	$\mathbb{P}(\bar{Y}^j, \bar{Y}^i)$	$\mathbb{P}(\bar{Y}^i Y^j)$ is known	✓

APPENDIX K

PROOF OF THEOREM 5

We have

$$\begin{aligned} \|T^j - \hat{T}^j\|_1 &\leq \|T^j - \bar{T}^j\|_1 \\ &\leq \|T^j - \mathbb{E}[\bar{T}^j] + \mathbb{E}[\bar{T}^j] - \bar{T}^j\|_1 \\ &\leq \|T^j - \mathbb{E}[\bar{T}^j]\|_1 + \|\mathbb{E}[\bar{T}^j] - \bar{T}^j\|_1. \end{aligned} \quad (25)$$

As $\bar{T}^j = \arg \min_{\bar{T}^j} \sum_{r=1}^R \|\bar{T}^j - \hat{T}_r^j\|_1 = \sum_{r=1}^R \frac{\hat{T}_r^j}{R}$, we first consider the r -th estimation

$$\hat{T}_r^j = \begin{pmatrix} 1 - \hat{\rho}_+^r & \hat{\rho}_-^r \\ \hat{\rho}_+^r & 1 - \hat{\rho}_-^r \end{pmatrix}, r \in \{1, \dots, R\}.$$

Lemma 7. *When the training sample size n is large,*

$$\|T^j - \mathbb{E}[\hat{T}_r^j]\|_1 \leq 8C\Delta, \quad (26)$$

$$\text{Var}[\hat{\rho}_+^r] \leq C^2 \left(\frac{3}{4n} + \frac{1}{2\lambda_1 n} \right), \quad (27)$$

$$\text{Var}[\hat{\rho}_-^r] \leq C^2 \left(\frac{3}{4n} + \frac{1}{2\lambda_1 n} \right), \quad (28)$$

where C is the maximum absolute value of the first derivative of $\hat{\rho}_+^r$ and $\hat{\rho}_-^r$ w.r.t. the estimated co-occurrence probabilities.

The proof of Lemma 7 is provided in Appendix K.1.

After that, according to Lemma 7, we can bound $\|T^j - \mathbb{E}[\bar{T}^j]\|_1$ by

$$\begin{aligned} \|T^j - \mathbb{E}[\bar{T}^j]\|_1 &= \|T^j - \mathbb{E}\left[\sum_{r=1}^R \frac{\hat{T}_r^j}{R}\right]\|_1 = \|T^j - \sum_{r=1}^R \frac{1}{R} \mathbb{E}[\hat{T}_r^j]\|_1 \\ &= \left\| \sum_{r=1}^R \frac{1}{R} T^j - \sum_{r=1}^R \frac{1}{R} \mathbb{E}[\hat{T}_r^j] \right\|_1 \leq \sum_{r=1}^R \frac{1}{R} \|T^j - \mathbb{E}[\hat{T}_r^j]\|_1 \leq \sum_{r=1}^R \frac{1}{R} 8C\Delta = 8C\Delta. \end{aligned} \quad (29)$$

Also, let

$$\bar{T}_r^j = \begin{pmatrix} 1 - \bar{\rho}_- & \bar{\rho}_- \\ \bar{\rho}_+ & 1 - \bar{\rho}_+ \end{pmatrix} = \begin{pmatrix} 1 - \sum_{r=1}^R \frac{1}{R} \hat{\rho}_-^r & \sum_{r=1}^R \frac{1}{R} \hat{\rho}_-^r \\ \sum_{r=1}^R \frac{1}{R} \hat{\rho}_+^r & 1 - \sum_{r=1}^R \frac{1}{R} \hat{\rho}_+^r \end{pmatrix}, \quad (30)$$

we can get

$$\begin{aligned} \text{Var}[\bar{\rho}_+] &= \text{Var}\left[\sum_{r=1}^R \frac{1}{R} \hat{\rho}_+^r\right] = \sum_{r=1}^R \frac{1}{R^2} \text{Var}[\hat{\rho}_+^r] \\ &\leq \sum_{r=1}^R \frac{C^2}{R^2} \left(\frac{3}{4n} + \frac{1}{2\lambda_1 n} \right) = \frac{C^2}{R} \left(\frac{3}{4n} + \frac{1}{2\lambda_1 n} \right). \end{aligned} \quad (31)$$

Similarly, we could prove

$$\text{Var}[\bar{\rho}_-] \leq \frac{C^2}{R} \left(\frac{3}{4n} + \frac{1}{2\lambda_1 n} \right). \quad (32)$$

Since $\|\mathbb{E}[\bar{T}^j] - \bar{T}^j\|_1 = 2|\mathbb{E}[\bar{\rho}_-] - \bar{\rho}_-| + 2|\mathbb{E}[\bar{\rho}_+] - \bar{\rho}_+|$, with the variances of $\bar{\rho}_+$ and $\bar{\rho}_-$ known, we consider to bound $\|\mathbb{E}[\bar{T}^j] - \bar{T}^j\|_1$ by employing certain concentration inequalities [70].

First, by employing Chebyshev's inequality [71], we can derive below bound:

Lemma 8. *for any $\delta > 0$, with probability at least $1 - \delta$, we have*

$$\|\mathbb{E}[\bar{T}^j] - \bar{T}^j\|_1 \leq 4C \sqrt{\left(\frac{3}{4n} + \frac{1}{2\lambda_1 n} \right) \frac{2}{R\delta}}. \quad (33)$$

The proof of Lemma 8 is provided in Appendix K.2.

Second, by employing Bernstein's inequality [72], we can derive below bound:

Lemma 9. *for any $\delta > 0$, with probability at least $1 - \delta$, we have*

$$\|\mathbb{E}[\bar{T}^j] - \bar{T}^j\|_1 \leq 4C \sqrt{\frac{2 \log(4/\delta)}{R} \left(\frac{3}{4n} + \frac{1}{2\lambda_1 n} \right)} + \frac{8 \log(4/\delta)}{3R}. \quad (34)$$

Proof of Lemma 9 is provided in Appendix K.3.

Finally, according to Eq. (29), Lemmas 8, and 9, we can conclude that for any $\delta > 0$, with probability at least $1 - \delta$,

$$\|T^j - \hat{T}^j\|_1 \leq 8C\Delta + \min \left(4C \sqrt{\left(\frac{3}{4n} + \frac{1}{2\lambda_1 n} \right) \frac{2}{R\delta}}, 4C \sqrt{\left(\frac{3}{4n} + \frac{1}{2\lambda_1 n} \right) \frac{2 \log(4/\delta)}{R}} + \frac{8 \log(4/\delta)}{3R} \right).$$

K.1 Proof of Lemma 7

First of all, as mentioned in Section 3.2 and Eq. (11), for the r -th estimation, our estimator need to first estimate $\{e_{00}^r, e_{01}^r, e_{10}^r, \rho_+^r, \rho_-^r\}$ by $\{\hat{e}_{00}^r, \hat{e}_{01}^r, \hat{e}_{10}^r, \hat{\rho}_+^r, \hat{\rho}_-^r\}$. For simplicity, we omitted the superscript r below when no confusion is caused.

According to Eq. (8) and Eq. (9), it is easy to get that

$$\hat{\rho}_+ = \frac{\hat{e}_{00} - (\hat{e}_{00} + \hat{e}_{01})(1 - \hat{\rho}'_-)}{\hat{e}_{10} + \hat{e}_{00} + \hat{\rho}'_- - 1}, \quad \text{and}$$

$$\hat{\rho}_- = \frac{\hat{e}_{10} - (1 - \hat{e}_{01} - \hat{e}_{00})\hat{\rho}'_+}{\hat{e}_{10} + \hat{e}_{00} - \hat{\rho}'_+},$$

which means $\hat{\rho}_+$ and $\hat{\rho}_-$ can be seen as the function of the estimated co-occurrence probabilities $\theta = \{\hat{e}_{00}, \hat{e}_{01}, \hat{e}_{10}, \hat{\rho}'_+, \hat{\rho}'_-\}$, and

$$\hat{T}_r^j(\theta) = \begin{pmatrix} 1 - \hat{\rho}_-(\theta) & \hat{\rho}_-(\theta) \\ \hat{\rho}_+(\theta) & 1 - \hat{\rho}_+(\theta) \end{pmatrix}. \quad (35)$$

Then, we begin to obtain the expectation and variance of $\hat{\rho}_+$ and $\hat{\rho}_-$.

Let $\theta^* = \{e_{00}, e_{01}, e_{10}, \rho'_+ + \Delta_1, \rho'_- + \Delta_0\}$ be the expectation of θ as derived in Section 4.1 (See Eq. (11)). According to Taylor's theorem [73], $\hat{\rho}_+(\theta)$ can be expressed as

$$\hat{\rho}_+(\theta) = \hat{\rho}_+(\theta^*) + \sum_{i=1}^5 (\theta_i - \theta_i^*) \frac{\partial \hat{\rho}_+}{\partial \theta_i}(\theta^*) + o(\theta). \quad (36)$$

Since the estimated co-occurrence probabilities θ will converge to their expectation θ^* exponentially fast by counting [70], when the training sample size is large, we have

$$\hat{\rho}_+(\theta) \approx \hat{\rho}_+(\theta^*) + \sum_{i=1}^5 (\theta_i - \theta_i^*) \frac{\partial \hat{\rho}_+}{\partial \theta_i}(\theta^*). \quad (37)$$

Hence, we can get the expectation and the variance of $\hat{\rho}_+$ as

$$\begin{aligned} \mathbb{E}_\theta[\hat{\rho}_+(\theta)] &\approx \hat{\rho}_+(\theta^*) + \sum_{i=1}^5 \mathbb{E}_\theta[(\theta_i - \theta_i^*)] \frac{\partial \hat{\rho}_+}{\partial \theta_i}(\theta^*) \\ &= \hat{\rho}_+(\theta^*), \quad \text{and} \\ \text{Var}_\theta[\hat{\rho}_+(\theta)] &\approx \mathbb{E}_\theta \left[(\hat{\rho}_+(\theta) - \hat{\rho}_+(\theta^*))^2 \right] \\ &\approx \mathbb{E}_\theta \left[\left(\sum_{i=1}^5 (\theta_i - \theta_i^*) \frac{\partial \hat{\rho}_+}{\partial \theta_i}(\theta^*) \right)^2 \right] \\ &= \sum_{i=1}^5 \left(\frac{\partial \hat{\rho}_+}{\partial \theta_i}(\theta^*) \right)^2 \text{Var}_\theta[\theta_i] + 2 \sum_{i>j} \frac{\partial \hat{\rho}_+}{\partial \theta_i}(\theta^*) \frac{\partial \hat{\rho}_+}{\partial \theta_j}(\theta^*) \text{Cov}_\theta[\theta_i, \theta_j] \\ &= \sum_{i=1}^5 \left(\frac{\partial \hat{\rho}_+}{\partial \theta_i}(\theta^*) \right)^2 \text{Var}_\theta[\theta_i], \end{aligned} \quad (38)$$

where the last equation holds because of the independence of the estimated co-occurrence probabilities. Similarly, as for $\hat{\rho}_-$, we have

$$\mathbb{E}_\theta[\hat{\rho}_-(\theta)] \approx \hat{\rho}_-(\theta^*), \quad \text{and} \quad (40)$$

$$\text{Var}_\theta[\hat{\rho}_-(\theta)] \approx \sum_{i=1}^5 \left(\frac{\partial \hat{\rho}_-}{\partial \theta_i}(\theta^*) \right)^2 \text{Var}_\theta[\theta_i]. \quad (41)$$

Now, we can obtain

$$\begin{aligned}\mathbb{E}[\hat{T}_r^j(\theta)] &= \begin{pmatrix} 1 - \mathbb{E}[\hat{\rho}_-(\theta)] & \mathbb{E}[\hat{\rho}_-(\theta)] \\ \mathbb{E}[\hat{\rho}_+(\theta)] & 1 - \mathbb{E}[\hat{\rho}_+(\theta)] \end{pmatrix} \\ &= \begin{pmatrix} 1 - \hat{\rho}_-(\theta^*) & \hat{\rho}_-(\theta^*) \\ \hat{\rho}_+(\theta^*) & 1 - \hat{\rho}_+(\theta^*) \end{pmatrix} = \hat{T}_r^j(\theta^*)\end{aligned}\quad (42)$$

Let $\theta^* = \{e_{00}, e_{01}, e_{10}, \rho'_+, \rho'_-\}$ be the true probabilities of θ . Since, according to Eq. (6), $\hat{T}^j(\theta^*) = T^j$, then

$$\begin{aligned}\|T^j - \mathbb{E}[\hat{T}_r^j]\|_1 &= \|\hat{T}^j(\theta^*) - \hat{T}^j(\theta^*)\|_1 \\ &= 2|\hat{\rho}_-(\theta^*) - \hat{\rho}_-(\theta^*)| + 2|\hat{\rho}_+(\theta^*) - \hat{\rho}_+(\theta^*)| \\ &\approx 2\left|\sum_{i=4}^5 (\theta_i - \theta_i^*) \frac{\partial \hat{\rho}_-}{\partial \theta_i}(\theta^*)\right| + 2\left|\sum_{i=4}^5 (\theta_i - \theta_i^*) \frac{\partial \hat{\rho}_+}{\partial \theta_i}(\theta^*)\right| \\ &\leq 2(\Delta_0 C + \Delta_1 C) + 2(\Delta_0 C + \Delta_1 C) \leq 8C\Delta,\end{aligned}$$

where C is the maximum absolute value of the first derivative of $\hat{\rho}_+^r$ and $\hat{\rho}_-^r$ w.r.t. the estimated co-occurrence probabilities θ . According to Eq. (11), it is easy to get that

$$\begin{aligned}\text{Var}[\hat{e}_{kv}] &= \frac{e_{kv}(1 - e_{kv})}{n}, \quad \text{for } k, v \in \{0, 1\}, \\ \text{Var}[\hat{\rho}'_+] &= \frac{(\rho'_+ + \Delta_1)(1 - \rho'_+ - \Delta_1)}{4\lambda_1 n}, \\ \text{Var}[\hat{\rho}'_-] &= \frac{(\rho'_+ + \Delta_1)(1 - \rho'_+ - \Delta_1)}{4\lambda_0 n}.\end{aligned}\quad (43)$$

Therefore,

$$\begin{aligned}\text{Var}[\theta_i] &\leq \frac{1}{4n}, \quad \text{for } i = 1, 2, 3, \\ \text{Var}[\theta_i] &\leq \frac{1}{4\lambda_1 n}, \quad \text{for } i = 4, 5.\end{aligned}$$

K.2 Proof of Lemma 8

According to Eq. (31), by employing Chebyshev's inequality, for any $\delta > 0$, with probability at least $1 - \delta$, we have

$$|\mathbb{E}[\bar{\rho}_+] - \bar{\rho}_+| \leq \sqrt{\frac{\text{Var}[\bar{\rho}'_+]}{\delta}} \leq C\sqrt{\left(\frac{3}{4n} + \frac{1}{2\lambda_1 n}\right)\frac{1}{R\delta}}.$$

Similarly, we could prove that, for any $\delta > 0$, with probability at least $1 - \delta$,

$$|\mathbb{E}[\bar{\rho}_-] - \bar{\rho}_-| \leq \sqrt{\frac{\text{Var}[\bar{\rho}'_-]}{\delta}} \leq C\sqrt{\left(\frac{3}{4n} + \frac{1}{2\lambda_1 n}\right)\frac{1}{R\delta}}.$$

Then, for any $\delta > 0$, with probability at least $1 - \delta$, we have

$$\begin{aligned}\|\mathbb{E}[\bar{T}^j] - \bar{T}^j\|_1 &= 2|\mathbb{E}[\bar{\rho}_-] - \bar{\rho}_-| + 2|\mathbb{E}[\bar{\rho}_+] - \bar{\rho}_+| \\ &\leq 4C\sqrt{\left(\frac{3}{4n} + \frac{1}{2\lambda_1 n}\right)\frac{2}{R\delta}}.\end{aligned}\quad (44)$$

K.3 Proof of Lemma 9

We consider to bound $\|\mathbb{E}[\bar{T}^j] - \bar{T}^j\|_1$ by employing the below theorem implied by Bernstein's inequality [70].

Theorem 8. *Let X_1, \dots, X_n be independent random variables with finite variances, and assume $\max_{1 \leq i \leq n} |X_i| \leq B$ almost surely for some constant $B > 0$. Let $V = \sum_{i=1}^n \mathbb{E}[X_i^2]$. Then, for any $\delta > 0$, with probability at least $1 - \delta$,*

$$\left|\frac{1}{n} \sum_{i=1}^n (\mathbb{E}[X_i] - X_i)\right| \leq \frac{\sqrt{2V \log(2/\delta)}}{n} + \frac{2B \log(2/\delta)}{3n}.$$

Since we can get

$$\begin{aligned}\|\mathbb{E}[\bar{T}^j] - \bar{T}^j\|_1 &= 2|\mathbb{E}[\bar{\rho}_-] - \bar{\rho}_-| + 2|\mathbb{E}[\bar{\rho}_+] - \bar{\rho}_+| \\ &= 2\left|\mathbb{E}\left[\sum_{r=1}^R \frac{1}{R} \hat{\rho}_-^r\right] - \sum_{r=1}^R \frac{1}{R} \hat{\rho}_-^r\right| + 2\left|\mathbb{E}\left[\sum_{r=1}^R \frac{1}{R} \hat{\rho}_+^r\right] - \sum_{r=1}^R \frac{1}{R} \hat{\rho}_+^r\right| \\ &= 2\left|\sum_{r=1}^R \frac{1}{R} (\mathbb{E}[\hat{\rho}_-^r] - \hat{\rho}_-^r)\right| + 2\left|\sum_{r=1}^R \frac{1}{R} (\mathbb{E}[\hat{\rho}_+^r] - \hat{\rho}_+^r)\right|,\end{aligned}\quad (45)$$

where we consider to bound $\sum_{r=1}^R \mathbb{E}[(\hat{\rho}_+^r)^2]$ and $\sum_{r=1}^R \mathbb{E}[(\hat{\rho}_-^r)^2]$.

According to Eq. (31), we have

$$\begin{aligned} \sum_{r=1}^R \mathbb{E}[(\hat{\rho}_+^r)^2] &= \sum_{r=1}^R (\text{Var}[\hat{\rho}_+^r] - \mathbb{E}[(\hat{\rho}_+^r)]^2) \leq \sum_{r=1}^R (\text{Var}[\hat{\rho}_+^r]) \\ &\leq \sum_{r=1}^R C^2 \left(\frac{3}{4n} + \frac{1}{2\lambda_1 n} \right) = RC^2 \left(\frac{3}{4n} + \frac{1}{2\lambda_1 n} \right). \end{aligned} \quad (46)$$

After that, since $\max_r |\hat{\rho}_+^r| \leq 1$, by employing Theorem 8, for any $\delta > 0$, with probability at least $1 - \delta$, we have

$$\left| \frac{1}{R} \sum_{r=1}^R (\mathbb{E}[\hat{\rho}_+^r] - \hat{\rho}_+) \right| \leq C \sqrt{\frac{2 \log(2/\delta)}{R} \left(\frac{3}{4n} + \frac{1}{2\lambda_1 n} \right)} + \frac{2 \log(2/\delta)}{3R}.$$

Similarly, we could prove that

$$\left| \frac{1}{R} \sum_{r=1}^R (\mathbb{E}[\hat{\rho}_-^r] - \hat{\rho}_-) \right| \leq C \sqrt{\frac{2 \log(2/\delta)}{R} \left(\frac{3}{4n} + \frac{1}{2\lambda_1 n} \right)} + \frac{2 \log(2/\delta)}{3R}.$$

Then, for any $\delta > 0$, with probability at least $1 - \delta$, we have

$$\begin{aligned} \|\mathbb{E}[\bar{T}^j] - \bar{T}^j\|_1 &= 2 \left| \sum_{r=1}^R \frac{1}{R} (\mathbb{E}[\hat{\rho}_-^r] - \hat{\rho}_-) \right| + 2 \left| \sum_{r=1}^R \frac{1}{R} (\mathbb{E}[\hat{\rho}_+^r] - \hat{\rho}_+) \right| \\ &\leq 4C \sqrt{\frac{2 \log(4/\delta)}{R} \left(\frac{3}{4n} + \frac{1}{2\lambda_1 n} \right)} + \frac{8 \log(4/\delta)}{3R}. \end{aligned}$$

APPENDIX L

PROOF OF THEOREM 6

For applying the Reweight algorithm [13] in noisy multi-label learning, we have

$$\begin{aligned} \bar{R}_{n,w}(\{T^j\}_{j=1}^q, f) &= \frac{1}{n} \sum_{i=1}^n \sum_{j=1}^q \frac{\hat{\mathbb{P}}(Y^j = \bar{y}_i^j | X = x_i)}{\hat{\mathbb{P}}(\bar{Y}^j = \bar{y}_i^j | X = x_i)} \ell(f_j(x_i), \bar{y}_i^j) \\ &= \frac{1}{n} \sum_{i=1}^n \sum_{j=1}^q \frac{[g'_j(x_i)]_{\bar{y}_i^j}}{[(T^j)^\top g'_j(x_i)]_{\bar{y}_i^j}} \ell(f_j(x_i), \bar{y}_i^j), \end{aligned} \quad (47)$$

where $g'_j(x) = [1 - g_j(x), g_j(x)]^\top$, $f_j(x) = \mathbb{I}[g_j(x) > 0.5]$, and $\mathbb{I}[\cdot]$ is the indicator function which takes 1 if the identity index is true and 0 otherwise.

Let $S = \{(x_1, \bar{y}_1), \dots, (x_i, \bar{y}_i), \dots, (x_n, \bar{y}_n)\}$, $S^i = \{(x_1, \bar{y}_1), \dots, (x_{i-1}, \bar{y}_{i-1}), (x'_i, \bar{y}'_i), (x_{i+1}, \bar{y}_{i+1}), \dots, (x_n, \bar{y}_n)\}$, and

$$\Phi(S) = \sup_f (\bar{R}_{n,w}(\{T^j\}_{j=1}^q, f) - \mathbb{E}_S[\bar{R}_{n,w}(\{T^j\}_{j=1}^q, f)]). \quad (48)$$

Lemma 10. Let \hat{f} be the learned classifier, and $U = \frac{1}{\min_j (1 - \max(\mathbb{P}(Y^j=0|Y^j=1), \mathbb{P}(Y^j=1|Y^j=0)))}$. For any $\delta > 0$, with probability at least $1 - \delta$, we have

$$\mathbb{E}[\bar{R}_{n,w}(\{T^j\}_{j=1}^q, \hat{f})] - \bar{R}_{n,w}(\{T^j\}_{j=1}^q, \hat{f}) \leq \mathbb{E}[\Phi(S)] + UM \sqrt{\frac{(\log 1/\delta)}{2n}}.$$

The proof of Lemma 10 is provided in Appendix L.1. Using the same tricks following [10], we can upper bound $\mathbb{E}[\Phi(S)]$ by the following lemma.

Lemma 11.

$$\mathbb{E}[\Phi(S)] \leq 2\mathbb{E} \left[\sup_f \frac{1}{n} \sum_{i=1}^n \sum_{j=1}^q \sigma_i \ell(f_j(x_i), \bar{y}_i^j) \right],$$

where $\sigma_1, \dots, \sigma_n$ are i.i.d. Rademacher random variables.

Proof of Lemma 11 is provided in Appendix L.2.

Recall that $f_j(x) = \mathbb{I}[g_j(x) > 0.5]$, $j = 1, \dots, q$, is the classifier, where g_j is the output of the sigmoid function, i.e., $g_j(x) = 1/(1 + \exp(-h_j(x)))$, $j = 1, \dots, q$, and $h(x)$ is defined by a d -layer neural network, i.e., $h : x \mapsto W_d \sigma_{d-1}(W_{d-1} \sigma_{d-2}(\dots \sigma_1(W_1 x))) \in \mathbb{R}^q$, W_1, \dots, W_d are the parameter matrices, and $\sigma_1, \dots, \sigma_{d-1}$ are activation functions.

To further upper bound the Rademacher complexity, we need to consider the Lipschitz continuous property of the loss function w.r.t. to $h_j(x)$. To avoid more assumptions, We discuss the widely used binary cross-entropy loss, *i.e.*,

$$\mathcal{L}(f(X), Y) = \sum_{j=1}^q \ell(f_j(X), Y^j) = \sum_{j=1}^q Y^j \log(g_j(X)) + (1 - Y^j) \log(1 - g_j(X)). \quad (49)$$

Then, we can further upper bound the Rademacher complexity by the following lemma.

Lemma 12.

$$\mathbb{E} \left[\sup_f \frac{1}{n} \sum_{i=1}^n \sum_{j=1}^q \sigma_i \ell(f_j(x_i), \bar{y}_i^j) \right] \leq qL \mathbb{E} \left[\sup_{h \in H} \frac{1}{n} \sum_{i=1}^n \sigma_i h(x_i) \right],$$

where H is the function class induced by the deep neural network.

The proof of Lemma 12 is provided in Appendix L.3. Note that $\mathbb{E} \left[\sup_{h \in H} \frac{1}{n} \sum_{i=1}^n \sigma_i h(x_i) \right]$ measures the hypothesis complexity of deep neural networks, which can be bounded by the following theorem.

Theorem 9. Assume the Frobenius norm of the weight matrices W_1, \dots, W_d are at most M_1, \dots, M_d . Let the activation functions be 1-Lipschitz, positive-homogeneous, and applied element-wise (such as the ReLU). Let x is upper bounded by B , *i.e.*, for any $x \in \mathcal{X}$, $\|x\| \leq B$. Then,

$$\mathbb{E} \left[\sup_{h \in H} \frac{1}{n} \sum_{i=1}^n \sigma_i h(x_i) \right] \leq \frac{B(\sqrt{2d \log 2} + 1) \prod_{i=1}^d M_i}{\sqrt{n}}.$$

The proof of Theorem 9 can be found in [43] (Theorem 1 therein). Theorem 6 follows by combining Lemmas 1, 2, 3, and Theorem 9.

L.1 Proof of Lemma 10

We employ McDiarmid's concentration inequality [70] to prove the lemma. We first check the bounded difference property of $\Phi(S)$, *i.e.*,

$$\Phi(S) - \Phi(S^i) \leq \sup_f \frac{1}{n} \sum_{j=1}^q \left(\frac{[g'_j(x_i)]_{\bar{y}_i^j} \ell(f_j(x_i), \bar{y}_i^j)}{[(T^j)^\top g'_j(x_i)]_{\bar{y}_i^j}} - \frac{[g'_j(x'_i)]_{\bar{y}_i^j} \ell(f_j(x'_i), \bar{y}_i^j)}{[(T^j)^\top g'_j(x'_i)]_{\bar{y}_i^j}} \right). \quad (50)$$

Before further upper bounding the above difference, we show that the importance weight $\frac{[g'_j(x)]_{\bar{y}^j}}{[(T^j)^\top g'_j(x)]_{\bar{y}^j}}$ is upper bounded by $U = \frac{1}{\min_j(1 - \max(\mathbb{P}(\bar{Y}^j=0|Y^j=1), \mathbb{P}(\bar{Y}^j=1|Y^j=0)))}$ for any (x, \bar{y}^j) and g'' . Specifically, if $\bar{y}^j = 0$ and let $\mathbb{P}(\bar{Y}^j = 1 | Y^j = 0) = \rho_-$, $g_j(x) = p$, we have

$$w = \frac{[g'_j(x)]_{\bar{y}^j}}{[(T^j)^\top g'_j(x)]_{\bar{y}^j}} = \frac{[g'_j(x)]_0}{[(T^j)^\top g'_j(x)]_0} = \frac{(1-p)}{(1-p)(1-\rho_-) + p\rho_-} \quad (51)$$

Since $\frac{dw}{dp} = \frac{-\rho_-}{[(1-p)(1-\rho_-) + p\rho_-]^2} < 0$, then $w \leq w|_{p=0} = \frac{1}{1-\rho_-}$, *i.e.*,

$$\frac{[g'_j(x)]_{\bar{y}^j}}{[(T^j)^\top g'_j(x)]_{\bar{y}^j}} \leq \frac{1}{1 - \mathbb{P}(\bar{Y}^j = 1 | Y^j = 0)}, \text{ when } \bar{y}^j = 0. \quad (52)$$

Similarly, we could get that

$$\frac{[g'_j(x)]_{\bar{y}^j}}{[(T^j)^\top g'_j(x)]_{\bar{y}^j}} \leq \frac{1}{1 - \mathbb{P}(\bar{Y}^j = 0 | Y^j = 1)}, \text{ when } \bar{y}^j = 1. \quad (53)$$

Hence, according to Eq. (52) and (53), for any (x, \bar{y}^j) and g'' , $\frac{[g'_j(x)]_{\bar{y}^j}}{[(T^j)^\top g'_j(x)]_{\bar{y}^j}} \leq \frac{1}{\min_j(1 - \max(\mathbb{P}(\bar{Y}^j=0|Y^j=1), \mathbb{P}(\bar{Y}^j=1|Y^j=0)))}$.

Then, we can conclude that the weighted loss is upper bounded by UM and that

$$\begin{aligned} \Phi(S) - \Phi(S^i) &\leq \frac{U}{n} \sup_f \sum_{j=1}^q \ell(f_j(x_i), \bar{y}_i^j) \\ &\leq \frac{U}{n} \sup_f \mathcal{L}(f(x), \bar{y}) \leq \frac{UM}{n}. \end{aligned} \quad (54)$$

Similarly, we could prove that $\Phi(S^i) - \Phi(S) \leq \frac{UM}{n}$.

By employing McDiarmid's concentration inequality, for any $\delta > 0$, with probability at least $1 - \delta$, we have

$$\Phi(S) - \mathbb{E}[\Phi(S)] \leq UM \sqrt{\frac{\log(1/\delta)}{2n}}. \quad (55)$$

L.2 Proof of Lemma 11

Using the same trick to derive Rademacher complexity [74], we have

$$\mathbb{E}[\Phi(S)] \leq 2\mathbb{E} \left[\sup_f \frac{1}{n} \sum_{i=1}^n \sum_{j=1}^q \sigma_i \frac{[g'_j(x_i)]_{\bar{y}_i^j}}{[(T^j)^\top g'_j(x_i)]_{\bar{y}_i^j}} \ell(f_j(x_i), \bar{y}_i^j) \right],$$

where $\sigma_1, \dots, \sigma_n$ are i.i.d. Rademacher random variables.

Then, the proof of Lemma 2 is transformed to prove the following inequality:

$$\mathbb{E} \left[\sup_f \frac{1}{n} \sum_{i=1}^n \sum_{j=1}^q \sigma_i \frac{[g'_j(x_i)]_{\bar{y}_i^j}}{[(T^j)^\top g'_j(x_i)]_{\bar{y}_i^j}} \ell(f_j(x_i), \bar{y}_i^j) \right] \leq \mathbb{E} \left[\sup_f \frac{1}{n} \sum_{i=1}^n \sum_{j=1}^q \sigma_i \ell(f_j(x_i), \bar{y}_i^j) \right]. \quad (56)$$

Note that

$$\mathbb{E}_\sigma \left[\sup_f \sum_{i=1}^n \sum_{j=1}^q \sigma_i \frac{[g'_j(x_i)]_{\bar{y}_i^j}}{[(T^j)^\top g'_j(x_i)]_{\bar{y}_i^j}} \ell(f_j(x_i), \bar{y}_i^j) \right] \leq \mathbb{E}_{\sigma_1, \dots, \sigma_{n-1}} \left[\mathbb{E}_{\sigma_n} \left[\sup_f \sum_{i=1}^n \sum_{j=1}^q \sigma_i \ell(f_j(x_i), \bar{y}_i^j) \right] \right]. \quad (57)$$

$$\text{Let } s_{n-1}(f) = \sum_{i=1}^{n-1} \sum_{j=1}^q \sigma_i \frac{[g'_j(x_i)]_{\bar{y}_i^j}}{[(T^j)^\top g'_j(x_i)]_{\bar{y}_i^j}} \ell(f_j(x_i), \bar{y}_i^j).$$

By definition of the supremum, for any $\epsilon > 0$, there exist f^1 and f^2 (also g^{1^*} and g^{2^*}) such that

$$\sum_{j=1}^q \frac{[g_j^{1^*}(x_i)]_{\bar{y}_i^j}}{[(T^j)^\top g_j^{1^*}(x_i)]_{\bar{y}_i^j}} \ell(f_j^1(x_i), \bar{y}_i^j) + s_{n-1}(f^1) \geq (1 - \epsilon) \sup_f \left(\sum_{j=1}^q \frac{[g'_j(x_i)]_{\bar{y}_i^j}}{[(T^j)^\top g'_j(x_i)]_{\bar{y}_i^j}} \ell(f_j(x_i), \bar{y}_i^j) + s_{n-1}(f) \right),$$

and

$$-\sum_{j=1}^q \frac{[g_j^{2^*}(x_i)]_{\bar{y}_i^j}}{[(T^j)^\top g_j^{2^*}(x_i)]_{\bar{y}_i^j}} \ell(f_j^2(x_i), \bar{y}_i^j) + s_{n-1}(f^2) \geq (1 - \epsilon) \sup_f \left(-\sum_{j=1}^q \frac{[g'_j(x_i)]_{\bar{y}_i^j}}{[(T^j)^\top g'_j(x_i)]_{\bar{y}_i^j}} \ell(f_j(x_i), \bar{y}_i^j) + s_{n-1}(f) \right).$$

Thus, for any ϵ , we have

$$\begin{aligned} & (1 - \epsilon) \mathbb{E}_{\sigma_n} \left[\sup_f \left(\sum_{j=1}^q \sigma_n \frac{[g'_j(x_i)]_{\bar{y}_i^j}}{[(T^j)^\top g'_j(x_i)]_{\bar{y}_i^j}} \ell(f_j(x_i), \bar{y}_i^j) + s_{n-1}(f) \right) \right] \\ &= \frac{(1 - \epsilon)}{2} \sup_f \left(\sum_{j=1}^q \frac{[g'_j(x_i)]_{\bar{y}_i^j}}{[(T^j)^\top g'_j(x_i)]_{\bar{y}_i^j}} \ell(f_j(x_i), \bar{y}_i^j) + s_{n-1}(f) \right) \\ &+ \frac{(1 - \epsilon)}{2} \sup_f \left(-\sum_{j=1}^q \frac{[g'_j(x_i)]_{\bar{y}_i^j}}{[(T^j)^\top g'_j(x_i)]_{\bar{y}_i^j}} \ell(f_j(x_i), \bar{y}_i^j) + s_{n-1}(f) \right) \\ &\leq \frac{1}{2} \left(\sum_{j=1}^q \frac{[g_j^{1^*}(x_i)]_{\bar{y}_i^j}}{[(T^j)^\top g_j^{1^*}(x_i)]_{\bar{y}_i^j}} \ell(f_j^1(x_i), \bar{y}_i^j) + s_{n-1}(f^1) - \sum_{j=1}^q \frac{[g_j^{2^*}(x_i)]_{\bar{y}_i^j}}{[(T^j)^\top g_j^{2^*}(x_i)]_{\bar{y}_i^j}} \ell(f_j^2(x_i), \bar{y}_i^j) + s_{n-1}(f^2) \right) \\ &\leq \frac{1}{2} \left(s_{n-1}(f^1) + s_{n-1}(f^2) + U \left| \sum_{j=1}^q \ell(f_j^1(x_i), \bar{y}_i^j) - \sum_{j=1}^q \ell(f_j^2(x_i), \bar{y}_i^j) \right| \right), \end{aligned} \quad (58)$$

where the last inequality holds because $\frac{[g'_j(x)]_{\bar{y}_i^j}}{[(T^j)^\top g'_j(x)]_{\bar{y}_i^j}} \leq U$ for any (x, \bar{y}^j) and g' .

Let $s = \text{sgn} \left[\sum_{j=1}^q \ell(f_j^1(x_i), \bar{y}_i^j) - \sum_{j=1}^q \ell(f_j^2(x_i), \bar{y}_i^j) \right] U$, where $\text{sgn}[z]$ is the sign of a real number z . We have

$$\begin{aligned}
& (1 - \epsilon) \mathbb{E}_{\sigma_n} \left[\sup_f \left(\sum_{j=1}^q \sigma_n \frac{[g_j'(x_i)]_{\bar{y}_i^j}}{[(T^j)^\top g_j'(x_i)]_{\bar{y}_i^j}} \ell(f_j(x_i), \bar{y}_i^j) + s_{n-1}(f) \right) \right] \\
& \leq \frac{1}{2} \left(s_{n-1}(f^1) + s_{n-1}(f^2) + s \left(\sum_{j=1}^q \ell(f_j^1(x_i), \bar{y}_i^j) - \sum_{j=1}^q \ell(f_j^2(x_i), \bar{y}_i^j) \right) \right) \\
& = \frac{1}{2} \left(s_{n-1}(f^1) + s \sum_{j=1}^q \ell(f_j^1(x_i), \bar{y}_i^j) \right) + \frac{1}{2} \left(s_{n-1}(f^2) - s \sum_{j=1}^q \ell(f_j^2(x_i), \bar{y}_i^j) \right) \\
& \leq \frac{1}{2} \sup_f \left(s_{n-1}(f) + s \sum_{j=1}^q \ell(f_j(x_i), \bar{y}_i^j) \right) + \frac{1}{2} \sup_f \left(s_{n-1}(f) - s \sum_{j=1}^q \ell(f_j(x_i), \bar{y}_i^j) \right) \\
& = \mathbb{E}_{\sigma_n} \left[\sup_f \left(\sum_{i=1}^n \sum_{j=1}^q \sigma_i \ell(f_j(x_i), \bar{y}_i^j) + s_{n-1}(f) \right) \right].
\end{aligned} \tag{59}$$

Since the above inequality holds for any $\epsilon > 0$, we have

$$\mathbb{E}_{\sigma_n} \left[\sup_f \left(\sum_{j=1}^q \sigma_n \frac{[g_j'(x_i)]_{\bar{y}_i^j}}{[(T^j)^\top g_j'(x_i)]_{\bar{y}_i^j}} \ell(f_j(x_i), \bar{y}_i^j) + s_{n-1}(f) \right) \right] \leq \mathbb{E}_{\sigma_n} \left[\sup_f \left(\sum_{i=1}^n \sum_{j=1}^q \sigma_i \ell(f_j(x_i), \bar{y}_i^j) + s_{n-1}(f) \right) \right]. \tag{60}$$

Proceeding in the same way for all other σ , we have

$$\mathbb{E}_{\sigma} \left[\sup_f \frac{1}{n} \sum_{i=1}^n \sum_{j=1}^q \sigma_i \frac{[g_j'(x_i)]_{\bar{y}_i^j}}{[(T^j)^\top g_j'(x_i)]_{\bar{y}_i^j}} \ell(f_j(x_i), \bar{y}_i^j) \right] \leq \mathbb{E}_{\sigma} \left[\sup_f \frac{1}{n} \sum_{i=1}^n \sum_{j=1}^q \sigma_i \ell(f_j(x_i), \bar{y}_i^j) \right], \tag{61}$$

and thus

$$\mathbb{E} \left[\sup_f \frac{1}{n} \sum_{i=1}^n \sum_{j=1}^q \sigma_i \frac{[g_j'(x_i)]_{\bar{y}_i^j}}{[(T^j)^\top g_j'(x_i)]_{\bar{y}_i^j}} \ell(f_j(x_i), \bar{y}_i^j) \right] \leq \mathbb{E} \left[\sup_f \frac{1}{n} \sum_{i=1}^n \sum_{j=1}^q \sigma_i \ell(f_j(x_i), \bar{y}_i^j) \right]. \tag{62}$$

L.3 Proof of Lemma 12

Before proving Lemma 12, we show that the base loss function $\ell(f_j(x), \bar{y}^j)$ is 1-Lipschitz-continuous w.r.t. $h_j(x)$, $j = \{1, \dots, q\}$.

Recall that

$$\begin{aligned}
\ell(f_j(x), \bar{y}^j) &= -(1 - \bar{y}^j) \log(1 - g_j(x)) - \bar{y}^j \log(g_j(x)) \\
&= (\bar{y}^j - 1) \log(1 + e^{h_j(x)}) + \bar{y}^j \log(1 + e^{-h_j(x)}).
\end{aligned}$$

Take the derivative of $\ell(f_j(x), \bar{y}^j)$ w.r.t. $h_j(x)$. If $\bar{y}^j = 0$, we have

$$\frac{d\ell(f_j(x), \bar{y}^j)}{dh_j(x)} = -\frac{e^{h_j(x)}}{1 + e^{h_j(x)}}. \tag{63}$$

If $\bar{y}^j = 1$, we have

$$\frac{d\ell(f_j(x), \bar{y}^j)}{dh_j(x)} = -\frac{e^{-h_j(x)}}{1 + e^{-h_j(x)}}. \tag{64}$$

According to Eqs. (63) and (64), it is easy to conclude that $-1 \leq \frac{d\ell(f_j(x), \bar{y}^j)}{dh_j(x)} \leq 1$, which indicates that the loss function is 1-Lipschitz with respect to $h_j(x)$, $\forall j \in \{1, \dots, q\}$.

Now we are ready to prove Lemma 3. Let H be the hypothesis space of h_j , We have

$$\begin{aligned}
& \mathbb{E} \left[\sup_{f=\{f_1, \dots, f_q\}} \frac{1}{n} \sum_{i=1}^n \sum_{j=1}^q \sigma_i \ell(f_j(x_i), \bar{y}_i^j) \right] \\
& \leq \mathbb{E} \left[\sum_{j=1}^q \sup_{f_j} \frac{1}{n} \sum_{i=1}^n \sigma_i \ell(f_j(x_i), \bar{y}_i^j) \right] \\
& = \mathbb{E} \left[\sum_{j=1}^q \sup_{h_j \in H} \frac{1}{n} \sum_{i=1}^n \sigma_i \ell(f_j(x_i), \bar{y}_i^j) \right] \\
& = \sum_{j=1}^q \mathbb{E} \left[\sup_{h_j \in H} \frac{1}{n} \sum_{i=1}^n \sigma_i \ell(f_j(x_i), \bar{y}_i^j) \right] \\
& \leq qL \mathbb{E} \left[\sup_{h_j \in H} \frac{1}{n} \sum_{i=1}^n \sigma_i h_j(x_i) \right] \\
& = qL \mathbb{E} \left[\sup_{h \in H} \frac{1}{n} \sum_{i=1}^n \sigma_i h(x_i) \right],
\end{aligned} \tag{65}$$

where the second equation holds because f_j and h_j are in one-to-one correspondence; the fourth inequality holds because of the Talagrand Contraction Lemma [75].

APPENDIX M

THE WILCOXON SIGNED-RANKS TEST FOR REWEIGHT-OURS AGAINST BASELINES

Wilcoxon signed-ranks test [76] is employed to show whether Reweight-Ours has a significant performance than other comparing approaches. Note that the performance of these methods used for the Wilcoxon signed-ranks test is from both class-dependent label noise cases and instance-dependent label-noise cases. As shown in Tab. 15, Reweight-Ours outperforms all baselines on both OF1 and CF1 metrics at 0.01 significance level.

TABLE 15: Summary of the Wilcoxon signed-ranks test for Reweight-Ours against other comparing approaches at 0.01 significance level. The p-values are shown in the brackets.

Reweight-Ours against	Standard	GCE	CDR	AGCN	CSRA	WSIC	Reweight-T max	Reweight-T 97%	Reweight-DualT max	Reweight-DualT 97%
mAP	win [0.000]	win [0.004]	win [0.004]	win [0.000]	tie [0.772]	win [0.000]	win [0.000]	win [0.000]	win [0.000]	win [0.000]
OF1	win [0.000]	win [0.000]	win [0.000]	win [0.000]						
CF1	win [0.000]	win [0.000]	win [0.000]	win [0.000]						

APPENDIX N

LIMITATIONS

This work still has certain limitations, including:

- This work exploits the memorization effect [32] in deep learning to perform sample selection, while the memorization effect has not been found in other traditional machine learning methods, and therefore, the proposed estimator can not be applied to such learning methods.
- This work estimates occurrence probabilities using frequency counting. Although this estimation error will converge to zero exponentially fast [41], when the number of one label appearing is too small, *e.g.*, less than 50, the estimation of the transition matrix for this class label is still difficult to be accurate.
- Since our work assumes label noise is class-dependent but instance-independent, when this assumption does not hold, the estimation is not guaranteed. The discussions about the relaxation of instance-independent assumption can be found in Appendix E, which reveals its applicability in certain typical instance-dependent cases.

APPENDIX O

COMPLETE NUMERICAL EXPERIMENTAL RESULTS

In the main paper, we have provided illustrations comparing the classification performance of Reweight-Ours with several state-of-the-art methods. Here, complete numerical experimental results are presented in Tab. 16- 23 for checks and references.

TABLE 16: Complete numerical results for classification performance on Pascal-VOC2007 dataset with class-dependent label noise.

	Noise rates (ρ_-, ρ_+)	(0,0.2)	(0,0.6)	(0.2,0)	(0.6,0)	(0.1,0.1)	(0.2,0.2)	(0.017,0.2)	(0.034,0.4)	
mAP	Standard	84.25±1.07	77.16±0.94	82.70±0.54	68.65±1.57	83.07±0.45	78.87±0.52	83.92±0.59	80.97±0.42	
	GCE	83.83±1.09	73.32±2.22	83.03±0.51	67.47±1.74	83.68±0.66	79.39±0.95	84.40±0.34	80.68±0.52	
	CDR	84.60±0.43	77.45±1.23	82.76±0.53	68.86±2.05	83.22±0.57	79.02±0.62	84.37±0.25	81.14±0.28	
	AGCN	83.24±0.67	75.50±0.56	81.09±0.51	66.47±1.29	81.09±0.48	73.79±0.76	82.21±0.42	76.55±1.11	
	CSRA	85.11±0.51	79.47±1.22	82.93±0.65	67.36±2.25	83.69±0.69	78.10±0.53	84.94±0.36	81.51±0.14	
	WSIC	84.14±0.26	76.17±1.31	82.30±0.64	66.82±3.87	83.41±0.31	77.93±1.00	84.17±0.48	80.74±0.44	
	Reweight-T max	84.20±0.46	76.97±1.20	83.04±0.39	71.36±2.47	83.48±0.15	79.10±0.52	84.06±0.24	81.01±0.99	
	Reweight-T 97%	84.00±0.68	78.97±0.69	83.07±0.29	73.96±1.69	82.71±0.30	78.80±0.28	84.37±0.22	81.42±0.25	
	Reweight-DualT max	84.46±0.20	77.65±1.06	83.75±0.44	73.75±1.61	83.94±0.31	79.48±1.24	84.60±0.30	81.77±0.26	
	Reweight-DualT 97%	82.36±0.45	77.72±0.73	84.56±0.40	75.76±2.11	79.69±1.40	75.26±1.70	81.84±0.81	77.40±1.86	
	Reweight-Ours	84.43±0.46	78.72±0.41	84.08±0.24	74.46±0.56	84.03±0.29	80.44±0.52	84.09±0.62	80.97±1.03	
	Reweight-TrueT	84.47±0.58	77.60±1.23	84.20±0.42	75.68±1.55	84.23±0.46	80.29±0.35	84.39±0.53	81.53±0.56	
	OF1	Standard	75.24±1.40	32.02±5.49	78.85±0.43	15.08±0.25	79.24±0.43	75.85±0.84	75.98±1.04	59.67±1.65
		GCE	76.17±1.57	36.13±4.07	79.28±0.44	14.85±0.22	79.73±0.70	76.27±0.55	76.80±0.68	60.26±2.43
CDR		76.05±0.68	34.11±3.43	79.04±0.46	14.99±0.19	79.34±0.60	76.00±0.47	76.56±0.52	59.31±1.04	
AGCN		74.92±1.02	30.97±3.78	75.45±2.06	16.85±0.56	78.69±0.31	72.64±0.51	75.16±0.58	56.56±1.64	
CSRA		76.94±1.03	33.65±2.73	77.71±1.23	15.94±0.32	80.36±0.53	76.92±0.34	77.91±0.63	62.62±1.97	
WSIC		75.01±1.18	16.48±6.78	79.02±0.59	14.88±0.21	78.55±1.05	72.88±3.44	72.30±2.82	53.26±9.44	
Reweight-T max		76.97±0.45	41.54±2.64	79.65±0.44	47.68±5.65	80.00±0.27	73.58±1.67	76.94±0.37	66.77±0.93	
Reweight-T 97%		77.71±0.65	68.28±2.03	80.16±0.24	70.67±0.70	75.28±0.97	65.03±2.20	78.45±0.63	74.11±0.67	
Reweight-DualT max		78.38±0.41	68.81±1.41	80.02±1.12	65.41±1.84	79.87±0.27	65.36±7.31	78.55±0.36	47.04±4.15	
Reweight-DualT 97%		68.17±3.53	61.81±3.29	80.74±0.50	72.53±2.65	52.99±5.06	36.75±6.71	67.55±0.64	57.41±0.70	
Reweight-Ours		78.62±0.58	65.68±1.67	80.85±0.25	67.43±4.65	79.64±0.29	75.52±0.86	79.25±0.52	74.35±1.65	
Reweight-TrueT		78.92±0.72	65.95±2.04	80.72±0.51	73.71±1.95	80.27±0.14	75.25±1.82	79.26±0.58	75.44±0.45	
CF1		Standard	72.53±1.11	30.64±3.90	76.83±0.65	14.97±0.24	75.86±1.23	70.68±1.76	73.11±0.54	52.07±2.34
		GCE	73.10±1.27	33.07±4.65	77.25±0.66	14.77±0.20	76.73±1.57	71.24±1.42	73.37±0.98	56.89±2.84
	CDR	73.08±0.47	33.06±1.84	76.95±0.79	14.88±0.17	76.09±1.42	70.78±1.09	73.33±0.85	54.16±3.19	
	AGCN	73.45±1.04	33.41±1.65	72.65±1.97	16.67±0.55	76.20±0.51	69.09±0.49	72.81±1.02	55.09±3.28	
	CSRA	74.10±0.56	33.44±3.65	75.28±1.32	15.71±0.23	77.52±0.94	73.44±0.62	74.98±0.48	58.60±2.24	
	WSIC	70.13±2.04	13.64±6.97	75.32±2.00	14.77±0.16	74.17±1.87	64.95±6.47	65.41±4.40	43.43±11.31	
	Reweight-T max	74.05±0.51	39.37±1.36	77.28±0.47	50.35±5.52	77.20±0.39	73.32±0.47	74.08±0.29	62.99±1.80	
	Reweight-T 97%	76.81±0.74	71.24±1.33	77.22±0.56	67.65±1.37	74.99±0.37	68.07±0.74	77.62±0.42	74.56±0.26	
	Reweight-DualT max	75.27±0.56	45.31±1.86	76.56±1.80	63.99±0.42	77.27±0.40	69.48±4.48	75.66±0.35	68.32±1.22	
	Reweight-DualT 97%	71.93±1.64	63.85±3.69	77.95±0.79	68.44±2.93	62.84±2.51	50.49±2.43	70.99±0.98	60.58±1.67	
	Reweight-Ours	76.86±0.48	61.29±1.94	77.89±0.42	66.79±2.50	78.04±0.40	74.08±0.79	77.28±0.48	72.18±0.74	
	Reweight-TrueT	76.22±0.63	62.91±1.25	77.92±0.99	68.51±2.29	77.60±0.45	68.89±3.06	76.39±0.77	71.54±0.86	

TABLE 17: Complete numerical results for classification performance on Pascal-VOC2012 dataset with class-dependent label noise.

	Noise rates (ρ_-, ρ_+)	(0,0.2)	(0,0.6)	(0.2,0)	(0.6,0)	(0.1,0.1)	(0.2,0.2)	(0.017,0.2)	(0.034,0.4)	
mAP	Standard	85.97±0.09	80.02±0.62	85.70±0.19	76.13±0.86	85.91±0.10	82.54±0.51	86.03±0.24	82.91±0.74	
	GCE	86.02±0.21	78.71±0.72	85.96±0.19	75.02±1.50	86.29±0.15	83.18±0.33	85.84±0.37	82.96±0.83	
	CDR	86.09±0.14	80.52±1.61	85.61±0.18	76.53±1.26	86.01±0.19	82.79±0.42	85.92±0.38	83.48±0.62	
	AGCN	85.16±0.12	79.67±0.43	84.91±0.38	77.54±0.29	84.69±0.30	80.15±0.49	84.75±0.12	81.85±0.35	
	CSRA	86.88±0.23	81.75±0.97	85.39±0.27	75.08±0.84	86.14±0.14	80.98±1.22	86.51±0.15	83.86±0.49	
	WSIC	86.39±0.38	80.75±0.49	85.53±0.28	77.00±1.03	85.67±0.17	82.01±0.87	86.07±0.22	83.19±0.19	
	Reweight-T max	85.40±0.43	79.06±1.69	85.80±0.32	78.59±0.69	85.98±0.32	82.88±0.41	85.51±0.51	82.38±1.67	
	Reweight-T 97%	85.97±0.27	81.04±0.79	85.81±0.21	80.12±0.75	85.66±0.55	82.81±0.52	85.99±0.51	83.28±1.07	
	Reweight-DualT max	85.93±0.41	78.69±2.62	86.47±0.26	80.00±0.66	86.23±0.34	84.21±0.18	86.15±0.44	83.42±1.26	
	Reweight-DualT 97%	83.93±0.52	79.97±1.42	86.37±0.25	81.84±0.87	82.39±0.85	78.61±1.01	83.33±1.40	80.95±1.15	
	Reweight-Ours	86.01±0.54	80.33±1.85	86.12±0.10	80.54±1.30	86.23±0.28	83.42±0.51	85.92±0.42	83.56±1.31	
	Reweight-TrueT	86.33±0.33	82.19±0.58	86.28±0.31	81.61±0.47	86.35±0.40	83.72±0.28	85.97±0.50	84.26±0.21	
	OF1	Standard	77.91±0.20	27.84±4.17	80.47±0.34	14.93±0.28	81.27±0.22	78.51±0.13	77.83±0.36	61.67±2.10
		GCE	78.25±0.28	24.67±3.13	80.89±0.19	14.73±0.28	81.47±0.34	78.78±0.11	78.32±0.37	63.26±1.40
CDR		78.02±0.23	29.45±6.39	80.65±0.36	14.91±0.26	81.34±0.35	78.58±0.14	77.82±0.34	61.94±1.91	
AGCN		76.11±0.76	31.06±4.73	80.49±0.51	15.42±0.35	80.28±0.44	76.02±1.33	75.83±1.18	61.59±4.20	
CSRA		78.61±0.56	32.36±6.27	79.88±0.57	15.71±0.50	81.82±0.35	78.12±1.11	79.05±0.59	61.77±3.46	
WSIC		78.56±0.78	27.90±6.72	80.56±0.32	15.09±0.24	80.98±0.49	77.36±1.51	78.52±0.65	57.56±4.11	
Reweight-T max		77.76±0.72	43.96±6.52	81.24±0.31	48.88±2.45	81.53±0.49	78.63±0.17	78.66±0.22	68.04±2.70	
Reweight-T 97%		79.31±0.20	71.79±2.35	81.56±0.29	75.10±1.81	77.81±1.09	71.28±1.99	79.20±0.35	73.90±1.81	
Reweight-DualT max		80.44±0.69	63.68±5.75	82.01±0.28	74.17±2.34	81.04±0.36	78.71±0.83	80.47±0.35	75.56±1.72	
Reweight-DualT 97%		60.81±1.36	58.42±2.41	82.20±0.20	75.96±1.47	56.42±1.24	30.28±1.82	64.36±1.42	58.49±1.73	
Reweight-Ours		80.54±0.61	69.08±4.58	81.77±0.43	75.38±3.05	81.11±0.56	77.78±0.37	80.75±0.43	77.31±1.49	
Reweight-TrueT		80.65±0.14	74.79±1.00	81.82±0.29	77.94±0.65	81.66±0.43	78.63±0.28	80.83±0.55	78.18±0.43	
CF1		Standard	75.15±0.62	29.76±3.77	79.06±0.35	14.87±0.29	79.05±0.26	75.61±0.52	76.07±0.46	60.32±1.90
		GCE	75.25±0.84	26.25±4.40	79.68±0.32	14.69±0.27	79.13±0.32	75.84±0.51	76.05±0.84	61.99±0.71
	CDR	75.32±0.66	31.49±4.03	79.20±0.20	14.85±0.25	79.14±0.45	75.56±0.49	76.11±0.44	60.02±1.91	
	AGCN	74.16±1.06	33.33±4.55	78.81±0.12	15.42±0.76	78.09±0.99	73.28±1.80	73.91±1.39	58.57±4.67	
	CSRA	75.91±0.98	32.83±4.88	78.86±0.25	15.48±0.49	79.87±0.26	75.53±1.12	76.40±0.73	59.53±3.12	
	WSIC	76.46±1.39	30.19±5.09	79.49±0.57	14.98±0.23	78.50±0.91	74.10±2.39	76.05±0.90	55.11±4.30	
	Reweight-T max	75.54±0.59	39.66±5.13	79.79±0.27	49.60±3.31	79.60±0.48	76.45±0.29	76.82±0.42	65.53±2.66	
	Reweight-T 97%	78.94±0.10	73.66±1.10	79.73±0.29	73.38±1.41	77.54±0.88	72.39±1.57	78.78±0.35	75.54±1.13	
	Reweight-DualT max	78.37±0.54	58.96±3.99	80.06±0.22	72.61±1.76	79.29±0.35	76.37±1.44	78.69±0.25	65.68±1.37	
	Reweight-DualT 97%	67.96±1.13	61.89±2.49	80.11±0.33	71.87±3.50	65.09±1.07	52.28±1.03	69.26±0.82	63.10±1.57	
	Reweight-Ours	78.81±0.53	66.76±3.38	79.82±0.43	72.84±2.16	79.90±0.39	75.90±0.81	79.37±0.35	75.16±1.42	
	Reweight-TrueT	78.95±0.28	71.82±1.45	79.95±0.53	73.87±1.65	79.69±0.58	75.82±0.78	79.12±0.40	75.99±0.37	

TABLE 18: Complete numerical results for classification performance on MS-COCO dataset with class-dependent label noise.

	Noise rates (ρ_-, ρ_+)	(0,0.2)	(0,0.6)	(0.2,0)	(0.6,0)	(0.1,0.1)	(0.2,0.2)	(0.008,0.2)	(0.015,0.4)
mAP	Standard	69.92±0.06	63.81±0.16	66.77±0.52	55.45±0.48	67.77±0.28	62.50±0.23	69.76±0.09	66.82±0.05
	GCE	69.90±0.05	62.58±0.17	67.32±0.11	54.01±0.70	68.62±0.16	63.21±0.35	69.99±0.11	66.72±0.19
	CDR	70.06±0.05	63.85±0.28	67.32±0.08	55.20±1.62	68.01±0.08	62.65±0.21	69.87±0.09	66.85±0.19
	AGCN	71.48±0.14	65.75±0.32	69.44±0.10	55.71±0.61	69.42±0.23	63.96±0.11	70.90±0.13	67.86±0.26
	CSRA	71.18±0.10	65.28±0.11	67.93±0.18	51.49±0.73	68.83±0.12	61.80±0.98	70.76±0.16	68.02±0.15
	WSIC	68.92±0.09	63.09±0.28	66.22±0.06	53.61±0.36	67.41±0.15	62.33±0.18	68.95±0.15	66.29±0.21
	Reweight-T max	69.99±0.18	63.94±0.11	67.40±0.13	58.27±0.25	67.85±0.05	63.28±0.12	69.76±0.07	66.24±0.51
	Reweight-T 97%	67.98±0.57	62.52±0.46	68.00±0.17	59.44±0.81	65.69±0.48	60.03±0.11	68.13±0.04	64.40±0.18
	Reweight-DualT max	67.57±0.21	60.39±0.53	68.57±0.25	58.42±0.82	68.01±0.51	62.17±0.32	68.76±0.08	65.75±0.15
	Reweight-DualT 97%	64.97±0.20	58.85±0.43	69.68±0.25	49.17±0.02	56.36±0.62	49.41±0.38	63.27±0.36	58.21±0.86
	Reweight-Ours	70.57±0.11	63.28±0.92	69.38±0.36	61.88±0.66	68.70±0.15	64.46±0.10	70.06±0.06	67.03±0.08
	Reweight-TrueT	70.78±0.17	65.50±0.42	69.45±0.07	62.40±0.12	69.49±0.06	65.27±0.36	70.46±0.06	68.03±0.12
OFI	Standard	66.48±0.50	19.18±0.97	69.58±0.38	7.05±0.01	68.64±0.18	64.84±0.54	66.07±0.15	51.70±0.42
	GCE	66.67±0.38	19.61±1.61	69.82±0.25	7.03±0.02	69.44±0.18	64.98±0.79	66.58±0.32	52.04±0.51
	CDR	66.46±0.54	19.60±2.86	69.72±0.31	7.06±0.04	68.75±0.09	64.68±0.54	66.03±0.39	52.49±1.18
	AGCN	67.14±0.52	16.02±0.76	70.63±0.12	7.04±0.02	69.66±0.25	66.07±0.55	66.61±0.48	52.38±1.05
	CSRA	67.98±0.40	24.08±2.60	70.14±0.17	7.06±0.02	69.70±0.31	64.89±1.22	67.37±0.28	51.81±0.53
	WSIC	66.67±0.15	23.02±4.70	69.02±0.06	7.02±0.00	67.78±0.58	62.31±0.69	66.38±0.25	52.07±1.94
	Reweight-T max	67.13±0.41	39.47±1.47	69.84±0.11	59.26±1.76	64.03±2.00	57.68±4.00	66.45±0.30	53.63±1.28
	Reweight-T 97%	57.66±0.56	54.06±1.19	69.72±0.39	64.79±0.85	43.81±0.54	33.65±2.93	55.44±0.56	51.78±1.37
	Reweight-DualT max	65.22±0.28	55.01±0.86	70.16±0.26	56.90±4.55	59.62±1.59	49.79±0.18	65.64±0.71	61.73±2.11
	Reweight-DualT 97%	29.39±0.36	29.30±0.74	70.24±0.26	48.87±6.87	25.83±0.16	8.51±0.26	39.29±0.45	35.78±1.10
	Reweight-Ours	70.10±0.10	61.74±0.64	70.52±0.26	65.78±0.56	64.45±0.47	58.60±3.30	69.40±0.31	65.93±0.42
	Reweight-TrueT	70.61±0.14	65.96±0.45	70.45±0.06	66.46±0.15	70.26±0.09	67.27±0.13	70.21±0.30	68.55±0.18
CFI	Standard	60.27±0.52	22.73±0.15	64.66±0.82	7.07±0.02	62.38±0.27	56.78±1.31	60.04±0.17	45.35±0.60
	GCE	60.76±0.08	21.06±1.12	65.27±0.22	7.04±0.03	63.60±0.25	56.72±1.56	60.66±0.19	44.28±1.12
	CDR	60.26±0.55	22.42±1.78	65.27±0.10	7.07±0.04	62.63±0.08	56.41±1.36	59.85±0.38	45.41±0.85
	AGCN	61.79±0.98	19.30±1.20	66.29±0.11	7.05±0.04	64.09±0.39	58.97±1.15	60.35±0.54	43.89±1.46
	CSRA	62.46±0.53	24.17±2.76	65.80±0.02	7.06±0.02	63.90±0.48	55.97±2.29	61.30±0.42	44.25±2.33
	WSIC	61.12±0.08	27.16±1.54	63.71±0.34	7.03±0.01	61.12±1.30	52.47±0.99	60.51±0.25	45.52±1.32
	Reweight-T max	61.59±0.51	32.78±0.70	64.82±0.24	56.68±0.80	63.35±0.16	59.93±0.50	60.92±0.08	48.40±0.33
	Reweight-T 97%	55.67±0.45	52.79±1.04	63.97±0.74	56.70±2.11	48.47±0.70	40.20±0.82	55.33±0.12	52.19±0.29
	Reweight-DualT max	64.79±0.23	52.16±2.08	63.51±0.35	54.62±1.12	66.29±0.34	61.33±0.09	65.18±0.22	60.88±0.59
	Reweight-DualT 97%	32.15±0.43	30.32±0.91	65.23±0.28	33.76±8.88	29.99±0.10	12.77±0.21	41.29±0.83	37.08±1.29
	Reweight-Ours	67.18±0.17	57.46±0.52	65.42±0.49	58.63±1.30	66.65±0.15	61.13±1.01	66.42±0.10	62.94±0.28
	Reweight-TrueT	65.67±0.15	59.74±0.37	65.43±0.20	58.78±0.05	65.10±0.02	60.25±0.50	65.02±0.55	63.09±0.62

TABLE 19: Complete numerical results for classification performance on Pascal-VOC2007 dataset with instance-dependent label noise.

	Noise type	Pair-wise 10%	Pair-wise 20%	Pair-wise 30%	PMD-Type-I	PMD-Type-II	PMD-Type-III
mAP	Standard	84.76±0.29	82.64±0.28	79.94±0.35	77.99±0.63	83.11±0.18	82.69±0.38
	GCE	84.92±0.22	83.16±0.27	79.81±0.93	77.30±0.67	83.02±0.33	82.59±0.14
	CDR	84.69±0.23	82.69±0.28	79.94±0.42	77.91±0.91	83.01±0.23	82.61±0.34
	AGCN	83.09±0.51	80.27±0.30	74.80±1.07	75.90±0.52	81.48±0.20	81.69±0.38
	CSRA	85.47±0.59	82.90±0.79	80.34±1.26	79.63±0.15	83.56±0.56	83.62±0.47
	WSIC	84.42±0.30	82.26±0.30	79.16±0.46	77.81±0.56	82.65±0.34	82.51±0.24
	Reweight-T max	84.47±0.31	82.02±0.46	79.57±0.69	78.02±0.56	82.14±0.38	81.68±0.70
	Reweight-T 97%	83.98±0.44	80.82±0.86	79.49±0.48	78.01±0.71	82.30±0.58	81.36±0.38
	Reweight-DualT max	84.60±0.34	82.37±0.38	80.20±0.60	78.20±0.75	82.29±0.81	81.83±0.66
	Reweight-DualT 97%	83.48±0.56	81.60±0.51	73.85±2.04	75.03±1.89	79.91±0.45	80.35±0.35
	Reweight-Ours	84.45±0.38	82.29±0.44	79.11±1.07	78.72±0.61	82.35±0.65	81.77±0.60
	OFI	Standard	80.04±0.27	78.13±0.34	75.29±0.47	58.08±1.93	76.97±0.76
GCE		79.96±0.29	78.62±0.31	74.90±0.98	56.90±3.62	77.10±0.77	76.24±0.45
CDR		79.86±0.41	78.10±0.37	75.28±0.60	59.04±1.39	76.93±0.85	76.33±0.41
AGCN		78.85±0.74	76.30±0.37	71.64±0.86	56.02±3.92	76.49±0.39	76.06±0.75
CSRA		81.21±0.74	79.31±0.56	76.17±0.89	59.08±1.98	78.45±0.51	77.67±0.29
WSIC		78.03±1.77	77.25±0.25	73.19±2.50	55.89±1.54	72.04±1.16	74.86±1.56
Reweight-T max		80.04±0.23	78.54±0.35	75.68±0.65	63.56±1.33	77.27±0.35	76.17±0.51
Reweight-T 97%		79.21±0.72	76.78±0.73	74.35±0.41	72.19±0.49	76.81±0.48	76.27±0.21
Reweight-DualT max		80.26±0.26	79.11±0.45	76.68±0.44	69.53±1.07	77.49±0.32	76.29±0.38
Reweight-DualT 97%		70.59±0.19	59.64±0.37	57.40±0.18	60.17±1.18	67.20±0.32	70.03±2.10
Reweight-Ours		80.45±0.13	79.42±0.45	74.34±0.35	73.66±0.73	77.62±0.40	77.18±0.40
CFI		Standard	77.21±0.38	73.96±0.35	69.46±0.69	50.84±3.44	73.70±0.95
	GCE	77.37±0.13	74.48±0.21	69.56±0.78	51.05±3.00	73.68±1.10	72.71±0.89
	CDR	77.08±0.36	73.76±0.49	69.49±0.68	52.67±2.00	73.53±1.05	72.87±0.61
	AGCN	76.71±0.67	72.50±0.67	66.35±1.42	53.73±2.90	73.15±0.42	73.12±0.91
	CSRA	78.98±0.88	75.93±0.55	71.39±1.16	56.91±1.17	75.78±0.66	75.10±0.18
	WSIC	73.57±3.03	72.08±0.42	65.45±4.66	48.03±2.78	63.49±2.59	70.06±2.83
	Reweight-T max	77.62±0.21	74.75±0.65	71.00±0.78	60.28±1.39	74.39±0.52	73.43±0.40
	Reweight-T 97%	77.53±0.51	74.14±0.87	71.10±0.61	72.27±0.57	75.81±0.64	74.76±0.31
	Reweight-DualT max	77.65±0.32	75.66±0.48	72.50±0.77	65.85±1.54	74.85±0.75	73.45±0.46
	Reweight-DualT 97%	73.90±0.14	65.79±0.10	60.23±0.18	62.28±1.36	71.22±1.00	71.50±1.02
	Reweight-Ours	78.32±0.21	76.57±0.51	71.42±0.62	72.41±0.62	76.23±0.63	75.05±0.38

TABLE 20: Complete numerical results for classification performance on Pascal-VOC2012 dataset with instance-dependent label noise.

	Noise type	Pair-wise 10%	Pair-wise 20%	Pair-wise 30%	PMD-Type-I	PMD-Type-II	PMD-Type-III
mAP	Standard	86.19±0.49	84.21±0.27	81.46±0.33	80.11±0.62	84.42±0.36	84.53±0.24
	GCE	86.70±0.33	84.67±0.23	82.14±0.37	79.98±0.58	84.59±0.29	84.44±0.29
	CDR	86.38±0.30	84.41±0.40	81.56±0.38	80.36±0.60	84.52±0.30	84.53±0.20
	AGCN	85.28±0.25	82.75±0.29	78.88±1.18	77.25±1.57	84.10±0.46	83.96±0.22
	CSRA	86.45±0.69	84.60±0.19	80.95±0.78	80.30±0.69	85.45±0.22	85.10±0.28
	WSIC	86.41±0.21	84.47±0.56	82.41±0.64	80.20±0.59	84.70±0.15	84.64±0.37
	Reweight-T max	85.79±0.10	83.98±0.30	81.09±0.67	79.84±0.80	84.34±0.34	83.41±0.42
	Reweight-T 97%	85.86±0.20	83.92±0.54	81.33±0.28	81.22±0.43	84.34±0.26	83.22±0.36
	Reweight-DualT max	86.36±0.18	84.79±0.33	82.11±0.50	80.75±0.41	84.49±0.35	83.52±0.38
	Reweight-DualT 97%	83.90±0.80	79.15±1.74	75.36±0.91	76.93±1.11	82.22±0.42	81.64±0.51
	Reweight-Ours	86.30±0.20	84.75±0.32	82.30±0.52	80.87±0.70	84.50±0.36	83.65±0.45
OFI	Standard	81.27±0.23	79.85±0.27	77.62±0.57	60.01±2.13	78.02±0.53	77.05±0.39
	GCE	81.49±0.34	79.81±0.20	77.96±0.39	58.80±1.92	77.90±0.43	76.88±0.32
	CDR	81.36±0.32	79.90±0.19	77.68±0.56	59.06±2.49	77.98±0.38	76.92±0.57
	AGCN	80.79±0.44	78.79±0.61	75.74±0.90	56.91±4.16	77.76±0.63	76.76±1.06
	CSRA	82.01±0.90	80.77±0.40	77.66±0.58	58.06±4.14	78.62±0.41	77.51±0.36
	WSIC	81.36±0.35	79.95±0.63	77.78±0.21	52.39±5.61	77.49±0.83	76.48±0.89
	Reweight-T max	81.47±0.33	80.39±0.38	78.01±0.35	66.39±0.76	78.18±0.53	76.93±0.46
	Reweight-T 97%	79.18±0.74	77.33±0.86	74.90±0.37	72.42±1.02	77.34±0.43	76.30±0.68
	Reweight-DualT max	81.95±0.20	81.45±0.15	79.08±0.46	73.13±0.75	78.16±0.58	77.07±0.40
	Reweight-DualT 97%	65.02±1.97	60.00±1.68	56.34±0.79	56.86±1.49	64.86±1.78	65.03±0.91
	Reweight-Ours	82.03±0.28	81.27±0.13	77.08±0.57	73.42±0.78	77.86±0.56	77.66±0.40
CFI	Standard	78.89±0.60	76.29±0.45	72.50±0.74	56.57±4.64	76.00±0.80	75.51±0.52
	GCE	79.15±0.72	76.08±0.55	72.92±0.31	55.47±5.42	75.95±0.85	74.85±0.56
	CDR	79.15±0.39	76.36±0.36	72.44±0.60	56.40±5.18	76.02±0.64	75.66±0.69
	AGCN	79.31±0.40	75.22±0.51	70.26±1.08	53.36±3.38	76.28±0.30	75.37±1.16
	CSRA	80.25±0.79	77.37±0.63	72.59±0.68	57.37±3.93	77.06±0.27	76.06±0.46
	WSIC	78.97±0.64	76.41±0.73	72.43±0.53	49.99±6.30	75.82±0.46	74.45±1.13
	Reweight-T max	79.64±0.27	77.03±0.70	73.06±0.89	63.28±1.59	76.68±0.34	75.45±0.75
	Reweight-T 97%	78.89±0.34	75.60±0.94	71.68±0.38	73.77±0.46	77.43±0.45	76.82±0.51
	Reweight-DualT max	78.49±0.39	76.64±0.18	75.57±0.88	65.35±2.36	74.90±0.65	73.86±0.67
	Reweight-DualT 97%	71.38±1.03	63.15±1.99	58.79±0.53	61.46±0.91	71.80±0.62	71.86±0.56
	Reweight-Ours	80.48±0.32	79.01±0.32	73.58±0.68	74.12±0.62	77.57±0.49	77.02±0.60

TABLE 21: Complete numerical results for classification performance on MS-COCO dataset with instance-dependent label noise.

	Noise type	Pair-wise 10%	Pair-wise 20%	Pair-wise 30%	PMD-Type-I	PMD-Type-II	PMD-Type-III
mAP	Standard	70.50±0.11	67.78±0.07	65.45±0.12	61.02±0.19	64.90±0.16	64.66±0.20
	GCE	70.99±0.16	68.40±0.17	66.24±0.13	60.77±0.27	65.06±0.18	64.67±0.10
	CDR	70.52±0.04	67.99±0.16	65.40±0.22	61.00±0.12	65.02±0.27	64.82±0.11
	AGCN	71.97±0.11	69.54±0.17	67.01±0.14	62.12±0.11	65.46±0.22	65.19±0.10
	CSRA	71.62±0.29	68.76±0.10	66.03±0.09	61.82±0.21	65.49±0.20	64.99±0.06
	WSIC	69.22±0.08	66.85±0.09	64.46±0.15	61.14±0.17	64.75±0.01	64.38±0.12
	Reweight-T max	70.42±0.12	67.85±0.11	65.58±0.17	61.29±0.21	64.95±0.02	64.54±0.28
	Reweight-T 97%	68.31±0.05	64.93±0.22	61.83±0.53	59.28±0.16	62.97±0.28	62.50±0.10
	Reweight-DualT max	68.24±0.24	65.40±0.57	62.88±0.77	60.17±0.33	63.02±0.09	62.05±0.26
	Reweight-DualT 97%	64.13±0.11	59.83±0.11	56.70±0.77	53.37±0.51	58.28±0.15	57.95±0.31
	Reweight-Ours	70.80±0.13	68.34±0.19	66.59±0.06	62.25±0.36	64.97±0.06	64.51±0.16
OFI	Standard	70.35±0.17	67.86±0.04	65.53±0.26	48.45±2.43	61.39±0.44	59.30±0.40
	GCE	70.91±0.14	68.30±0.05	66.22±0.17	46.62±0.85	61.70±0.55	59.14±0.31
	CDR	70.43±0.27	68.09±0.18	65.66±0.52	48.25±1.76	61.46±0.73	59.35±0.28
	AGCN	71.07±0.23	68.75±0.27	66.04±0.17	42.82±1.86	61.74±0.45	59.63±0.78
	CSRA	70.73±0.33	68.32±0.25	65.98±0.14	47.15±1.43	61.97±0.61	59.10±0.59
	WSIC	69.40±0.16	67.66±0.15	65.47±0.43	50.92±0.98	62.72±0.42	61.31±0.30
	Reweight-T max	70.34±0.53	68.54±0.34	66.16±0.44	56.60±0.29	62.16±0.12	59.80±0.62
	Reweight-T 97%	56.52±0.32	54.00±0.68	54.13±0.95	51.43±1.34	52.35±0.04	51.93±0.74
	Reweight-DualT max	67.18±0.63	64.80±0.80	62.88±1.34	61.06±1.06	58.86±0.60	59.63±1.04
	Reweight-DualT 97%	35.60±0.29	33.68±0.42	34.19±0.62	31.45±0.88	33.84±1.24	33.70±0.90
	Reweight-Ours	71.15±0.13	69.68±0.21	66.54±0.46	63.75±0.12	64.94±0.19	63.60±0.40
CFI	Standard	64.81±0.26	61.41±0.27	57.70±0.58	42.38±1.28	54.53±0.33	52.34±0.16
	GCE	65.65±0.19	61.86±0.26	58.51±0.31	40.51±0.39	55.08±0.80	52.37±0.32
	CDR	64.91±0.38	61.58±0.36	57.65±0.49	42.83±1.22	54.72±0.77	52.30±0.36
	AGCN	66.92±0.48	63.41±0.50	58.40±0.37	39.44±0.31	55.00±0.13	53.12±0.29
	CSRA	66.38±0.40	62.87±0.53	58.41±0.43	41.52±1.18	55.39±0.98	52.63±0.70
	WSIC	64.08±0.24	61.78±0.40	58.39±0.73	46.75±0.51	56.80±0.28	55.51±0.26
	Reweight-T max	65.09±0.63	62.46±0.52	58.65±0.49	47.58±0.37	55.93±0.30	53.30±0.33
	Reweight-T 97%	54.88±0.52	51.90±0.56	53.18±1.04	48.72±0.86	51.04±0.13	51.18±0.13
	Reweight-DualT max	66.37±0.36	64.28±0.63	60.67±0.86	59.75±0.21	58.78±0.40	58.05±0.60
	Reweight-DualT 97%	38.34±0.39	36.92±0.20	43.24±0.44	31.85±0.55	36.89±0.48	36.73±0.23
	Reweight-Ours	68.24±0.39	66.68±0.35	63.50±0.21	60.93±0.48	61.16±0.15	60.44±0.36

TABLE 22: Complete numerical results for classification performance with different loss correction ways on Pascal-VOC2007 dataset with class-dependent label noise. The best performances are in **bold**.

	Noise rates (ρ_-, ρ_+)	(0,0.2)	(0,0.6)	(0.2,0)	(0.6,0)	(0.1,0.1)	(0.2,0.2)	(0.017,0.2)	(0.034,0.4)
mAP	Reweight-Ours	84.43±0.46	78.72±0.41	84.08±0.24	74.46±0.56	84.03±0.29	80.44±0.52	84.09±0.62	80.97±1.03
	Backward-Ours	83.41±0.18	67.22±2.97	81.13±0.45	63.82±1.36	79.00±0.88	70.44±1.80	81.27±0.37	69.22±1.96
	Forward-Ours	84.96±0.28	80.23±0.25	83.41±0.72	71.45±3.65	83.19±0.24	76.77±2.14	84.31±0.51	80.46±1.02
	Revision-Ours	84.99±0.33	79.26±0.51	84.37±0.24	74.44±1.16	84.49±0.36	80.61±0.73	84.98±0.11	82.14±0.10
OFI	Reweight-Ours	78.62±0.58	65.68±1.67	80.85±0.25	67.43±4.65	79.64±0.29	75.52±0.86	79.25±0.52	74.35±1.65
	Backward-Ours	74.98±0.56	16.35±5.06	78.55±0.33	14.57±0.29	74.35±1.12	63.60±4.39	71.68±0.78	36.38±4.13
	Forward-Ours	80.09±0.45	70.38±0.29	80.44±0.50	59.35±10.36	79.77±0.35	73.92±2.33	79.92±0.62	75.18±1.24
	Revision-Ours	79.07±0.94	63.97±3.14	81.20±0.32	68.74±4.18	80.22±0.40	75.68±1.16	79.83±0.33	75.23±0.56
CFI	Reweight-Ours	76.86±0.48	61.29±1.94	77.89±0.42	66.79±2.50	78.04±0.40	74.08±0.79	77.28±0.48	72.18±0.74
	Backward-Ours	70.64±0.59	15.01±4.66	75.48±0.84	14.55±0.26	66.26±2.15	46.19±8.35	65.56±1.59	23.78±2.95
	Forward-Ours	77.85±0.56	64.64±1.69	77.14±0.35	62.26±3.06	77.72±0.25	70.45±4.38	77.74±0.80	71.76±1.45
	Revision-Ours	76.82±0.90	58.56±3.72	78.26±0.51	66.89±1.46	78.55±0.58	73.94±1.06	77.86±0.33	72.12±1.16

TABLE 23: Complete numerical results for classification performance with different base learning algorithms on Pascal-VOC2007 dataset with class-dependent label noise. The best performances are in **bold**.

	Noise rates (ρ_-, ρ_+)	(0,0.2)	(0,0.6)	(0.2,0)	(0.6,0)	(0.1,0.1)	(0.2,0.2)	(0.017,0.2)	(0.034,0.4)
mAP	Standard	84.25±1.07	77.16±0.94	82.70±0.54	68.65±1.57	83.07±0.45	78.87±0.52	83.92±0.59	80.97±0.42
	+R-Ours	84.43±0.46	78.72±0.41	84.08±0.24	74.46±0.56	84.03±0.29	80.44±0.52	84.09±0.62	80.97±1.03
	AGCN	83.24±0.67	75.50±0.56	81.09±0.51	66.47±1.29	81.09±0.48	73.79±0.76	82.21±0.42	76.55±1.11
	+R-Ours	85.07±0.56	80.35±0.69	83.41±0.68	66.07±4.32	83.79±0.41	78.18±2.53	84.38±0.30	80.76±0.91
	CSRA	85.11±0.51	79.47±1.22	82.93±0.65	67.36±2.25	83.69±0.69	78.10±0.53	84.94±0.36	81.51±0.14
+R-Ours	85.83±0.53	77.64±3.21	84.66±0.60	75.41±1.77	84.68±0.44	81.01±0.57	85.74±0.29	82.64±0.35	
OFI	Standard	75.24±1.40	32.02±5.49	78.85±0.43	15.08±0.25	79.24±0.43	75.85±0.84	75.98±1.04	59.67±1.65
	+R-Ours	78.62±0.58	65.68±1.67	80.85±0.25	67.43±4.65	79.64±0.29	75.52±0.86	79.25±0.52	74.35±1.65
	AGCN	74.92±1.02	30.97±3.78	75.45±2.06	16.85±0.56	78.69±0.31	72.64±0.51	75.16±0.58	56.56±1.64
	+R-Ours	80.28±0.41	71.36±2.52	79.18±1.38	46.77±3.34	79.06±0.92	73.14±2.63	79.49±0.76	75.78±2.11
	CSRA	76.94±1.03	33.65±2.73	77.71±1.23	15.94±0.32	80.36±0.53	76.92±0.34	77.91±0.63	62.19±1.97
+R-Ours	80.61±0.80	61.48±3.61	81.22±0.45	57.48±9.33	80.43±0.44	76.04±0.80	81.22±0.34	77.21±0.45	
CFI	Standard	72.53±1.11	30.64±3.90	76.83±0.65	14.97±0.24	75.86±1.23	70.68±1.76	73.11±0.54	52.07±2.34
	+R-Ours	76.86±0.48	61.29±1.94	77.89±0.42	66.79±2.50	78.04±0.40	74.08±0.79	77.28±0.48	72.18±0.74
	AGCN	73.45±1.04	33.41±1.65	72.65±1.97	16.67±0.55	76.20±0.51	69.09±0.49	72.81±1.02	55.09±3.28
	+R-Ours	78.74±0.95	68.58±3.35	77.62±0.65	51.45±1.57	78.02±0.61	71.84±3.18	78.09±0.24	74.32±1.45
	CSRA	74.10±0.56	33.44±3.65	75.28±1.32	15.71±0.23	77.52±0.94	73.44±0.62	74.98±0.48	58.60±2.24
+R-Ours	78.65±0.75	59.28±3.71	78.32±0.73	62.59±6.25	78.98±0.45	75.28±0.37	79.52±0.39	74.38±0.98	